A Novel Control Mechanism of Mitotic Exit in *Saccharomyces cerevisiae*

by

Betül Sarı

A Dissertation Submitted to the
Graduate School of Sciences and Engineering

in Partial Fulfillment of the Requirements for

the Degree of

Master of Science

in

Molecular Biology and Genetics

January 4, 2021

A Novel Control Mechanism of Mitotic Exit in *Saccharomyces cerevisiae*

Koç University

Graduate School of Sciences and Engineering

This is to certify that I have examined this copy of a master's thesis by

Betül Sarı

and have found that it is complete and satisfactory in all respects,

and that any and all revisions required by the final

examining committee have been made.

Committee Members:

Asst. Prof.Dr. Ayşe KOCA ÇAYDAŞI (Advisor - Koç University)

Assoc. Prof. Dr. Nurhan ÖZLÜ SICAKKAN (Koç University)

Prof. Dr. Ahmet KOÇ (İnönü University)

Date: _____

[Dedicated to my lab members]

ABSTRACT

A Novel Control Mechanism of Mitotic Exit in *Saccharomyces cerevisiae*

Betül Sarı

Master of Science in Molecular Biology and Genetics

January 4, 2021

Mitotic exit is the cell cycle stage in which the cell transits from M phase to a new G1 phase. While mitosis is under control of cyclin-dependent kinases (CDK), mitotic exit depends on inactivation of CDKs. Timely coordination of mitotic CDK inactivation with respect to chromosome segregation is important to avoid aneuploidy and maintain ploidy. A comprehensive understanding of regulation of mitotic exit is missing.

In budding yeast, mitotic exit is achieved by the use of a special network, called Mitotic Exit Network. An inhibitor to Mitotic Exit Network, Kin4 kinase, leads to lethality for the cells when is expressed in high doses. Our goal is to find out novel mechanisms of mitotic exit control. In this thesis, we identified a temperature sensitive mutant that rescues the lethality of Kin4 overexpression. Through a "dosage suppressive genetic screening", we found two genes, *SAN1* and *PHO2*, that retarded growth this temperature sensitive mutant when Kin4 was overexpressed. We further characterized the effect of these genes on mitotic exit, with a focus on *SAN1*.

Our results indicate a novel regulatory mechanism for mitotic exit. Data presented in this thesis will pave the way to illuminate a new section in the process of exiting from mitosis. Owing to the fact that the basic cellular tasks are preserved from yeast to human, we envisage that characterization of this newly emerged role in the mitotic exit of *S. cerevisiae* would contribute to the understanding of analogous control mechanisms in more complex organisms.

ÖZETÇE

***Saccharomyces cerevisiae'nin* Hücre Döngüsünde, Mitoz Fazından Çıkışın Yeni Bir Kontrol Mekanizması Tarafından Kontrolü**

Betül Sarı

Moleküler Biyoloji ve Genetik, Yüksek Lisans

4 Ocak 2021

Mitotik çıkış, hücrenin M fazından yeni bir G1 fazına geçtiği hücre döngüsü aşamasıdır. Mitoz, sikline bağımlı kinazların (CDK) kontrolü altındayken, mitotik çıkış CDK'lerin inaktivasyonuna bağlıdır. Mitotik CDK inaktivasyonunun kromozomların ayrılmasına göre zamanında koordinasyonu, anöploidiyi engellemek ve ploidi sürdürmek için önemlidir. Mitotik çıkış düzenlemesine ilişkin kapsamlı bir anlayış eksiktir.

Tomurcuklanan mayada, mitotik çıkış, Mitotic Exit Network (Mitozdan Çıkış Ağı) adı verilen özel bir ağın kullanılmasıyla sağlanır. Mitozdan Çıkış Ağı için bir inhibitör olan Kin4 kinaz, yüksek dozlarda ifade edildiğinde hücreler için ölüme yol açar. Amacımız, mitotik çıkış kontrolünün yeni mekanizmalarını bulmaktır. Bu tezde, Kin4 aşırı ifadesinin ölümcüllüğünü kurtaran sıcaklığa duyarlı bir mutant belirledik. Bir "dozaj baskılayıcı genetik tarama" yoluyla, Kin4 aşırı ifade edildiğinde bu sıcaklığa duyarlı mutantın büyümesini geciktiren iki gen bulduk, *SAN1* ve *PHO2*. SAN1'e odaklanarak bu genlerin mitotik çıkış üzerindeki etkisini daha da karakterize ettik.

Sonuçlarımız, mitotik çıkış için yeni bir düzenleyici mekanizmaya işaret etmektedir. Bu tezde sunulan veriler, mitozdan çıkış sürecinde yeni bir bölüme ışık tutmanın yolunu açacaktır. Mayadan insana temel hücresel görevlerin korunduğu gerçeğinden dolayı, S. cerevisiae'nin mitotik çıkışında yeni ortaya çıkan bu rolün karakterizasyonunun, daha karmaşık organizmalarda benzer kontrol mekanizmalarının anlaşılmasına katkıda bulunacağını öngörmekteyiz.

ACKNOWLEDGEMENTS

At first, I need to thank to Asst. Prof. Ayşe Koca Çaydaşı for accepting me in her lab and enable my journey to begin. I feel lucky to start my research career with her. Beside all the practical skills I learnt from her, such as designing and completing an experiment, analyze data and present my finding in a proper way, I have also gained the ability in being resilient, thinking critically and being a solution-oriented person, especially when I experience a failure.

And my beloved lab members: Şeyma, Hüseyin, Barış, Dilara, Idil, Cansu and Mukadder… We were not only colleagues in a team, but also good friends who enjoy doing the things together. Thank you for all the memories we experienced together, even including our arguments, which will be stayed as invaluable parts of my life. I love you all and the present me would not be possible without your existence, you all know that.

Lastly, I thank to my beloved family, for providing me a life-time support and care when I need without any hesitation.

TABLE OF CONTENTS

LIST OF TABLES

LIST OF FIGURES

ABBREVIATIONS

FEAR	Cdc14 early anaphase release network
SPOC	spindle position checkpoint
MEN	mitotic exit network
G1	Gap 1
G2	Gap 2
S	Synthesis
DNA	Deoxyribonucleic acid
RNA	Ribonucleic acid
CDK	Cyclin dependent kinase
SCF	Skp, Cullin, F-box containing complex
APC	Anaphase-Promoting Complex or Cyclosome
Cln	Cyclin or G1 cyclin
Clb	B-type cyclin
Cdc	Cell division cycle
dSPB	Daughter spindle pole body
mSPB	Mother spindle pole body
WT	wild type
mt	mutant
ts	temperature sensitive
E. coli	*Escherichia coli DH5α* bacteria

Chapter 1:
INTRODUCTION

1.1 The Cell Cycle

The cell cycle encompasses the most precious assets of life and comprises a series of events during a eukaryotic cell grows, splits its genome into two daughter cells and duplicates itself. Cells pass through four sequential stages during the course of cell cycle. The first phase of cell cycle is the G1 phase in which macromolecules such as proteins, RNA, and cellular membranes are produced. If the cells commit for cell division, the phase of DNA synthesis (S) follows G1 phase. Non-dividing cells, however, exit from cell cycle through transition from G1 into a quiescence state (G0), which blocks the progression of cells into S phase. The S phase is followed by another period of growth (G2), after which the cells become ready to enter the mitotic phase (mitosis (M)), in which the genetic material is segregated equally into two daughter cells (nuclear division). Cytoplasmic division (cytokinesis) comes at the end of mitosis. Two daughter cells are split from each other by these processes. The completion of one cell cycle requires transition from M phase to G1 phase of the next cell cycle. The phases in between two mitotic phases have been frequently named as “interphase” (see figure 1.1).

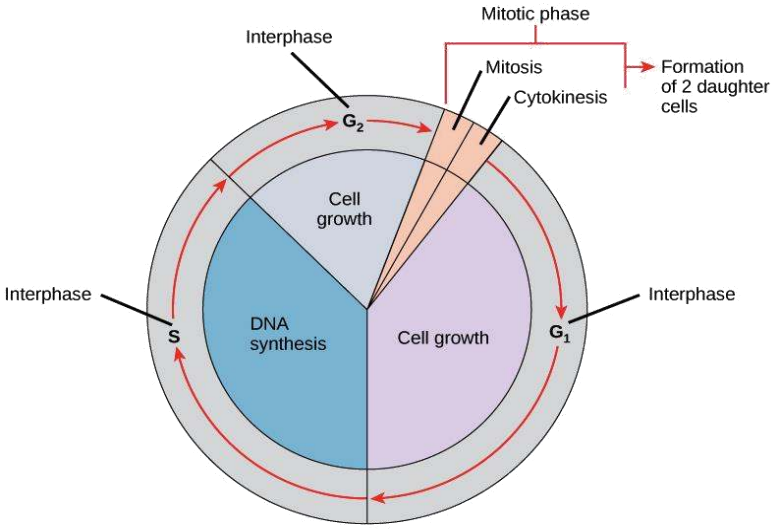

Figure 1.1: The cell cycle consists of interphase and the mitotic phase.

The figure is adapted from Rye, C., Wise, R., Jurukovski, V., Desaix., Choi, J. & Avissar, Y. (2017). Biology. Houston, Texas: OpenStax College, Rice University.

The eukaryotic cell cycle is under control of a family of evolutionarily conserved protein kinases (Hartwell et al., 1974; Nasmyth and Nurse, 1981; Nurse and Bissett, 1981). These protein kinases are called cyclin-dependent kinases (CDKs) as their activity requires their association with cyclins, the phase-specific oscillators during cell cycle. The level of CDK activity fluctuates at different phases of the cell cycle according to their coupling with their respective cyclins. This is due to cyclins which are present in the cells for a limited time and therefore bind to CDKs at specific cell cycle stages (Evans et al., 1983). Importantly, CDKs turn on and off in response to several protein–protein interactions and modifications including interaction with cyclin dependent kinase inhibitors (CKI), phosphorylation by activating and inhibiting kinases, and ubiquitin-mediated proteolysis of cyclins and regulatory proteins (Deshaies et al., 1995; Ducommun et al., 1991; Mendenhall, 1993; Willems et al., 1996) .

Hereafter, we will focus on budding yeast cell cycle - as in this thesis we use budding yeast as our model eukaryote.

1.2 Budding Yeast Cell Cycle

In budding yeast, the cell cycle is mainly commanded by a single cyclin-dependent protein kinase (Cdc28) (Hartwell et al., 1974). The activity of Cdc28 is determined by cyclins that it interacts (Table 1.1): Cln1-3 for G1 phase, Clb5-6 for G1-S transition, Clb3-4 for S phase and transition to G2 and Clb1-Clb2 which act throughout the mitosis.

Table 1.1: Cyclin and CDK types in different cell stages

Cell cycle stage	Cyclin	CDK
G1	Cln3	Cdc28 (Cdk1)
G1/S	Cln1,2	Cdc28 (Cdk1)
S	Clb5,6	Cdc28 (Cdk1)
M	Clb1,2	Cdc28 (Cdk1)

Due to the minute levels of cyclins, CDKs are inactive during early G1 phase (Tyers et al., 1992). Cells accumulate the necessary monomers to produce essential macromolecules and grow until the G1-cyclin levels increase. In this phase, cells also

repair their DNA if DNA is damaged (i.e. by reactive oxygen species or by chemical agents, ultraviolet or ionizing radiation) (Branzei and Foiani, 2008).

G1 cyclins (Cln1-3) are highly unstable proteins. However, the mRNA and protein levels of the precedent cyclin Cln3 is constant through cell cycle (Tyers et al., 1993; Wittenberg et al., 1990). In early G1 phase, Cln3 levels are relatively low. During G1, absolute Cln3 abundance starts to increase regularly, as the cell grows in size, which is proportional to total protein amount in the cell. However, there is no such an increase in the transcription or translation level of Cln3 relative to cell volume. (Sillje et al., 1997; Tyers et al., 1993). Consistently, Cln3-Cdc28 complex is present in very small amounts in the cells in the beginning of G1 and the level of the complex elevates slightly throughout G1.

When sufficient amount of Cln3-Cdc28 is present, the complex phosphorylates and activates two transcription factors, SBF (Swi4/6 cell cycle box binding factor), and MBF (Mlu1 cell cycle box binding factor- Mbp1&Swi6 heterodimer). SBF/MBF controls transcription of late G1 cyclins Cln1 and Cln2. Cln3-Cdc28 complex also phosphorylates Whi5, which is a repressor of SBF. Phosphorylated Whi5 moves from nucleus to cytoplasm and hence cannot inhibit SBF anymore (Costanzo et al., 2004). This way Cln1 and Cln2 levels increase (Koch et al., 1993; Nasmyth and Dirick, 1991). Cln1 and Cln2 are then able to bind and activate CDK, thus start the budding, spindle pole body duplication and DNA replication (Charvin et al., 2010). This way, cells pass from G1 to S phase – also known as START checkpoint. START is a main cell cycle checkpoint in *Saccharomyces cerevisiae* ("Restriction Point" in mammalian cells), in which the cells choose whether or not to begin irreversibly to the next round of cell division (Hartwell et al., 1974). The level of Cln3 presumably reflects the size of the cell and the nutrient conditions. Therefore, one popular model of cell division suggests that the cell reaches to the START when the level of Cln3 reaches a threshold value (Hartwell et al., 1974). Beyond START cells progress into mitosis almost independently of size and environment (Johnston et al., 1977).

Progression into S phase requires blockage of Sic1 and Cdh1 activity (Schneider et al., 1996; Zachariae et al., 1998). Sic1 is a cyclin dependent kinase inhibitor (CKI) directly binds S- and M-phase cyclin-CDK complexes to inhibit their activity, but not G1/S-Cdk1 complexes (Cln-Cdk1) (Schwob et al., 1994). Cln-Cdk1 complexes phosphorylate Sic1 (Verma et al., 1997), which in turn leads to its ubiquitylation by the

Skp, Cullin, F-box containing (SCF) complex (Nash et al., 2001). Once Sic1 is ubiquitylated, it is degraded in the proteasome. Cdh1 is an activatory subunit of anaphase promoting complex (APC) which is a E3 ubiquitin ligase. APC-Cdh1 destines the mitotic (Clb1-2) cyclins for proteasomal degradation. G1/S cyclin-CDKs phosphorylate Cdh1 to block its interaction with APC and therefore results in the elevation of mitotic cyclin levels. Clb1,2-Cdc28 also inactivates SBF and MBF (Koch et al., 1996), which result in the drop of Cln1,2 expression.

At the metaphase–anaphase transition, Cdc20, another activating subunit of the APC, takes stage. APC-Cdc20 targets mitotic cyclins. Clb1,2 protein levels do not completely run out due to APC-Cdc20 activity at anaphase onset, their total removal occurs in telophase by re-activation of Cdh1 (Visintin et al., 1997). Additionally, at the onset of anaphase, Pds1 - the inhibitor of Esp1- is degraded via APC-Cdc20 complex (Shirayama et al., 1999). Absence of Pds1 makes Esp1 available to the cleave cohesin from its Scc1 subunit and leads to separation of sister chromatids later in anaphase (Shirayama et al., 1999).

To begin a new cell cycle, exit from mitosis is crucial. Mitotic exit requires CDK inactivation and removal of phosphorylation from CDK-cyclin targets. CDK inactivation is achieved by two interrelated events: first, proteolytic degradation of mitotic cyclins and second activation of cyclin-dependent kinase inhibitors.

In the budding yeast, the exit from mitosis occurs in charge of Cdc14 phosphatase which reverts CDK-based activation through removal of phosphorylation from CDK targets directly, directs cyclin subunits to proteasomal degradation and activates CKI Sic1 indirectly (Visintin et al., 1998). To achieve CDK inactivation, Cdc14 dephosphorylates Cdh1 which, in turn, promotes its APC binding. APC-Cdh1 complex drives multi-ubiquitylation of mitotic cyclins which could be detected and disintegrated by proteasomes. Cdc14 also drives accumulation of the CDK inhibitor Sic1 via dephosphorylation-based stabilization. (Verma et al., 1997). Additionally, *SIC1* transcription factor Swi5 is a dephosphorylation target of Cdc14, to promote *SIC1* gene expression (Knapp et al., 1996; Visintin et al., 1998). Stabilized Sic1 binds to CDK and blocks CDK activity (Donovan et al., 1994). Sic1, Swi5 and Cdh1 are not the only targets for Cdc14. During the transition from M to G1 phase, Cdc14 reverts the phosphorylation of most, possibly all, CDK targets (Stegmeier and Amon, 2004). Also, rDNA segregation-related protein Nur1 (Godfrey et al., 2015), some of the kinetochore proteins (Akiyoshi

and Biggins, 2010; Olafsson and Thorpe, 2015), microtubule-associated proteins such as Ase1 (Khmelinskii et al., 2007), Ask1 (Higuchi and Uhlmann, 2005), Fin1 (Woodbury and Morgan, 2007), or Sli15 (Pereira and Schiebel, 2003) are also substrates of Cdc14 phosphatase. Finally, Cdc14 also dephosphorylates substrates that are necessary for septin ring clearance and actomyosin ring constriction during cytokinesis: it acts on septin splitting independently of its role in mitotic exit progression (Tamborrini et al., 2018) and regulates actomyosin ring constriction via modulating actomyosin ring proteins such as in Chs2 trafficking (Chin et al., 2012), Iqg1 stability (Miller et al., 2015), Inn1 localization (Meitinger et al., 2010) or the association of Cyk3 with Inn1 (Palani et al., 2012).

Cdc14 activity is blocked by its inhibitor Net1/Cfi1 in a complex known as regulator of nucleolar silencing and telophase (RENT) up to early anaphase (Straight et al., 1999). Nucleolar localization of Cdc14 blocks it to interact with its targets. Two networks, FEAR (Cdc fourteen early anaphase release) network and MEN (mitotic exit network) regulate the localization, and therefore, the activity of Cdc14 (Jaspersen et al., 1998; Shou et al., 1999; Stegmeier et al., 2002; Visintin et al., 2003).

1.3 FEAR Network in Budding Yeast

Activation of Cdc14 is induced by the FEAR network. FEAR network consists of Separase (Esp1 in the budding yeast) (Stegmeier et al., 2002), the kinetochore/spindle protein Slk19 (Sullivan et al., 2001), Spo12 and its homolog Bns1 (Tomson et al., 2009), the polo like kinase Cdc5 (Visintin et al., 2003), the Separase inhibitor Securin (Pds1 in yeast) (Tinker-Kulberg and Morgan, 1999), the nucleolar protein Fob1 (Stegmeier et al., 2004) and protein phosphatase type 2A-regulating proteins Zds1 and Zds2 (Queralt and Uhlmann, 2008).

FEAR network could be divided into two sets of components to differentiate its actions: Esp1-based set and Spo12-based set. Esp1 is mostly known with its protease activity on cohesin cleavage at early anaphase (Uhlmann et al., 2000). FEAR network related function of Esp1 is not well understood (Yellman and Roeder, 2015), whereas its protease function for separation of sister chromatids at the anaphase onset is clearly established. Besides, it was proposed that downregulation of PP2A-Cdc55 could depend on Esp1 (Queralt et al., 2006). At the beginning of anaphase, Esp1 becomes activated by the degradation of its inhibitor, Pds1, and functions together with Slk19 and the proteins

Zds1/2 to downregulate the protein phosphatase PP2A-Cdc55 (Queralt et al., 2006). This downregulation enable Clb-CDKs to phosphorylate Net1, the inhibitor of Cdc14 (Azzam et al., 2004; Queralt et al., 2006). This phosphorylation causes a temporary release of Cdc14 from Net1 during early anaphase. Interestingly, its protease activity seems not to be essential to perform its FEAR network-related functionality (Sullivan and Uhlmann, 2003).

Epistasis analysis positioned *SPO12* and *BNS1* in parallel to *ESP1* and *SLK19,* and *CDC5* at their downstream (Visintin et al., 2003). Spo12 is a nucleolus-localized phosphoprotein which binds to a FEAR network inhibitor, Fob1. Fob1 normally associates with Net1 and negatively regulate the release of Cdc14. Spo12 likely has an effect on the conformation of Fob1 that would decrease the binding of Net1 to Cdc14 (Stegmeier et al., 2004). Slk19, on the other hand, exerts its activity in mitotic exit by encaging Cdc14 into the nucleus until the end of anaphase (Faust et al., 2013). Lastly, Cdc5 contributes the phosphorylation of Net1, which causes the disassociation of RENT complex (Shou et al., 2002). Thus, Cdc14 could relocate from nucleolus to nucleoplasm (Shou et al., 2002; Visintin et al., 2003).

All these mechanisms act in concert to achieve the release of Cdc14 from nucleolus. However, FEAR activity is limited to a short time which is only enough to transiently translocate Cdc14 to the nucleus where it could interact with spindle pole bodies (SPB, centrosomes) and mitotic spindle. Although Net1 is kept as phosphorylated, Cdc14 returns into the nucleolus at the late anaphase, unless mitosis-specific phosphorylation of Cdk substrates is reversed by dephosphorylation (Shou et al., 1999; Visintin et al., 1999). Upon FEAR activity, MEN keeps the Cdc14 activity stable by controlling its spindle pole body localization (Yoshida et al., 2002). When MEN-mediated Cdc14 is released, Cdc14 could reach the cytoplasm and be able to dephosphorylate its cytoplasmic substrates such as Cdh1 or Sic1 (Visintin et al., 1998). Hence, to achieve both nuclear and cytoplasmic localization of Cdc14 and the exit from mitosis, MEN-but not FEAR-is essential (Table 1.2).

Table 1.2: The differences between FEAR and MEN networks in mitotic exit

FEAR	**MEN**

Not essential for mitotic exit, only lead to a delay in mitotic exit and in separation of rDNA regions	Essential for accomplishing mitotic exit, the defects in MEN components lead to mitotic arrest
Results in only a transient release of Cdc14, from nucleolus to nucleus and is transient	Cdc14 is fully released by MEN into cytoplasm where it can associate with its most targets
FEAR network is specific for budding yeast to promote mitotic exit	MEN network is a conserved pathway from yeast to human (see Section 1.5).

FEAR is not essential for mitotic exit, however, it has essential functions in following anaphase related tasks:

(1) FEAR network regulates the condensation and segregation of lately segregated parts of the genome such as the ribosomal DNA (rDNA) array and telomeres (Clemente-Blanco et al., 2011; Sullivan et al., 2004). Cdc14 phosphatase positively regulates sister-chromatid telomeres' separation through transcription repression (Clemente-Blanco et al., 2011; D'Amours et al., 2004). In difference, Cdc14 induces rDNA condensation in a way which rely on Aurora B complex and condensin (Sullivan et al., 2004).

(2) Stabilization of spindle midzone during anaphase is regulated by FEAR network (Pereira and Schiebel, 2003; Sullivan et al., 2001; Zeng et al., 1999). The FEAR network directs the Ipl1-Sli5-Bir1 complex (Aurora B kinase complex or chromosomal passenger complex in higher eukaryotes) to the spindle midzone to activate spindle-stabilizing factors. This complex has multiple functions, such as the establishment of kinetochore biorientation (Pereira and Schiebel, 2003; Tanaka et al., 2002), anaphase spindle stability (Tanaka et al., 2002) the activation of the spindle tension checkpoint (Biggins and Murray 2001), mitotic spindle disintegration (Buvelot et al., 2003) and chromosome condensation (Lavoie et al., 2004; Petersen and Hagan, 2003). In early anaphase, The FEAR network is required to target Ipl1 and Sli15 to the spindle midzone (Lavoie et al., 2004). This localization depends on Cdc14 phosphatase, which dephosphorylates the microtubule binding sites of Ipl1 and Sli15 to allow them to interact with the microtubules (Mirchenko and Uhlmann, 2010; Nakajima et al., 2011; Pereira and Schiebel, 2003). In this way, the chromosomal passenger complex associates with the anaphase spindle and becomes the main regulator of the spindle stability during mitotic exit (Rozelle et al., 2011).

1.4 Spindle Pole Bodies of Budding Yeast

Before starting to explain MEN and its role in mitotic exit, we need to give a brief information about Spindle Pole Bodies (SPBs) - equivalent of the centrosomes in budding yeast.

Spindle pole bodies are multi-layered structures which reside in the nuclear envelope and they are the only microtubule nucleation centers in the budding yeast. Like centrioles, the SPBs duplicate itself one time per cell cycle and the 'new' SPB is produced in close to the pre-existing 'old' one. Differently, the new SPB remains connected to the old one via a half-bridge until the bridge in between them is cleaved in S phase. (Byers and Goetsch, 1975). After the separation of two SPBs, the old SPB is oriented to the daughter cell (the new cell - bud), while the newly synthesized SPB is located at the mother (old) cell (Pereira et al., 2001). The spindle pole bodies are named as the mother-cell-localized SPB (mSPB) and the daughter-cell-localized SPB (dSPB) (Figure 1.2).

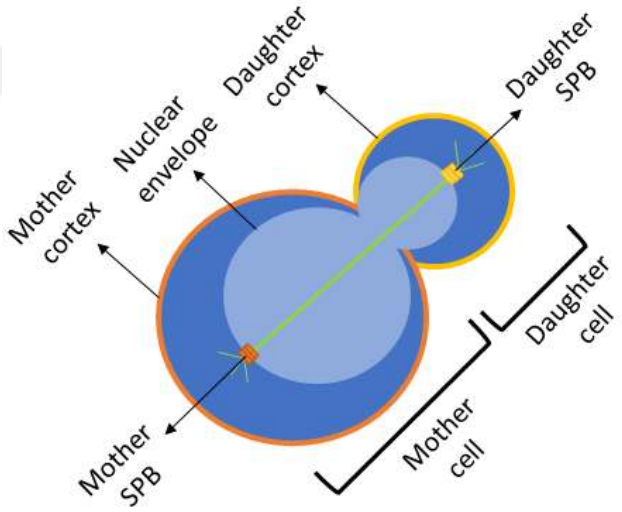

Figure 1.2: The basic structure of the the budding yeast.

Budding yeast undergoes closed mitosis; hence, nuclear envelop does not break down during mitosis. SPBs are located at the two opposite edges of nucleus to create the mitotic spindle. Mitotic spindle and astral microtubules are shown in green. Nuclear envelope is shown in light blue. SPBs are shown as three layers at the edges of the nuclear envelope. Mother SPB is shown in yellow and daughter SPB is shown in orange. The cortex of daughter cell is shown in yellow, whereas the mother cell cortex is shown in orange.

Spindle pole bodies consist of three main layers. These are (1) the outer plaque that faces the cytoplasm and the cytoplasmic microtubules, (2) central plaque that contains an electron dense region which is the site for construction of new SPB and (3) inner plaque that faces the nucleoplasm and the nuclear microtubules (Jaspersen and

Winey, 2004) (Figure 1.3). MEN components locate at the outer plaque of SPBs via the scaffold protein Nud1 (see Figure 1.5). SPBs act as signal amplifiers for MEN signaling (See *section 1.5*).

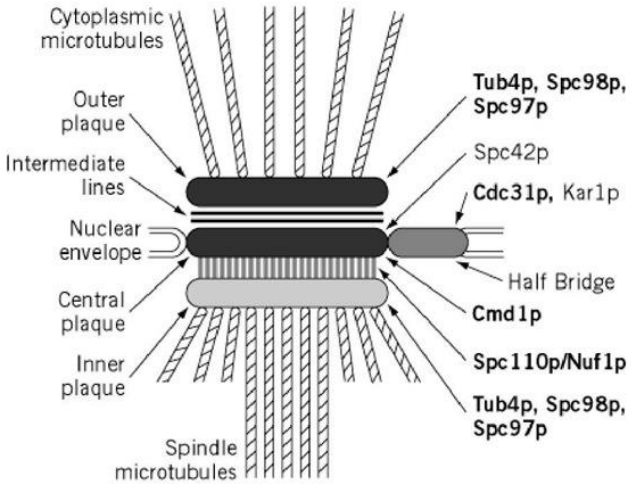

Figure 1.3: Diagram of the localizations of Spindle Pole Body components and the spindle pole microtubules.

The figure is adapted from Wigge, P.A. et al. The Journal of Cell Biology 14:967-977 (1998).

1.5 Mitotic Exit Network (MEN)

The MEN is a signaling pathway of budding yeast that promote cells to exit from mitosis in order for cells to complete a full cell cycle (Lee et al., 2001; Visintin et al., 1998; Visintin et al., 1999). The MEN cascade is analogous to Septation Initiation Network in fission yeast (Furge et al., 1999; Nurse et al., 1976; Schmidt et al., 1997) and the Hippo pathway in animals (Cai et al., 2009; Hao et al., 2008; Harvey et al., 2003; Justice et al., 1995; Kang et al., 2009; Oka et al., 2008; Tapon et al., 2002; Xu et al., 1995) (Figure 1.4).

The budding yeast MEN consists of several components: Tem1 which is a GTPase, Bfa1/Bub2 complex which works as a GAP (GTPase activating protein) for Tem1 protein, Lte1 as the putative GEF (guanine nucleotide exchange factor) and protein kinases Cdc5, Cdc15 and Dbf2 (with its associated factor Mob1) (Lee et al., 2001) and SPB protein Nud1 as a scaffold for MEN components (Gruneberg et al., 2000; Valerio-Santiago and Monje-Casas, 2011).

GTPase Tem1 is the most upstream element in MEN (Lee et al., 2001; Shou et al., 1999). It is likely active when it is bound to GTP (Shirayama et al., 1994b). Movement of a SPB into the daughter cell during early anaphase leads to the MEN GTPase Tem1 to accumulate at the dSPB. Tem1 localization on SPB is crucially important for activation of MEN, as well as SPB localization of Cdc5, Cdc15, Dbf2, and Mob1 (Rock and Amon, 2011). Not only Nud1 but also Spc72 and Cnm67 proteins have roles on localization of these proteins. It is also shown that Cdc5 phosphorylates Spc72 and Nud1 during its localization onto SPBs (Gruneberg et al., 2000; Knop and Schiebel, 1997).

The MEN pathway initiates with the activation of Tem1. When Tem1 is active, it associates with its downstream component Cdc15 and enables its accumulation around outer plaque of SPBs (Cenamor et al., 1999; Visintin and Amon, 2001). Also, Cdc5 and Cdc14 are thought to promote its accumulation at SPBs (Jaspersen and Morgan, 2000; Rock and Amon, 2011; Shirayama et al., 1998). Once at the SPB, Cdc15 kinase phosphorylates the MEN scaffold Nud1, creating a SPB docking site for Dbf2-Mob1 (Rock et al., 2013). SPB-localized Cdc15 phosphorylates Dbf2 and catalytically activates Dbf2-Mob1 complex, the most downstream component in MEN signaling (Cheng et al., 1998; Lee et al., 2001). Nuclear Dbf2-Mob1, then, drives the disassembly of Cdc14-Net1 complex by phosphorylating and blocking nuclear localization signal of Cdc14 (Mohl et al., 2009; Stoepel et al., 2005). In addition, it was suggested that Cdc5 activates Dbf2, probably via promoting FEAR induced Cdc14 activation (Lee et al., 2001; Visintin and Amon, 2001). Recently, it was shown that Dbf2-Mob1 drives the phosphorylation of both Net1 and Cdc14, to promote Cdc14 release (Zhou et al., 2020). Overall, Dbf2-Mob1 finishes Cdc14's full delivery into cytoplasm. Thus, Cdc14 could associate with its cytoplasmic CDK substrates to dephosphorylate them and converse CDK phosphorylation. (Caydasi et al., 2010a).

Two main actors are proposed to regulate the MEN at the level of its uppermost component Tem1: putative GEF (guanine-nucleotide exchange factor) Lte1 and two-component GAP complex. Lte1 is presumed to function as a GEF for Tem1, due to the presence of a GEF homology domain in Lte1 (Keng et al., 1994),. Lte1 is thought to increase the speed of the MEN signaling by converting GDP-bound Tem1 to GTP-bound Tem1, which enables Tem1 to transmit MEN signaling through MEN components (Bos et al., 2007). The requirement of Lte1 in low temperatures to achieve mitotic exit (Shirayama et al., 1994a) supports this hypothesis. However, the hypothesis is still not

proven, due to the lack of evidence for the *in vitro* GEF activity of Lte1 in the literature (Geymonat et al., 2009). Conversely, the GAP complex interrupts the MEN by inducing GTP hydrolysis of Tem1, thereby inactivating Tem1 (Fraschini et al., 2006; Geymonat et al., 2002). Whereas only Bub2 has the GAP-homology domain (Richardson and Zon, 1995), the presence of Bfa1 in the complex is required to inactivate Tem1. Cdc5 kinase hyperphosphorylates Bfa1 and thereby inactivates Bfa1/Bub2 GAP complex, to keep Tem1 active (Geymonat et al., 2003; Hu et al., 2001; Kim et al., 2012; Stegmeier and Amon, 2004).

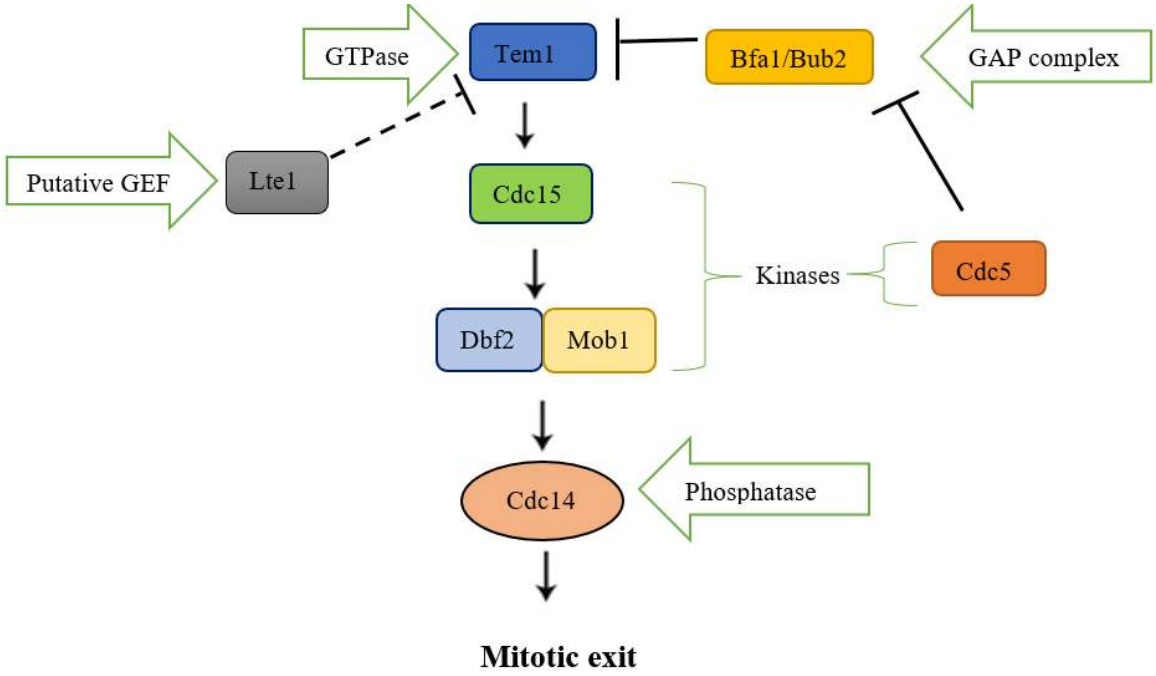

Figure 1.4: Mitotic exit network.

Dashed lines indicate uncertain interactions, whereas straight lines show certain interactions between components. The black arrows indicate the activation of the downstream components. The black lines ended in a small line perpendicularly indicate the inhibition lines for the downstream components.

1.6 Spindle Position Checkpoint (SPOC)

The mitotic spindle should be oriented along the mother to bud axis to faithfully segregate the chromosomes into the mother and daughter cells. Otherwise, chromosome segregation to the bud would fail and lead to multinucleation of the mother cell and anucleation of the daughter. Such divisions would drive aneuploidy and genomic instability.

A checkpoint called as Spindle Position Checkpoint (SPOC) senses the spindle misalignment and blocks mitotic exit until the anaphase spindle is properly positioned (Pereira et al., 2000; Wang et al., 2000; Yeh et al., 1995). SPOC components consist of Kin4 kinase, Bfa1/Bub2 GAP complex, Elm1 kinase, PP2A phosphatase with the regulatory subunit Rts1, 14-3-3 protein Bmh1 and cortical protein Lte1 (Figure 1.6).

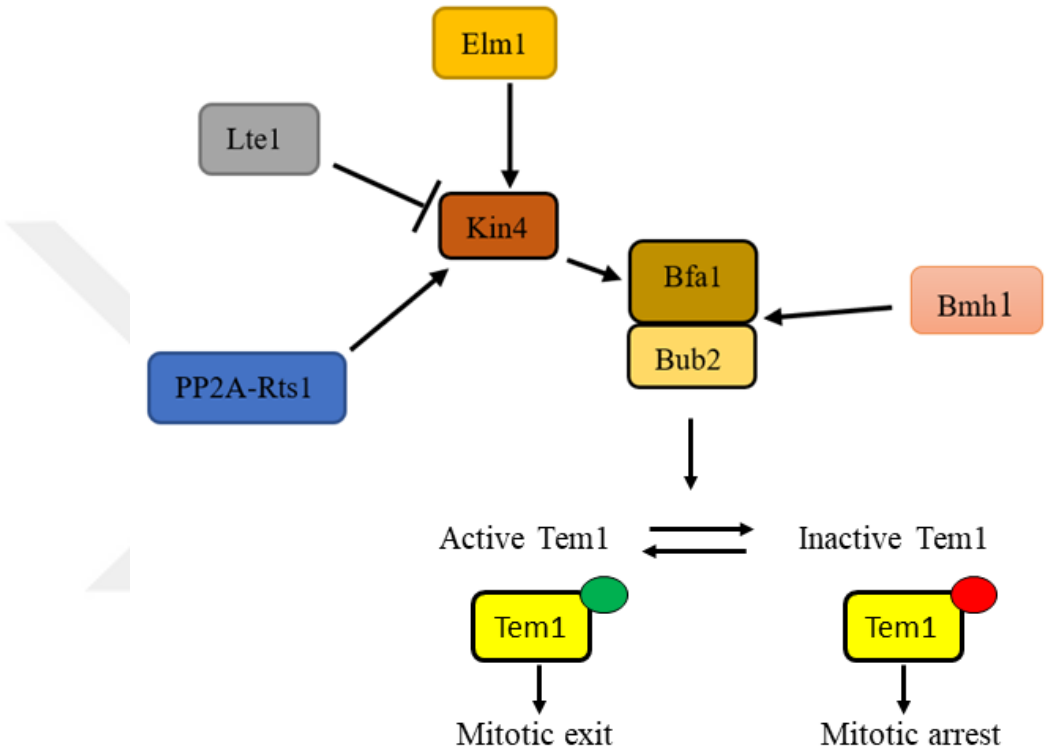

Figure 1.5: SPOC components and their interactions with each other.

Lte1, PP2A-Rts1 and Elm1 regulate Kin4 activity from different aspects (see the main text). Normally, GTP bound Tem1 (GTP shown in green) initiates MEN and lead to mitotic exit. However, when SPOC starts to act, active Kin4 phosphorylates Bfa1. In turn, Bfa1-Bub2 GAP complex accelerates the reaction for production of Tem1-GDP (GDP shown in red) and cause mitotic arrest. The black arrows indicate the activation of the downstream components. The black lines end in a perpendicular small line indicate the inhibition of the downstream components. Tem1 bound GTP is shown in green and Tem1 bound GTP is shown in red.

Mitotic spindle entrapment in the mother cell drives the mother cell cortex associated Kin4 to localize at both SPBs and therein to phosphorylate Bfa1 at two serine subunits (S150 and S180) (Maekawa et al., 2007). The activation and localization of Kin4 at the mother cell cortex and the mother SPB are regulated by at least two known regulators: Elm1 and PP2A phosphatase with Rts1 subunit (PP2A-Rts1).

Elm1 kinase is located at bud neck and phosphorylates mother cortex-localized Kin4 by means of from a threonine (T209) residue in its activation loop (T-loop), which

is the autoinhibitory site of Kin4. Hence, Elm1 phosphorylation prompts the complete initiation of Kin4. This phosphoregulation is needed for Kin4 kinase activity, whereas it does not have an effect for SPOC activation (Caydasi et al., 2010b).

PP2A-Rts1 complex is needed to direct the restriction of Kin4 localization to the mother cell cortex and the mother SPB. PP2A-Rts1 is essential for dephosphorylation of Kin4, as an immediate or roundabout regulator, which is thought to advance Kin4 confinement but not the kinase action (Chan and Amon, 2009).

Additionally, C-terminal region of Kin4 kinase was shown to be important in terms of both Kin4 localization. Kin4 that lacks the C-terminal is unable to localize at the mother cell cortex and to interact with the SPOC components (Chan and Amon, 2010). The daughter localized GEF Lte1, is a negative regulator of Kin4 which binds to Kin4 kinase and inhibits Kin4 activity (Bertazzi et al). Lte1 also prevents association of Kin4 with the dSPB (Bertazzi et al., 2011; Chan and Amon, 2010; Falk et al., 2011).

Other SPOC components, the 14-3-3 family protein Bmh1 acts downstream of Kin4 in the SPOC pathway. Briefly, Bmh1 binds Kin4 phosphorylated Bfa1 to affect Bfa1-Bub2 binding to SPBs (See section 1.7 for details).

1.7 Localization of MEN and SPOC components

Most MEN and SPOC components localize and accumulate at SPBs (Table 1.3) and this localization is essential for their function (Valerio-Santiago and Monje-Casas, 2011). Intriguingly, Bfa1, Bub2 and Tem1 have a bias towards the dSPB during an unperturbed anaphase (Pereira et al., 2002; Yoshida et al., 2002). Their localization at SPBs is asymmetric; mainly present at the dSPB and reduced or absent at the mSPB (Pereira et al., 2000) (Table 1.3). In cells lacking Bfa1, Bub2 or both, Tem1 fails to bind to SPBs until late anaphase, when a very faint Tem1 signal appears at SPBs (Caydasi et al., 2012; Pereira et al., 2000; Valerio-Santiago and Monje-Casas, 2011). Thus, SPB localization of Tem1 mainly relies on Bfa1/Bub2 (Caydasi et al., 2012; Pereira et al., 2000; Valerio-Santiago and Monje-Casas, 2011). Kin4 localizes to the mother cell cortex during the cell cycle and to the mSPB during anaphase (D'Aquino et al., 2005) with binding to SPBs via Spc72 (Maekawa et al., 2007) (Table 1.3). Only minute amount of Kin4 would associate with daughter cell. It is hypothesized that the activation of Tem1 could be conceivable only when the Tem1-bearing SPB relocates to the daughter cell (Bardin et al., 2000; Chan

and Amon, 2010; Pereira et al., 2000). In any case, in spindle misalignment, both the MEN and SPOC elements entrapped inside the mother cell, which permits Kin4 to connect with Bfa1/Bub2 to hinder inhibitory phosphorylation of Cdc5 on Bfa1 (Geymonat et al., 2003; Gryaznova et al., 2016) (see Table 1.3). In this fashion, Bfa1/Bub2 complex become catalytically active to function as a GAP for Tem1, which defers mitotic exit and causes mitotic arrest until the spindle is properly oriented (Gryaznova et al., 2016; Kim et al., 2012) (see Table 1.3 and Figure 1.5).

When the spindle is misaligned, in contrast, Kin4 starts to localize at both SPBs which makes Bfa1/Bub2 GAP complex reachable for it to phosphorylate them (Maekawa et al., 2007). However, Kin4 alone is unable to disrupt asymmetric localization of GAP complex at SPBs. Phosphorylation of Bfa1 by Kin4 creates a docking site on Bfa1 for the 14-3-3 family protein Bmh1 to weaken the Bfa1–SPB binding (Caydasi et al., 2014) and causes Bfa1 to move away from Spc72 where Bfa1 normally localizes nearby (Gryaznova et al., 2016). Thus, the interaction of Bfa1/Bub2 complex with the dSPB becomes loose, which leads to Bfa1/Bub2 (Pereira et al., 2000) and also Tem1 (Molk et al., 2004) release from SPBs and distribution into cytoplasm (Caydasi and Pereira, 2009). In this way, Cdc5 is not able to hyper-phosphorylate Bfa1, which leads to Tem1 inactivation through the GAP activity of Bfa1/Bub2 (Caydasi and Pereira, 2009).

Table 1.3: The localization of MEN and SPOC components in mitotic exit.

	LOCALIZATION OF THE COMPONENTS	
	NORMAL SPINDLE	**MISALIGNED SPINDLE**
Tem1	mainly at dSPB[1,8]	both SPBs – lower levels [2]
Lte1	the bud cell cortex[1]	the bud cortex[1,2]
Bfa1/Bub2	mainly at dSPB[2]	both SPBs – lower levels [2]
Cdc5	both SPBs[3] also bud neck in the telophase[4]	both SPBs[10]
Cdc15	both SPBs in anaphase[5] also bud neck in the telophase[8]	both SPBs – lower levels [12]
Dbf2/Mob1	both SPBs in anaphase[6,7] also bud neck in the telophase[6,7]	both SPBs – lower levels [12]
Kin4	Mother cell cortex and mSPB[9]	Mother cell cortex and both SPBs[9]

Elm1	Around bud neck[13]	Around bud neck[13]
Rts1	Cell periphery and cytoplasm[14]	Cell periphery and cytoplasm[14]
Bmh1	Cytoplasm[15]	Cytoplasm[15]
Cdc14	nucleolus (early anaphase), nucleus (later anaphase) and cytoplasm (telophase) [16]	nucleolus and nucleus[16,17]

[1]Bardin et al., 2000, [2]Pereira G., 2000, [3]Hu et al., 2001. [4]Song et al., 2000. [5]Xu et al., 2000. [6]Frenz et al., 2000. [7]Luca et al., 2001. [8]Molk et al., 2004. [9]Pereira et al., 2005. [10]Maekawa et al., 2007. [11]Caydasi et al., 2009. [12]Caydasi et al., 2017. [13]Aparna et al., 1999. [14]Gentry et al., 2002. [15]Caydasi et al., 2014. [16]Shou et al., 1999. [17]Jaspersen et al., 1998.

Chapter 2:

REVEALING A NOVEL MITOTIC EXIT REGULATOR THROUGH A DOSAGE SUPPRESOR GENETIC SCREEN

Aim of the thesis

Mitotic exit is the cell cycle stage in which the cell transits from M phase to a new G1 phase. While mitosis is under control of CDKs, mitotic exit depends on the inactivation of CDKs (Cdc28 in budding yeast), the turnover of mitotic cyclins and the removal of phosphorylation from CDK targets, such as Swi5 and Cdh1 (see Chapter 1). The time-wise coordination of these events in mitotic exit is important to avoid severe outcomes, such as genetic instability, aneuploidy, or cell death.

Our goal is to find out novel regulators in the process of mitotic exit. Preliminary data from our lab identified a novel temperature sensitive mutant that allowed mitotic exit of budding yeast cells that were otherwise arrested in telophase. This data suggests that the corresponding temperature sensitive gene has a potential role in mitotic exit inhibition. The aim of this thesis is to validate the preliminary data which indicates a novel mitotic exit regulatory mechanism and to illuminate the molecular mechanisms behind this regulation. For this, we **(1)** employed a dosage suppressor screen, **(2)** validated the results of the screen, **(3)** analyzed genetic interactions between the hits and known mitotic exit proteins and **(4)** performed preliminary functional characterization of one of the hits.

Results and Discussion

rkt1-1 rescues the lethality of Gal1-*KIN4*

The production of Kin4 at high doses is lethal for cells as it constitutively activates the Bfa1/Bub2 GAP complex (D'Aquino et.al., 2005) (Figure 2.1, row 1, Raf/Gal plates, all temperatures). Bfa1/Bub2 inhibits the MEN by inhibiting the GTPase Tem1 and hence its constitutive activation prevents mitotic exit. As a consequence, deletion of mitotic exit inhibiting genes such as *BFA1* or *BUB2*, allows growth of Kin4 overexpressing cells (Figure 2.1, row 2, Raf/Gal plates, all temperatures). We identified a yeast temperature sensitive mutant that rescues the lethality of Gal1-Kin4 overexpression (Figure 2.1, row 3, Raf/Gal plates, 30^{o}C). Through whole genome sequencing we identified the mutated

gene and found that it contains a premature stop codon. We prefer not to reveal the real identity of the gene here. We will rather refer to this gene as *RKT1* (Rescues Kin4 Toxicity) and the corresponding mutant as *rkt1-1*. This data indicates that the decrease in functionality of *rkt1-1* at the semi permissive temperature leads to the exit from mitosis of the cells arrested in telophase.

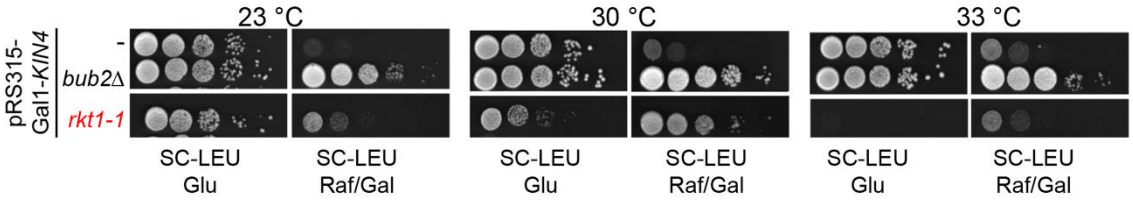

Figure 2.1: *rkt1-1* is able to rescue Kin4 overexpression-based lethality.

Serial dilutions of Gal1-*KIN4* bearing WT (-), *bub2*Δ or the temperature sensitive *rkt1-1* cultures were dropped on Glucose containing (Glu) or Raffinose and galactose containing (Raf/Gal) agar plates. Raf/Gal plates allow Gal1-*KIN4* overexpression. Gal1-*KIN4* is presented on a *LEU2*-based centromeric plasmid (pRS315-Gal1-*KIN4*), thus cells were grown on Leucine lacking synthetic medium (SC-LEU). Note that 33°C is the restrictive temperature for the *rkt1-1*, while 30°C is semi permissive (Table 2.1).

Table 2.1: Growth comparison of wild type and *rkt1-1* cells at different temperatures.

	Wild type	***rkt1-1***
23°C	(+++)[1]	(+++)[1]
30°C	(+++)[1]	(++)[2]
33°C	(+++)[1]	(-)[3]
35°C	(+++)[1]	(-)[3]
37°C	(+++)[1]	(-)[3]

[1] maximum growth. [2] moderate growth. [3] no growth.

2.1 Construction of a stable background strain to be used in the dosage suppressor genetic screen

In the aforementioned data (Figure 2.1), Kin4 overexpression is achieved by a Gal1-*KIN4* expressing centromeric plasmid that was introduced in the cells. We next constructed strains in which Gal1-*KIN4* was stably integrated into the yeast genome.

For this, first, a Gal-*KIN4* containing integration plasmid (pRS305-Gal1-*KIN4*) was constructed and this plasmid was restricted from the promoter region of the *URA3* gene and transformed into *WT* and *rkt1-1* strains. Restriction at the *URA3* locus creates plasmid ends that are homologous to the *URA3* locus on the chromosome and thus allows insertion of the plasmid into this locus after homologous recombination events.

Importantly, integration plasmids typically lack their yeast replication origin, therefore they cannot propagate in the cell unless they are integrated into the genome (Chan and Tye, 1980; Orr-Weaver et al., 1981). Transformants were selected on SC-URA medium that selects for the integration plasmid marker. Kin4 overexpression in these strains were confirmed by Western blotting using anti-Kin4 antibodies (Figure 2.2A). The obtained strains were also tested via colony growth tests (Figure 2.2B). Consistent with our previous observation (Figure 2.1), *rkt1-1* rescued the lethality caused by Kin4 overexpression at 30°C and to some extend at 23°C (Figure 2.2B).

We next analyzed the morphology of Kin4 overexpressing WT and *rkt1-1* cells. Cells overexpressing Kin4 arrest in telophase which is marked with accumulation of cells with separated nuclei (D'Aquino et al., 2005) (Figure 2.2C). As the arrest is prolonged these cells start emerging a new daughter cell on the top of the previous daughter cells forming chains of cell bodies without undergoing mitotic exit (Figure 2.2C-2.2D). We analyzed the effect of *rkt1-1* on this phenotype (Figure 2.2C-D). *rkt1-1* neither formed chained cells nor accumulated cells with separated nuclei (Figure 2.2 C-D). These results are in line with our previous conclusion that *RKT1* regulates mitotic exit in a negative manner.

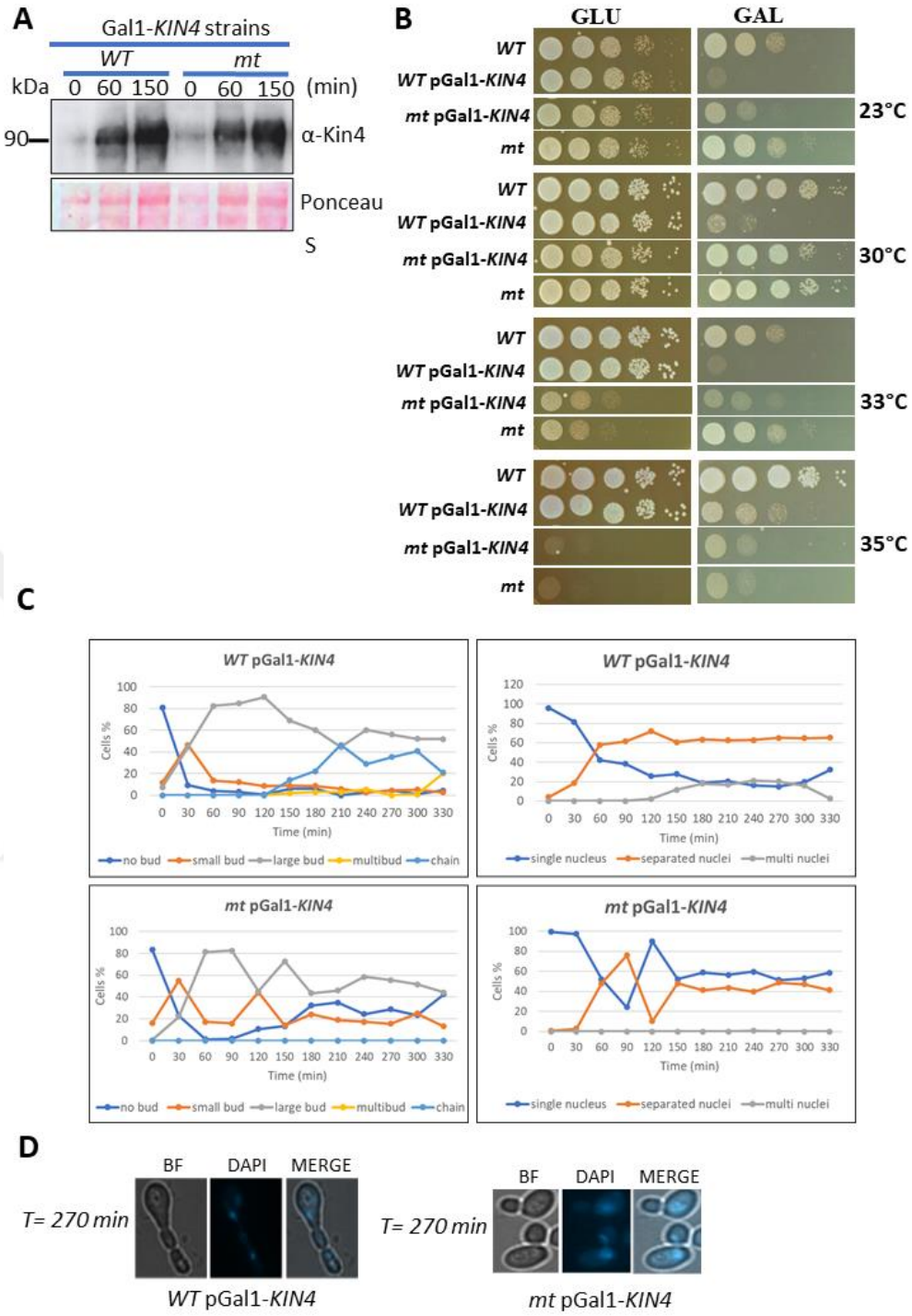

Figure 2.2: *rkt1-1* rescues Kin4 overexpression lethality

A) Comparison of Kin4 overexpression levels in *RKT1* (*WT)* Gal1-*KIN4* and *rkt1-1* Gal1-*KIN4* cells. WT: *RKT1*, mt: *rkt1-1*. Stationary phase liquid cultures of BSY007 (WT Gal1-*KIN4*) and BSY008 (*rkt1-1* Gal1-*KIN4*) grown in YP-RAF medium at 23°C until to log phase and Galactose (%2) was added to cultures to induce Kin4 overexpression (t=0). Samples are collected in every 30 min and analyzed in Western blot with anti-Kin4 antibodies. Ponceau S was shown as a loading control.

B) *rkt1-1* is able to rescue Kin4 overexpression-based lethality sourced from pGal1-*KIN4***.** BSY007 (*WT* pGal1-*KIN4*) and BSY008 (mt pGal1-*KIN4*) liquid cultures grown in YP-Raf medium until stationary phase and 10-fold serial dilutions of the indicated strains were spotted onto glucose (GLU) and raffinose/galactose (GAL) containing plates. Note that Kin4 overexpression is achieved on GAL plates. Plates were incubated at 23°C, 30°C, 33°C or 35°C.

C) *rkt1-1* leads to a decrease in anaphase arrested cells and prevents chain phenotype upon Kin4 overexpression. In the experiment explained in Figure 2.2A, ethanol fixated samples were also collected in every 30 min and cell cycle

progression was analyzed through microscopy. Budding index (left) and mitotic index (right) was calculated after DAPI staining of the nucleus. Note the accumulation of large budded (grey line, left top graph) and chained (blue line, left top graph) cells and cells in telophase (separated nuclei, orange line, right top graph) in the *WT* Gal1-Kin4 but not in the *mt* Gal1-Kin4 (bottom left and right graphs). At least 100 cells were count for each sample at each time point.
D) *rkt1-1* converts chain phenotype to normal phenotype. As a part of the experiment explained in Figure 2.2A, representative images of cells are shown for *RKT1* Gal1-*KIN4* and *rkt1-1* Gal1-*KIN4,* after 4,5 hours of Kin4 overexpression via galactose induction. (BF: bright field)

2.2 Dosage suppressor genetic screen to find the hits that revert rkt1-1 Gal1-KIN4 rescue phenotype

The dosage suppressor genetic screening was performed using a YEplac181-based multicopy (2-micron) yeast genomic library (Maier et al., 2008) (Gift from Prof. Dr. Michael Knop). Briefly, the *rkt1-1* Gal1-*KIN4* strain was transformed with the library to obtain enough number of transformant that allows coverage of the yeast genome 3-times (See materials methods for details). All transformants were replica plated onto glucose and galactose plates and their growth at 30ºC were compared (Figure 2.3A). The colonies that grow less on galactose-containing plates were selected for the further assessment. Initially, we started around 23.000 transformants which went down to 1185 by the first galactose-based selection (replica plating- see Figure 2.3B). After that, the transformants were individually transferred onto galactose plates and the growth phenotypes were carefully compared. This second selection reduced the number of colonies that poorly grows on galactose containing plates to 370 colonies (Figure 2.3B). 2-micron plasmids were purified from these 370 colonies. Then, purified plasmids were transformed into *E. coli*. 3 colonies were selected from each *E. coli* transformation for amplification of each plasmid. These plasmids were run on agarose gels to observe whether plasmids from the 3 colonies are identical (Appendix C) and one representative from each 370 plasmid were transformed back into the starting strain *rkt1-1* Gal1-*KIN4*. Using colony formation tests, 6 plasmids were confirmed to cause growth sickness on galactose-containing plates (Figure 2.3C-D). These 6 plasmids were sequenced. The insert fragments inside the plasmids are displayed in Table 2.2 and in Appendix D.

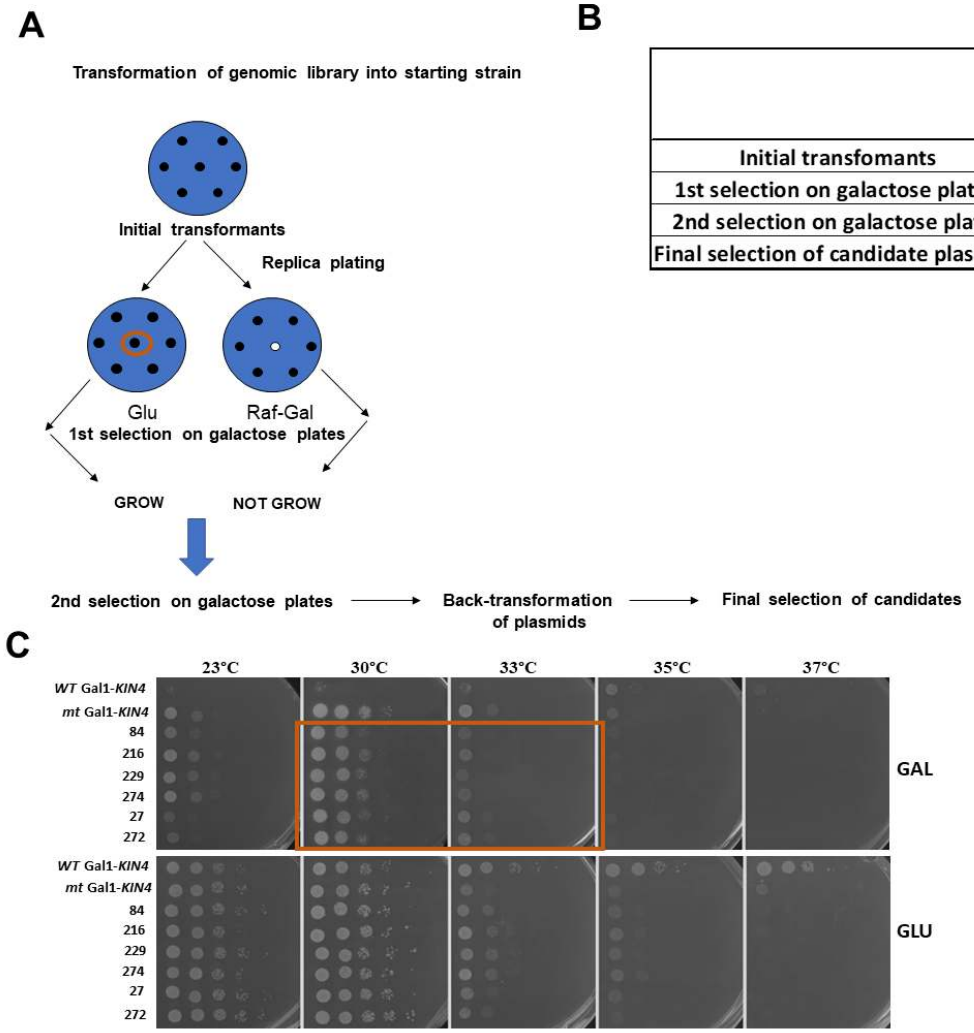

Figure 2.3: A dossage suppressor screen identifies genes that causes lethality of *rkt1-1* Gal1-*KIN4* on galactose plates

A) Schematic outline of the screening strategy. See text for details.
B) Screening results in numbers. See text for details.
C) Drop test showing the growth lethality phenotype of the 6 plasmids (indicated with the numbers 84, 216, 229, 274, 27, 272) that were identified as hits of the screen. GAL: Sc-Leu plates with raffinose galactose as carbon source; GLU: Sc-Leu plates with glucose as carbon source. Compare the growth of drops in the red box with the growth of mt Gal1-Kin4 (second row from the top). The synthetic sickness and lethality phenotype is seen at 30°C and 33°C respectively. WT: *RKT1*, mt: *rkt1-1*

Table 2.2: Chromosomal fragments contained in the plasmid hits

PLASMID	CHROMOSOME #	LOCATION (BP)	COVERED GENES
27	CHR IV	271.425 - 273.190	*PHO2* and *NSE4*
84	CHR IV	741.410 - 748.079	*SAN1, MKC7* and *TAF12*
216	CHR IV	741.135 - 744. 727	*SAN1*

229	CHR IV	741.135 - 744. 727	*SAN1*
272	CHR IV	271.429 - 273. 192	*PHO2* and *NSE4*
274	CHR IV	741.135 - 744.725	*SAN1*

Importantly these 6 plasmids contained common genes. The common gene in the inserts of plasmids numbered 84, 216, 229 and 274 is *SAN1* which is a nuclear ubiquitin ligase (Table 2.2). Plasmids numbered 27 and 272 possess two genes which both lack their C-termini: *NSE4* (component of the SMC5-SMC6 complex) and *PHO2* (homeobox transcription factor in phosphate metabolism).

2.3 Whereas PHO2 and SAN1 overexpression cause sickness, NSE4 overexpression does not affect the growth pattern of rkt1-1 Gal1-KIN4

As in the case of *SAN1* containing plasmids (84, 216, 229 and 274), single gene was present in majority of them, thus it was evident that the observed genetic interaction was due to *SAN1*. However, two linked genes were present in the remaining plasmids and in order to find the gene responsible for dosage suppressor we cloned individual genes in multicopy plasmids (see materials and methods). Using these plasmids, we analyzed the effect of individual genes' overexpression to the growth of *rkt1-1* Gal1-*KIN4* (Figure 2.4). *PHO2* overexpression led to sickness, whereas *NSE4* overexpression did not influence the growth of *rkt1-1* Gal1-*KIN4* cells on galactose containing plates (Figure 2.4A-B). As expected, the overexpression of *SAN1* caused sickness of *rkt1-1* Gal1-*KIN4* cells on galactose containing plates. Importantly, *SAN1* overexpression phenotype was more apparent than that of *PHO2* overexpression (Figure 2.4C vs Figure 2.4B).

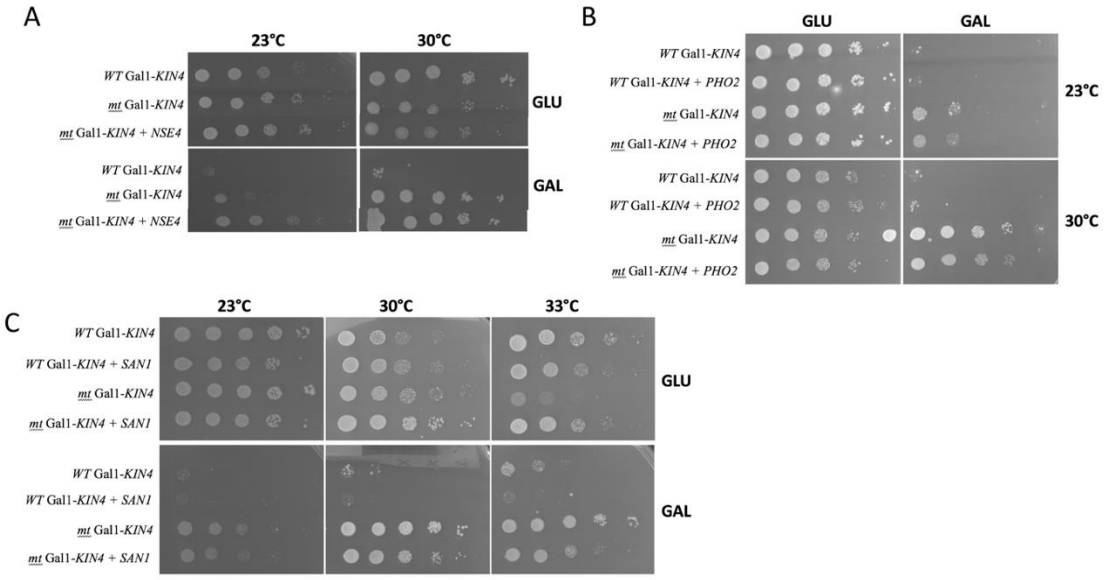

Figure 2.4: Analysis of individual gene overexpression.

Liquid cultures of indicates strains were grown in media lacking leucine (SC-Leu Raf) until stationary phase and 10-fold serial dilutions were spotted onto SC-LEU containing glucose (GLU) and SC-LEU containing raffinose and galactose (GAL) as carbon sources and then grown at indicated temperatures. *WT* Gal1-*KIN4*: BSY007 (*RKT1* pGal1-KIN4), *mt* Gal1 *KIN4*: BSY008 (*rkt1-1* pGal1-*KIN4.* Cells contain pRS425 (LEU-based 2µ) plasmid or single gene bearing pRS425 plasmid. The gene name is indicated as + *NSE1* in A, + *PHO2* in B, or + *SAN1* in C.
A) Nse4 overexpression does not have an effect on the growth of *rkt1-1 pGal1-KIN4.*
B) Pho2 overexpression leads to a slight sickness on *rkt1-1 pGal1-KIN4.*

2.4 Epistatic analysis of candidate genes

First we asked whether multicopy expression of *SAN1* or *PHO2* caused any growth defects in wild type cells (Figure 2.5A). Neither of the plasmids caused severe growth defects, however multicopy *SAN1* caused a slight growth retardation at 37 °C (Figure 2.4A). Then we analyzed the effect of multicopy *SAN1* or *PHO2* on temperature sensitivity of the *rkt1-1* mutant (Figure 2.5B). Indeed, multicopy *SAN1* but not *PHO2* was able to rescue *rkt1-1* temperature sensitivity. This suggest a function for SAN1 directly in *RKT1* pathway.

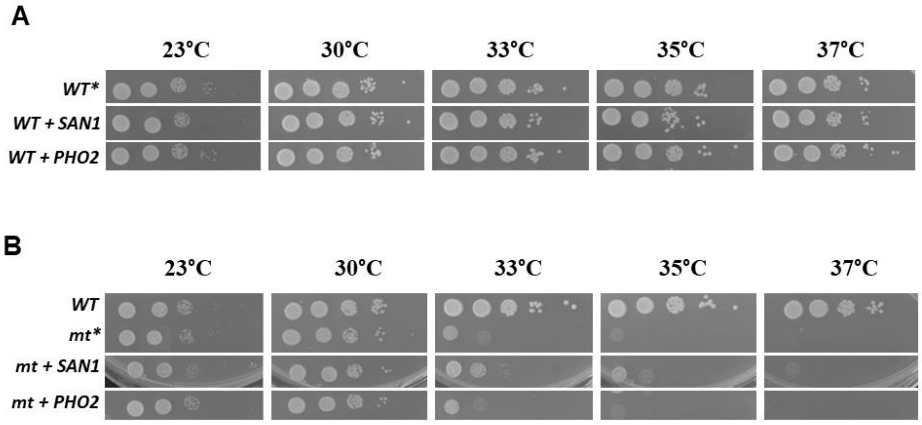

Figure 2.5: Affect of multi-copy *SAN1* and *PHO2* on growth of *WT* and *rkt1-1* strains.

Liquid cultures of indicated strains were grown in media lacking leucine (SC-Leu) until stationary phase and 10-fold serial dilutions were spotted onto SC-LEU. *WT*: BY4741; mt (*rkt1-1*): Y06322. Cells contain pRS425 (LEU-based 2μ) plasmid or single gene bearing pRS425 plasmid. The gene names are indicated as + *PHO2* or + *SAN1*.
A) Multi-copy *SAN1* or *PHO2* does not influence the growth of WT cells.
B) Multi-copy *SAN1* but not *PHO2* rescues temperature sensitivity of mt rkt1-1.
.

Our genetic screen placed *SAN1* and *PHO2* in a pathway that prevents mitotic exit. According to this conclusion, these genes' overexpression in temperature sensitive mutants of the MEN (MEN-ts) are expected to cause synthetic growth defects. We analyzed the influence of *SAN1* and *PHO2* on MEN-ts mutants. As a result, we encountered distinct patterns of growth in different MEN mutants (Figure 2.6). A summary of these interactions is presented in Table 2.3. Briefly, multicopy *SAN1* resulted in synthetic growth defect in the *cdc14-2* and *cdc5-10* mutants, whereas multicopy *PHO2* caused growth defects in *cdc15-10* and *dbf2-2* mutants (Figure 2.6). These synthetic genetic interactions are in line with our conclusion that *SAN1* and *PHO2* are mitotic exit inhibitors. Controversially, we observed that multicopy *SAN1* rescued the growth of *cdc15-1* mutant (Figure 2.6B). This result may indicate an additional role of *SAN1* that becomes essential in this mutant.

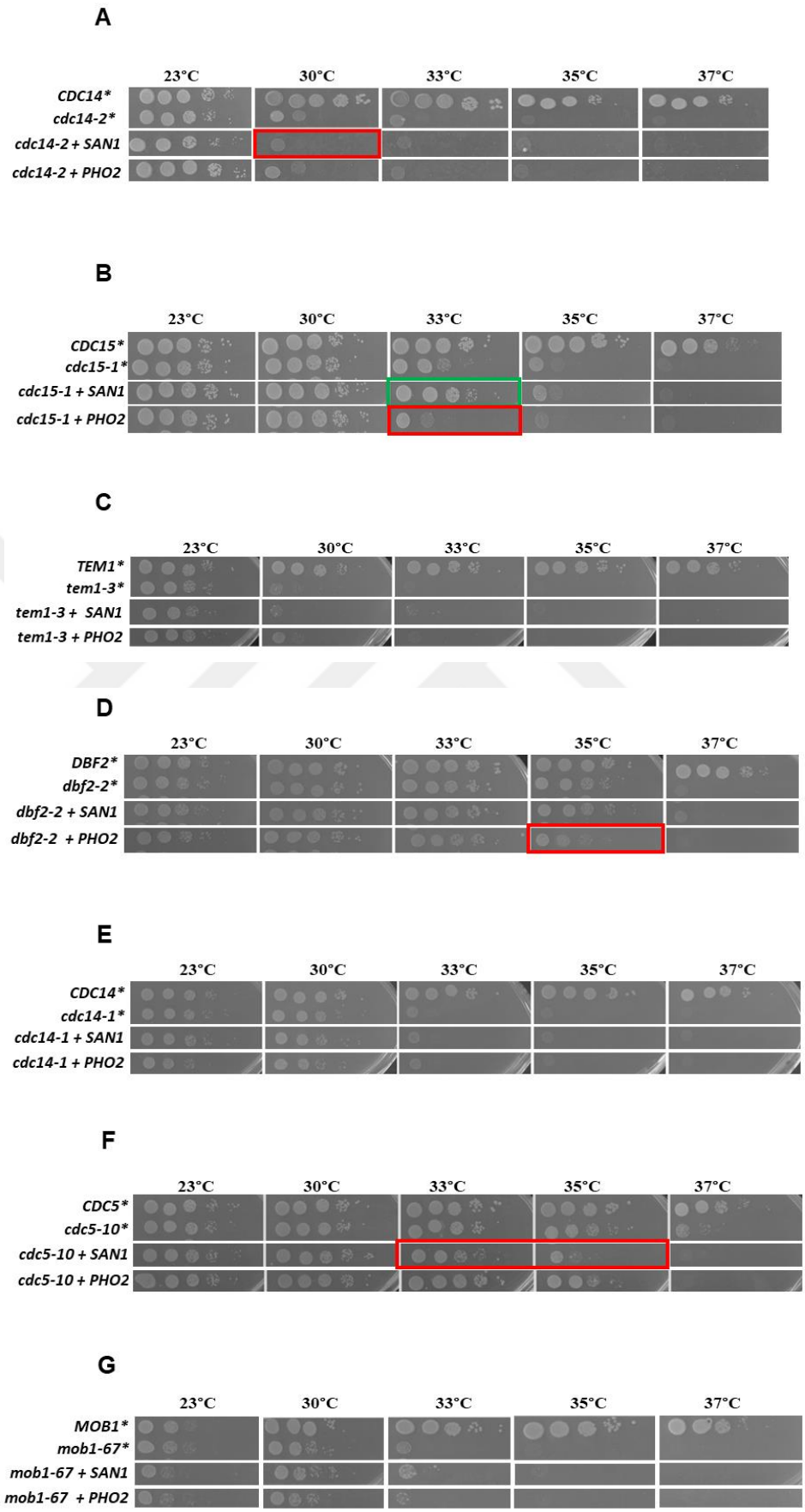
A
23°C
30°C
33°C
35°C
37°C
CDC14*
cdc14-2*
cdc14-2 + SAN1
cdc14-2 + PHO2
B
23°C
30°C
33°C
35°C
37°C
CDC15*
cdc15-1*
cdc15-1 + SAN1
cdc15-1 + PHO2
C
23°C
30°C
33°C
35°C
37°C
TEM1*
tem1-3*
tem1-3 + SAN1
tem1-3 + PHO2
D
23°C
30°C
33°C
35°C
37°C
DBF2*
dbf2-2*
dbf2-2 + SAN1
dbf2-2 + PHO2
E
23°C
30°C
33°C
35°C
37°C
CDC14*
cdc14-1*
cdc14-1 + SAN1
cdc14-1 + PHO2
F
23°C
30°C
33°C
35°C
37°C
CDC5*
cdc5-10*
cdc5-10 + SAN1
cdc5-10 + PHO2
G
23°C
30°C
33°C
35°C
37°C
MOB1*
mob1-67*
mob1-67 + SAN1
mob1-67 + PHO2

Figure 2.6: Multi-copy expression of *SAN1* and *PHO2* exhibit genetic interactions with MEN-ts mutants.

A-G) Different plasmids affect temperature sensitive (ts) allele of Mitotic Exit Network (MEN) component-bearing mutants, differently. Strains with asterisks (*) shows empty plasmid (pRS315, LEU2-base) transformed strains. Liquid cultures of wild type strain (YPH499) with empty plasmid (*) and indicated ts mutants with the empty plasmid (*) or *SAN1* bearing *(+ SAN1)* and *PHO2* bearing *(+ PHO2)* YEplac181plasmid were grown in media lacking leucine (SC-Leu) until stationary phase and 10-fold serial dilutions were spotted onto SC-LEU glucose plates and the plates were incubated at 23°C, 30°C, 33°C, 35°C or 37°C. The growth differences were indicated with green (rescue) and red (sickness/lethality) rectangles around relevant drops. To note, all 6 hit plasmids were tested using colony formation test. Here, one representative for each set was shown for simplicity. (ESM1249-1: YPH499 *tem1-3;* ESM1276-1: YPH499 *cdc14-2*; ESM1278-1: YPH499 *cdc15-1*; CVY16-1: YPH499 *cdc14-1*; ESM1309-1: YPH499 *dbf2-2*; ESM1361-1: YPH499 *mob1-67*; CLY169-2: YPH499 *cdc5-10.* All strains are of YPH499 origin.

Table 2.3: The summary of possible interactions of the genes inside selected plasmids with indicated MEN components, using the data from colony formation assays.

Plasmid no	Genes inside the plasmids	*cdc14-2*	*cdc15-1*	*cdc5-10*	*mob1-67*	*dbf2-2*
84, 216, 229, 274	*SAN1*					
27, 272	*NSE4, PHO2*					

(Dark green: synthetic rescue; red: synthetic sickness/synthetic lethality).

Our genetic screen identified genes, whose multi copy expression caused lethality of *rkt1-1* Gal1-*KIN4* cells on galactose plates. We next asked whether the same genes' multi copy overexpression causes lethality of *bub2*Δ Gal1-*KIN4, bfa1*Δ Gal1-*KIN4* or *rts1*Δ Gal1-*KIN4* cells on galactose plates. Bfa1, Bub2 and Rts1 are components of the spindle position checkpoint (SPOC) and their deletion rescues lethality of Kin4 overexpression, as does *rkt1-1*. So, we reasoned that if plasmids identified in our screen cause lethality in *bub2*Δ Gal1-*KIN4*, *bfa1*Δ Gal1-*KIN4* and *rts1*Δ Gal1-*KIN4* strain backgrounds upon Kin4 overexpression, the genes on the plasmids may participate in a pathway that inhibit mitotic exit independently of the SPOC or MEN. However, little or no differences were observed in the growth of *Δbfa1* Gal1-*KIN4, Δbub2* Gal1-*KIN4* and *Δrts1* Gal1-*KIN4* strains after transformation with *SAN1*-bearing and *PHO2*-bearing 2-micron plasmids (Figure 2.7).

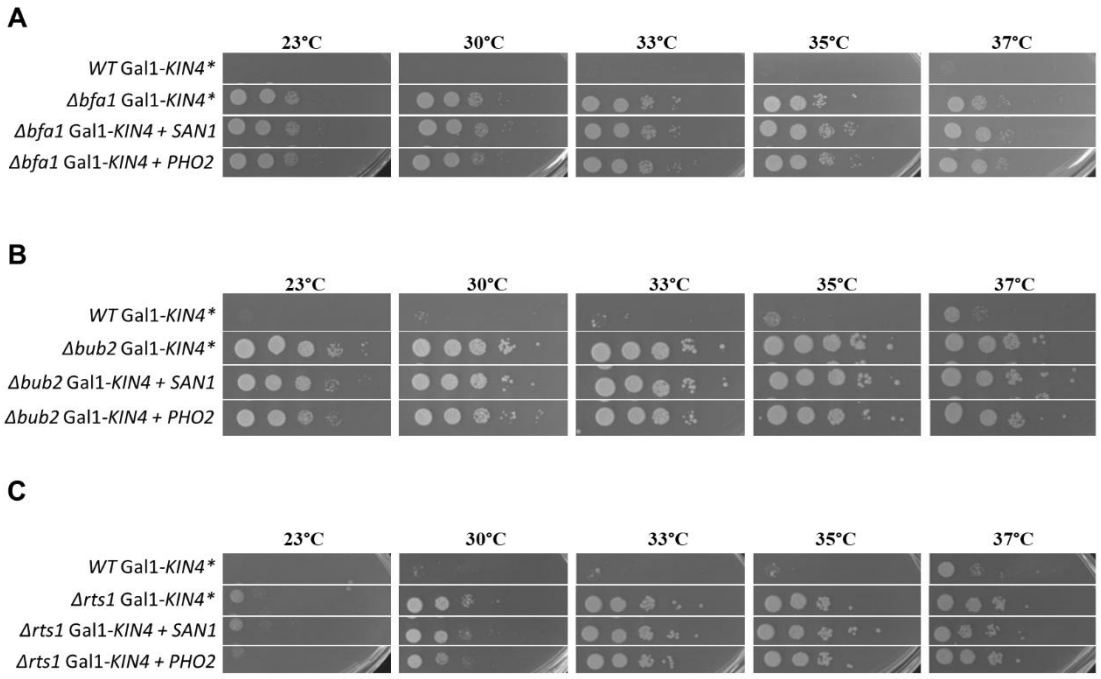

Figure 2.7: Multi-copy expression of *SAN1* and *PHO2* does not cause lethality on SPOC deficient cells overexpressing Kin4.

A-C) Liquid cultures of wild type strain with Gal1-*KIN4* (UJY011: *WT* Gal1-*KIN4*) with the empty plasmid (PRS315), null mutants (UJY013-1: UJY011 *Δbfa1*; UJY014-1: UJY011 *Δbub2*; UJY016-1: UJY011 *Δrts1*) with empty plasmid (PRS315) and, the indicated null mutants bearing *SAN1* (#274) or *PHO2* (#272) plasmids were grown in the raffinose-containing, leucine-lacking media (SC-Leu Raf) until stationary phase and 10-fold serial dilutions were spotted onto SC-LEU Glucose and SC-LEU Galactose plates and the plates were grown at 23°C, 30°C, 33°C, 35°C or 37°C. The strains with asterisk (*) showed the empty plasmid bearing strains. Only galactose plates were shown in the figure, for simplicity.

Taken together, our results indicate that San1 and Pho2 may have a function in regulating mitotic exit. Owing to the importance of protein degradation for mitotic exit and due to representing more possible interactions with MEN components, from this point on, we focused our analysis to San1, which is a nuclear E3 ubiquitin ligase.

Chapter 3:
SAN1 PROTEIN AS A HIT FROM GENETIC SCREENING

3.1 San1 Structure and Function

San1 is a E3 ubiquitin ligase (Dasgupta et al., 2004), which mainly acts on nuclear misfolded / aberrantly folded proteins to achieve their ubiquitin mediated proteasomal degradation (Gardner et al., 2005).

In nucleus, San1-mediated ubiquitin-dependent proteasomal degradation mechanism takes place as follows: Ubiquitin is transferred from E1 ubiquitin-activating enzyme (Uba1) to E2 ubiquitin conjugating enzyme (Ubc1-sometimes Cdc34) (Gardner et al., 2005). Via its RING domain (see figure 3.1), San1 attaches to charged E2 ubiquitin conjugated enzyme (Rosenbaum et al., 2011) (Figure 3.2). The E3 ubiquitin ligase San1 also directly recognizes the nuclear aberrant proteins and catalyzes the transfer of the ubiquitin from E2 ubiquitin conjugating enzyme-ubiquitin complex to the substrate (Gardner et al., 2005) (Figure 3.2). Repetitive reactions lead to the formation of the polyubiquitylated substrates which enables 26S proteasome to recognize these misfolded substrates and to degrade them into aminoacids and single ubiquitin proteins (Figure 3.2 and Figure 3.3).

Figure 3.1: Simplified figure of the domains of San1 protein.

The figure was taken from Fredrickson et al., 2012. Means of self-preservation: how an intrinsically disordered ubiquitin-protein ligase averts self-destruction (N-term: N-terminal, C-term: C-terminal, RING: Really Interesting New Gene).

Biochemical analysis has shown that San1 has a highly disordered structure located at both sides of its RING domain that gives San1 a great flexibility in recognizing its substrates (Rosenbaum et al., 2011) The affinity of San1 to hydrophobic substrates was found to be much greater than the affinity to hydrophilic ones and this exposed hydrophobicity degree was correlated with the substrate insolubility (Fredrickson et al., 2013). Thus, San1 targets proteins that are prone to aggregation.

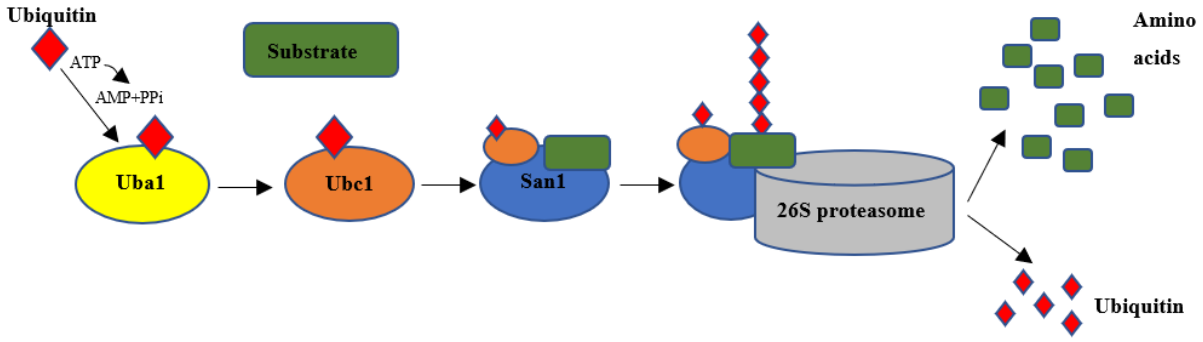

Figure 3.2: San1-based proteasomal pathway.

The figure is modified from Chen et al. (2013) Plant E3 Ligases: Flexible Enzymes in a Sessile World.

The localization of San1 is restricted to the nucleus and this localization is crucial for its activity on its substrates (Gardner et al., 2005; Prasad et al., 2010). Whereas San1 is a nuclear localized E3 ligase (Gardner et al., 2005), it was shown to be selectively polyubiquitylate misfolded substrates from cytoplasm, after their transfer to nucleus (Prasad et al., 2010). Recently, San1 is implicated in the degradation of outer mitochondrial membrane proteins, as well (Metzger et al., 2020). San1 uses the Hsp70 and the Hsp40 chaperone proteins for nuclear import of its cytosolic and mitochondrial substrates (Metzger et al., 2020; Prasad et al., 2010) Hsp110 chaperone also assists trafficking of the misfolded substrates that lack a nuclear localization sequence (Prasad et al., 2018) (see figure 3.3).

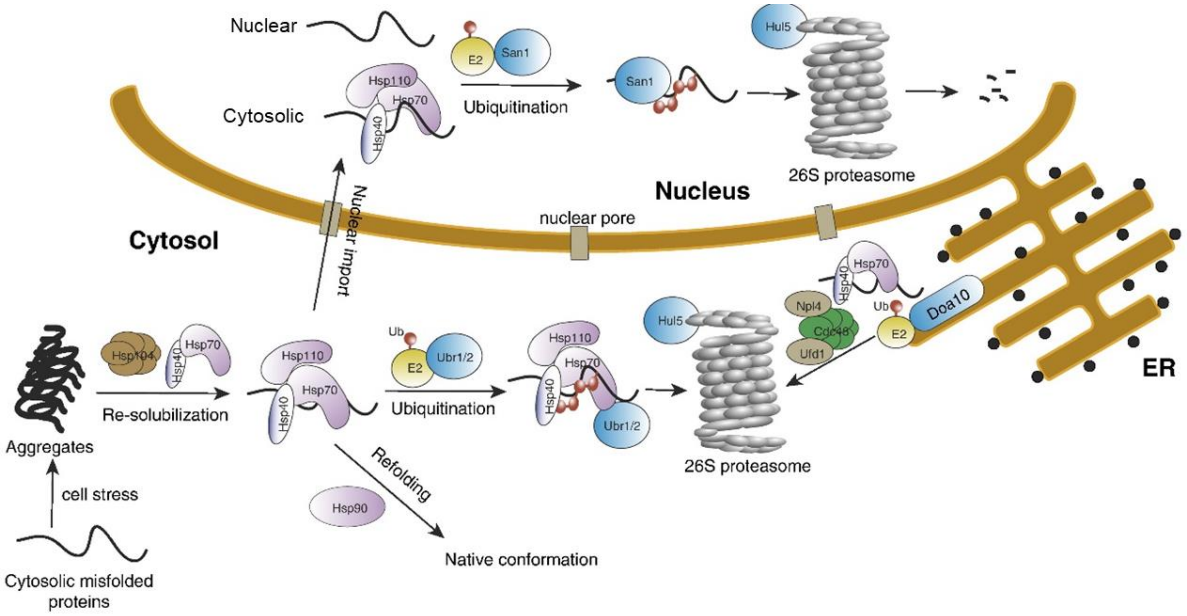

Figure 3.3: Protein quality control and degradation of the nuclear (above) and cytoplasmic proteins (below) via San1.

The figure is taken and modified from Shiber, A.; Ravid, T. Chaperoning Proteins for Destruction: Diverse Roles of Hsp70 Chaperones and their Co-Chaperones in Targeting Misfolded Proteins to the Proteasome.
Misfolded/aggregated proteins are ubiquitylated via E3 ligases with the help of chaperones. Nuclear substrates are recognized by San1 and San1 recruits the ubiquitin-bearing E2 ubiquitin-conjugating enzyme to transfer the ubiquitin to the misfolded protein. The 19S proteasome bound E3/E4 ligase Hul5 adds new ubiquitin proteins onto present ubiquitin chain. In the end, 26S proteasome is able to detect the misfolded protein and start degradation process. Some aberrantly folded cytoplasmic substrates could be under San1-based ubiquitylation after their transport into the nucleus. However, this event only becomes possible with the collective work of Hsp70, Hsp40 and Hsp110 chaperones, another E3 ligase Doa10 and various ERAD pathway members. The 19S proteasome bound E3/E4 ligase Hul5 adds new ubiquitin proteins onto present ubiquitin chain. In the end, 26S proteasome is able to detect the misfolded protein and start degradation process.

3.2 San1 and Cell Cycle

It was shown that San1 could interact with different "cell division cycle (cdc)" proteins. San1 has shown genetic interactions with Cdc5 (Ratsima et al., 2011) and Cdc9 (van Leeuwen et al., 2016) and Cdc13 (Downey et al., 2006); deletion of *SAN1* rescued the growth of their ts mutants. San1 is responsible for the ubiquitin mediated degradation of *cdc13-1* (Gardner et al., 2005). Similarly, our *SAN1*-bearing hits have shown some effects onto MEN-ts strains' growth when are overexpressed (see Figure 2.5). These lead us to think that San1 may have a role in the regulation of cell cycle. Due to our result in genetic screening, which showed a possible role of San1 in a pathway together with Kin4 or in parallel (see Figure 2.3), we hypothesized that San1 might act in mitotic exit.

3.2.1 San1 overexpression does not lead to a significant change on the duration of mitotic exit in an unperturbed cell cycle

Our genetic screen placed *SAN1* in a pathway that inhibits mitotic exit (see Chapter 2). In this screen, the overexpression of *SAN1* on a multicopy plasmid caused lethality of the cells defective in mitotic exit. Intriguingly, Niu et al., 2008 also has shown in a flow cytometry-based genetic screen that the overexpression of San1 lead to a G2/M arrest. We suggested that G2/M arrest might be related to an arrest during mitotic exit and the overexpressed San1 would be responsible for this phenotype. To investigate the effect of *SAN1* overexpression on cell cycle progression, we compared the cell cycle progression of cells carrying 2-micron plasmids with or without *SAN1* (pRS425-*SAN1* or pRS425). For this, we performed a time course experiment which started with the synchronization of cells in G1 (T=0). Cells were then released from the G1 arrest to allow

their synchronous progression through cell cycle. Samples were collected every 15 min for western blot and microscopy analysis. Comparison of the cycling pattern of the mitotic cyclin Clb2 suggested that the entry to and exit from mitosis is not influenced by the 2-micron *SAN1* (figure 3.4). Analysis of budding through microscopy indicated that cells with 2-micron *SAN1* may slightly delay bud formation but otherwise there is not a significant change.

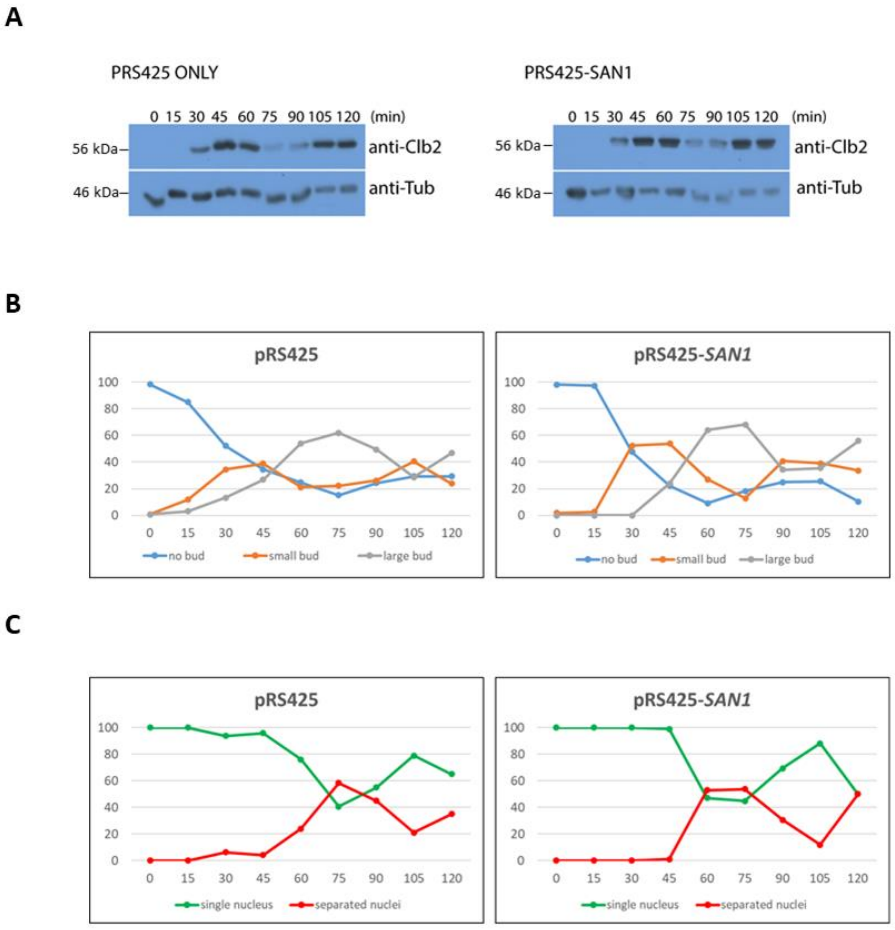

Figure 3.4: San1 overexpression does not lead an anaphase arrest

SEY039-1 was transformed with pRS425 and pRS425-*SAN1* plasmids. The obtained strains were grown to log phase in YPAD and synchronized in G1 using alpha factor. The cells were released from alpha factor arrest (t=0) and samples were collected every 15 minutes for western blot (A) and microscopy (B-C) analysis.
A) Levels of mitotic cyclin Clb2 was analyzed via western blot. Tubulin served as loading control.
B) Budding index was assessed by analyzing ethanol fixed samples by microscopy. A minimum of 100 cells were counted per time point, per sample. Percentage of no budded, small budded and large budded cells were calculated.
C) Mitotic index was assessed by analyzing ethanol fixed samples by microscopy after staining of their nuclei with DAPI. A minimum of 100 cells were counted per time point, per sample. Percentage of cells with separated nuclei (2 dapi stained regions) and single nucleus (1 dapi stained region) was plotted.

Aforementioned time course experiment had a time resolution of 15 min. We next analyzed mitotic exit in cells overexpressing *SAN1* with more time resolution. For this,

we performed time lapse experiments in which we monitored the anaphase onset and spindle breakage in living cells through fluorescence time lapse imaging. As a spindle marker, we used GFP-*TUB1*. Start of the fast spindle elongation indicated the anaphase onset whereas spindle breakdown was a marker for mitotic exit. The time period between these two landmarks was considered as the anaphase duration. We reasoned that a delay in mitotic exit would lead an increase in the anaphase duration and vice versa. In our experimental set up, there were no significant changes in the duration anaphase upon *SAN1* overexpression.

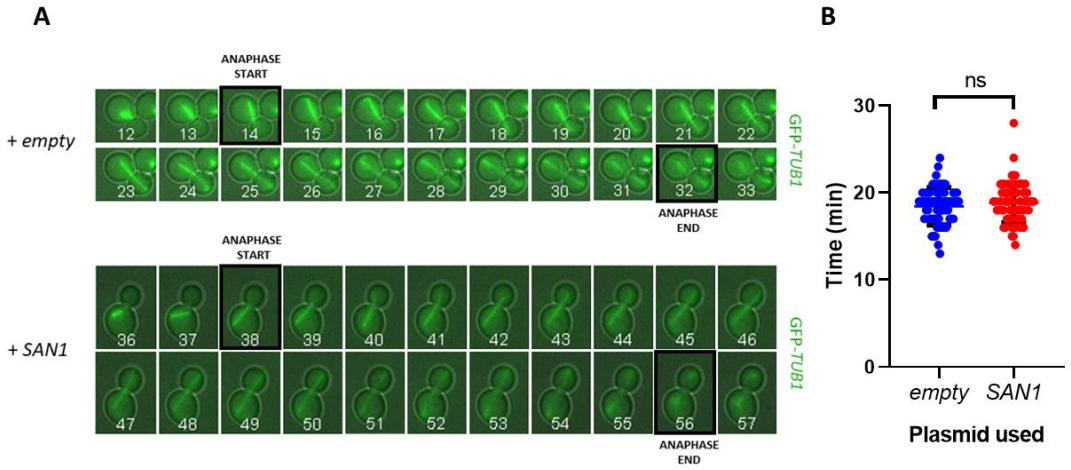

Figure 3.5: San1 overexpression does not change anaphase duration.

A) Time lapse series of representative SHM295 (ESM356 *GFP-TUB1*) cells with empty plasmid (above) and *SAN1* containing plasmid (below). The start and the end of anaphase for the respective cells were indicated with black frames. The numbers below the cells represented the time passed (as minutes) after the time lapse experiment has started.
B) Dot plot showing the anaphase duration. Each dot represented a single cell which underwent anaphase during the time lapses. Student t-test was applied for statistical analysis and no significant difference was found in between two strains (p=0.32). N_{empty}= 71, N_{SAN1}=75

3.2.2 Deletion of SAN1 does not alter the timing of mitotic exit

Previously, we analyzed the effect of multi copy *SAN1* on the growth of mitotic exit network mutants in which we observed a synthetic lethality with *cdc14-2* and *cdc5-10* mutants and a synthetic rescue phenotype with *cdc15-1* mutant (figure 2.5 and Table 2.3). Here, we analyzed the genetic interactions between *SAN1* and MEN-ts mutants upon *SAN1* deletion. Loss of *SAN1* lead to a synthetic lethality in *cdc14-1* and *dbf2-2* mutants (figure 3.6) and a slight growth rescue in *cdc5-10* mutant. We could suggest that San1 may have pleotropic effects on cell cycle or cell survival. Alternatively, the drop test experiments may not show the minute differences, if any (see Discussion).

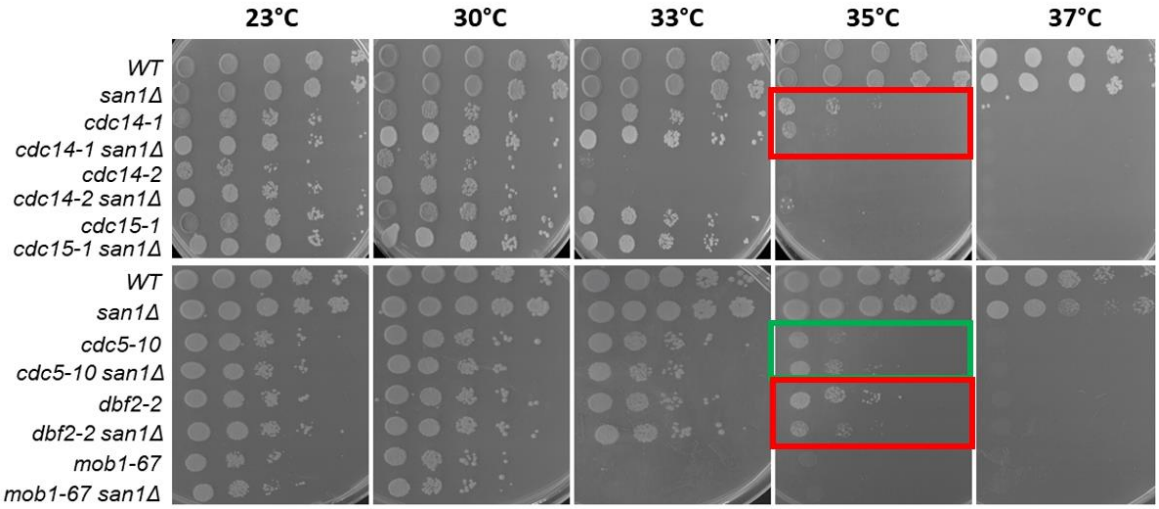

Figure 3.6: Synthetic genetic interactions between *san1*Δ and MEN-ts.

Serial dilutions of indicated strains are dropped on 5FOA plates. YPH499 (WT), BSY015 (WT san1Δ), BSY025 (*cdc5-10* san1Δ), BSY021 (*dbf2-2* san1Δ), BSY022 (*mob1-* san1Δ), JOY79-1 (*cdc5-10*), ESM2283 (*dbf2-2*), ESM2285 (*mob1-67*), BSY023 (*cdc15-1* san1Δ), BSY020 (*cdc14-1* san1Δ), BSY024 (*cdc14-2* san1Δ), GPY491-1 (*cdc14-1*), GPY490 (*cdc14-2*), ESM2282 (*cdc15-1*) strains contained wild type copy of the mutated MEN gene on URA3-based centromeric plasmid, which is negatively selected for on 5FOA plates. Red squares indicated growth sickness/lethality, while green square indicated growth rescue.

We also investigated the anaphase duration in *san1*Δ GFP-*TUB1* cells, during an unperturbed cell cycle (figure 3.7). Anaphase duration was not altered upon *SAN1* deletion.

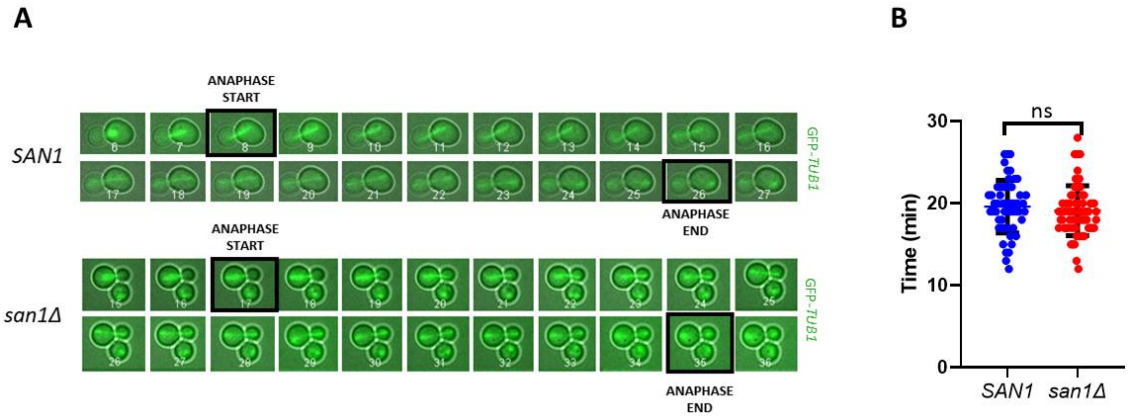

Figure 3.7: Deletion of *SAN1* does not make a difference in the duration of anaphase.

A) Time lapse series of representative SHM295 (ESM356 *GFP-TUB1 SAN1,* above) and BSY040-1 (ESM356 GFP-TUB1 *san1Δ,* below) cells. The start and the end of anaphase for the respective cells were indicated with black frames. The numbers below the cells represented the time passed (as minutes) after the time lapse experiment has started.
B) Dot plot showing the anaphase duration. Each dot represented a single cell which underwent anaphase during the time lapses. Student t-test was applied for statistical analysis and no significant difference was found in between two strains (p=0.38) (N_{SAN1}= 54; $N_{san1\Delta}$= 68).

3.2.3 San1 does not act on the SPOC pathway

After all, we suspected that San1 might be functioning as a mitotic exit inhibiting potentially as a SPOC-related element that blocks mitotic exit. To address whether San1 is a part of the SPOC, we analyzed SPOC functionality of *san1*Δ cell as well as Gal1-*SAN1* cells. For this, we used a *kar9Δ* strain background that frequently mispositions its spindles at 30°C or higher temperatures (Miller RK, 1998). We included *kar9Δ kin4Δ* cells in our analysis as a control for SPOC deficient phenotype. We grew the cells at 23°C until log phase and shifted the temperature to 30°C for 4 hours. Then we fixed the cells with 70 % EtOH and stained their nuclei using DAPI. This way, we could score the cells with mispositioned nuclei (2 DAPI signals in the mother cell), normal positioned nuclei (1 DAPI signal in the mother and 1 DAPI signal in the daughter cell) and multi nucleated cells (multiple DAPI signals). The latter is an indication of SPOC deficiency. Neither *san1Δ* nor Gal1-*SAN1* strains was significantly different from wild type control. This result presented that San1 is not a component of the SPOC pathway.

Deletion of SPOC related genes are usually able to rescue the lethality of mitotic exit deficient *lte1*Δ *spo12*Δ cells. In line with our above conclusion, deletion of *SAN1* did not rescue lethality of *lte1*Δ *spo12*Δ (figure 3.8).

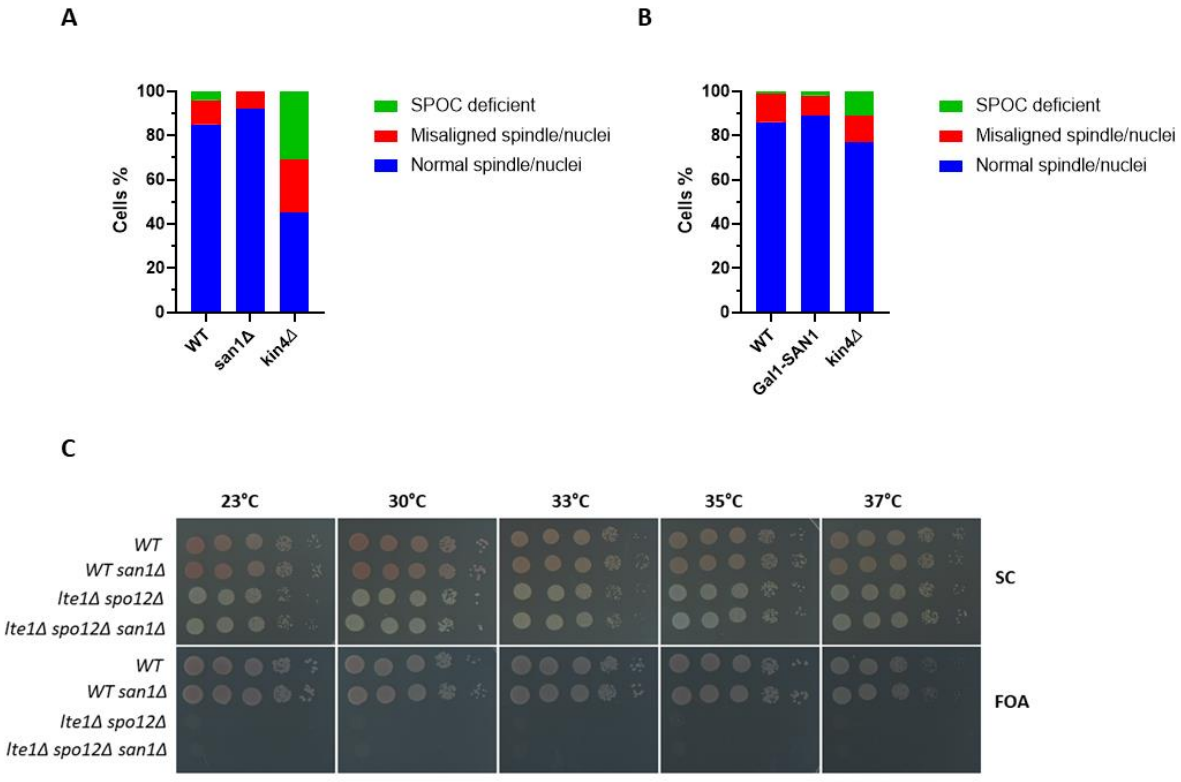

Figure 3.8: Neither *SAN1* deletion nor overexpression change the level of misaligned and SPOC deficiency phenotype

A-B) SPOC functionality analysis of *san1*Δ (A) and Gal1-*SAN1* (B) cells. % of cells with multi-nuclei (SPOC deficient), misaligned nuclei and normal aligned nuclei is plotted. 100 cells were count for each strain. The statistical analysis was done using chi-square test; $p>0.05$.
C) Serial dilutions of indicated cell cultures were dropped onto SC and 5 FOA agar plates and plates were incubated in respective temperatures.

3.2.4 Wild type SAN1 levels does not undergo cyclic changes during cell cycle

We next analyzed if wild type San1 levels underwent any cyclic change in different cell cycle phases. To understand this, we monitored protein levels of San1 in synchronously dividing cells. Cells were synchronized in G1 using the mating pheromone alpha factor (t=0) and released from this G1 arrest by removal of alpha factor. Samples were collected every 15 min and San1-6HA protein levels were analyzed with SDS-PAGE (Figure 3.9). Cells synchronous progression in cell cycle was assessed through microscopy by monitoring the budding index and mitotic index. In addition, the levels of mitotic cyclin Clb2, as a marker for mitotic phase of the cell cycle, was monitored by SDS-PAGE. The experiment showed that the were no significant changes in the protein levels of San1-6HA throughout the cell cycle.

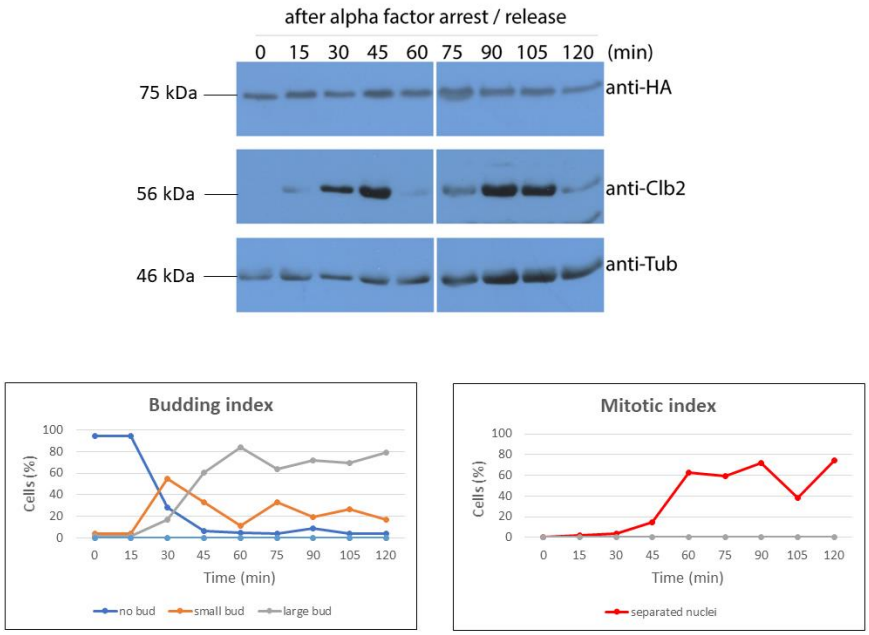

Figure 3.9: Wild type San1 levels does not fluctuate during cell cycle.

A) Western blot analyses are performed to check San1 levels during cell cycle. HA antibody was used for the demonstration of San1 levels. Clb2 was used for assessing cell cycle progression, while Tubulin acts as a loading control (anti-: antibody against specific protein or tag).

B) Budding index and mitotic index was plotted as a marker for cell cycle progression. A minimum of 100 cells were counted per time point, per sample. Percentage of cells with separated nuclei (2 dapi stained regions) and single nucleus (1 dapi stained region) was plotted.

Chapter 4:
DISCUSSION

In eukaryotic organisms, the event of mitosis relies on a specific set of protein kinases, known as cyclin-dependent kinases (CDKs) (Lee and Nurse, 1987). Through their differential binding with a variety of cyclins, CDKs drive the timely coordination of cell cycle events from the beginning to the end: G1-CDK/cyclin complexes lead to the entry of a new cell cycle, S-CDK/cyclin complexes are responsible for the initiation of DNA replication, and lastly, M-CDK/cyclin complexes enables the mitotic entry (Morgan, 1995). During exit from mitosis, these mitotic events need to be reversed and CDKs should be inactivated (Chibazakura et al., 2004). Spatiotemporal regulation of these reversion processes is crucial to achieve the accurate chromosome segregation which is vital for maintaining the proper ploidy and ensuring the viability of the organism (Chibazakura, 2004; Morgan, 1997). Despite the importance and the conservation of these pathways among all eukaryotes, a detailed mechanism of the regulation of mitotic exit is still missing.

The main aim of our thesis to find alternate proteins that regulate mitotic exit in budding yeast *Saccharomyces cerevisiae*. A preliminary genetic screening performed in our lab showed that a temperature sensitive mutant of *RKT1*, *rkt1-1*, was able to rescue the toxicity of Kin4 overexpression. This finding enabled us to couple Kin4 and Rtk1 and place them in the same or parallel pathway which interrupts mitotic exit. Additionally, because Kin4 starts to act in the anaphase, it could be supposed that the role of Rkt1 continues through anaphase/telophase/cytokinesis phases.

The first part of our aim is to understand the mechanism of which Rkt1 leads to mitotic exit inhibition. To reveal this novel mechanism, we needed to find out the components in the proposed pathway of Rkt1 and to construct the pathway. To achieve this goal, we performed a dosage-suppression genetic screening. Hence, we could come up with the proteins (hits) that potentially works with Rkt1 or in parallel to Rkt1 to affect mitotic exit. In the end, we obtained two candidates: San1 and Pho2. San1 is a E3 type ubiquitin ligase that detects the misfolded hydrophobic nuclear proteins and sends them to proteasome for their turnover (Dasgupta et al., 2004). Our second hit, Pho2, is a transcription factor which is very important in the regulation of the phosphate metabolism (Liu et al., 2000).

Intriguingly, Niu et al., 2008 has shown that overexpression of San1 lead to a G2/M arrest. We hypothesized that G2/M arrest of San1 might be related to an arrest during mitotic exit. In addition, *SAN1* represented more in the genetic screen (with 4 plasmids in comparison to 2 from *PHO2*) and more pronounced interaction with MEN components (figure 2.6) in its 2-micron plasmid form. Lastly, in difference to 2-micron *PHO2*, 2-micron *SAN1* has driven a rescued phenotype on *rtk1-1*, with (figure 2.3) and without (figure 2.5) the presence of Kin4 overexpression. This result might be a hint for San1 to be acting in the same pathway with Rtk1. For these reasons, we chose to examine this protein for its plausible role in Rtk1 a related pathway that may regulate in mitotic exit.

In the first sight, the sickness phenotype with the mutant MEN strains in the overexpression of San1 might be related to E3 ligase activity of San1 due to the turnover of those mutants. MEN mutant proteins could be considered as partially active at their semi permissive temperature, in which San1 overexpression showed its effect on the sickness of growth (figure 2.6) It could be quite logical to think that overexpressed San1 might direct the MEN-ts mutants to proteasomal degradation, which decrease the level of active MEN components to proceed the mitotic exit. However, the loss *SAN1* lead to some growth sickness in different MEN-ts mutants (figure 3.6). More interestingly, the lethal phenotype in MEN strains that were related to the overexpression *SAN1* were not always rescued by the San1 loss e.g., *cdc5-10* + Prs425-*SAN1* lethality was rescued in the *cdc5-10 san1Δ,* however, this situation was not valid for *cdc14-2* (figure 2.6 and figure 3.6). Moreover, San1 overexpression led to a growth rescue on *cdc15-1* strain, which stayed unchanged when *SAN1* was deleted (figure 2.6 and figure 3.6). These results were seemingly unexpected. Whereas San1 is most known with its E3 ubiquitin ligase activity, it was suggested that San1 may have roles in gene silencing (Dasgupta et al., 2004; Schnell et al., 1989), transcriptional elongation regulation (Sen et al., 2016), mating pheromone response (Dasgupta et al., 2004), resistance to chemicals (Svensson et al., 2011), vacuolar morphology (Arlt et al., 2011), vegetative growth (Pereira et al., 2014), and cell cycle progression (Niu et al., 2008). In this case, these controversial results might be sourced from the possible pleiotropic effects of San1.

To note, loss of San1 lead to sickness phenotype at 37°C, even in the presence of the wild type version of the ts mutant gene (figure 3.6 and SC plates - data not shown). This result may arise from San1's role in degradation of unfolded/aggregated proteins which may be happening more pronouncedly at 37°C.

Figure 2.3 showed that 2-micron *SAN1* reverted the lethal phenotype sourced from Kin4 toxicity, which constructed our initial hypothesis about the possible role of *SAN1* in the blockage of mitotic exit. However, in our time course experiment, we could not detect any differences in between San1 overexpressed plasmid and the empty plasmid in any of the cell cycle phases (figure 3.5). Additionally, there was no significant change in anaphase duration between the 2-micron San1-bearing strain and the empty plasmid-bearing strain, as well. Hence, further experiments are needed to reveal the unknowns in this issue.

As another point of view, MEN ts mutants were showing some genetic interactions with *san1Δ*. In contrast, the anaphase duration did not change in the loss of *SAN1*, compared to the wild type strain (figure 3.7). Repetition of the time course and time lapse experiments with the respective MEN ts mutant strains would be beneficial to examine the changes that are specifically related to these mutants, if any. This situation is applicable for both San1 overexpression and deletion status. Alternatively, the effect of San1 overexpression and deletion could be examined at different phases of cell cycle such as the duration of early mitosis (the time interval until the start of anaphase) or the duration of cytokinesis, with usage of different cellular markers (both for SDS-PAGE and fluorescence microscopy) to observe the possible differences in detail.

To examine if Kin4 and San1 were present in the same pathway, we distorted the correct alignment of mitotic spindle to activate SPOC. However, Figure 3.8 showed that San1 was not acting through SPOC pathway. Still, becoming an alternate pathway to alter the process of exit of mitosis could be a possibility for San1 and for Rkt1 pathway.

Rkt1 is a potent protein to be involved in different cellular processes. Previous works stated that it participates in mRNA decapping and catabolic processes of mRNA (Tucker et al., 2002), mating pheromone response (de Barros Lopes et al., 1990), transcriptional elongation (Tucker et al., 2001), protein ubiquitylation (Panasenko et al., 2006), and regulation of cell cycle (de Barros Lopes et al., 1990). San1 has known with its E3 ubiquitin ligase activity, which may link the protein ubiquitylation role of Rkt1 to San1. Similarly, San1 was shown to have genetic interactions with some of the transcription-related proteins such as Sir3, Sir4, Spt16 or Mex7 (see Section 3.1) and to be significantly related to mating pheromone response pathway (Dasgupta et al., 2004). As was stated above, the G2/M arrest occurred with the overexpression of San1 (Niu et al., 2008), which might state as a clue of San1 role in cell cycle. Thus, it is not surprising to connect Rkt1

and San1 into a cell cycle regulation pathway, whereas further experiments were needed to have a clearer understanding.

Appendix A: Tables

Table A1: PCR primer sets that are used in the study

PRIMER NAME	PRIMER SEQUENCE	Description
SAN1-S1	CCCCTTTGTTTTCTCTCATAGTCTTGTAACCTCAGCTTTTGTTCATTATGcgtacgctgcaggtcgac	binds 50 bp upstream of START, until START
SAN1-S2	CCAATAGGACATATTTTCATATTAACATACTTCAGAAGCGGTATTGTTTAatcgatgaattcgagctcg	binds 50 bp downstream of STOP, until STOP
SAN1-S3	CCATTCATAACGACGTCCCTAATGATAACAATGAGCAACGATCATCACAAcgtacgctgcaggtcgac	binds 50 bp upstream of START, except START
SAN1-S4	TTATTTGGTGATGTATTTGTGCCTCTGTTTTGTTCTTGACCACTTTCACTcatcgatgaattctctgtcg	binds 50 bp downstream of START, except START
SAN1-Fw-BamHI	CGC**GGATCC**GCTTCCACGTCTCATTCG	binds 658 bp upstream of START
SAN1-Rev-SalI	ACGC**GTCGAC**TACCGCGAGCCTGTTATC	binds 500 bp downstream STOP
San1-Col2	CAGAGGAGGTTATGTCGGTG	binds 243bp downstream of STOP
San1-Col1	CGCCAGGTTCATTACAGCTA	binds 473 bp upstream of START
NSE4-BamH1-Fw	CGC**GGATCC**TGAGGTCCACTATCTGATGC	binds 717 bp upstream of START
NSE4-SalI-Rev	ACGC**GTCGAC**GACGTTGAACTCCACAAGCT	binds 257 bp downstream of STOP
PHO2-BamHI-Fw	CGC**GGATCC**CGCTACTGTCAGGCTCAGTA	binds 551 bp upstream of START
PHO2-SalI-Rev	ACGC**GTCGAC**GTCATGGCTGAGTTGTATAG	binds 660bp downstream of STOP
Smc3-SacII-Rev	TCC**CCGCGG**TCGGACTCCGTATCGGATTC	binds 525bp downstream STOP, contains SacII flanking - used in cloning
Smc3-BamHI-Fw	CACTTGCT**GGATCC**GCAGTC	binds 530bp upstream START, contains BamHI - used in cloning

*The lowercase letters indicate the parts that is bound to the plasmids used in gene deletion or tagging studies.

**Bold sites are the restriction sites of restriction enzymes indicated in primer names.

***START indicates the beginning of Open Reading Frame (ORF) for the gene, whereas STOP indicates the end of ORF.

Table A2: Plasmids that are used in the study

Plasmid Name	Description
pRS315	*LEU2*-dependent CEN-based yeast-E. coli shuffle plasmid. Amp^R.
pRS316	*URA3*-dependent CEN-based yeast-E. coli shuffle plasmid. AmpR.
pRS406	*URA3*-based integration vector, blue-white selection. Amp^R.
pYM3	*6HA*-klTRP1. AmpR.
pFA6a-His3MX6	pFA6a-His3MX6. AmpR.
pGW410-1	p406-Gal1-*KIN4*. AmpR.
pBK030-1	pRS315-pGal1- *KIN4*-Cyc1term. AmpR.
pBS004	pRS425-*NSE4*. AmpR.
pBS005	pRS425-*PHO2*. AmpR.
pBS006	pRS425-*SAN1*. AmpR.
pRS425	*LEU2*-based 2 micron yeast/E. coli shuttle vector, blue-white selection. Amp^R.

Table A3: Yeast strains that are used in the study

All strains are derivatives of S288C.

Genotype/description	
YPH499*	MATa ura3-52 lys2-801amber ade2-101ochre trp1Δ63 his3Δ200 leu2Δ1.
ESM356-1*	(Spore 2.1) MATa ura3-52 leu2Δ1 his3Δ200 trp1Δ63.,
BY4741	MATa; his3Δ1; leu2Δ0; met15Δ0; ura3Δ0.
ESM1249-1	YPH499 tem1-3.
ESM1276-1	YPH499 cdc14-2.
ESM1278-1	YPH499 cdc15-1.
CVY16-1	YPH499 cdc14-1.
ESM1309-1	YPH499 dbf2-2.
ESM1361-1	YPH499 mob1-67.
CLY169-2	YPH499 cdc5-10.
Y06322	*rkt1-1kanMX6*.
GPY491-1	ESM1276 (YPH499 *cdc14-2*) pUG120 (*CDC14*-pRS316).
GPY490	CVY16 (YPH499 *cdc14-1*) pUG120 (*CDC14*-pRS316).
ESM2285	ESM1361 (YPH499 *mob1-67*) pSM926 (pRS316-*MOB1*)
JOY79-1	CLY169 (YPH499 *cdc5-10*) pCL33 (pRS316-*CDC5*).
ESM2283	ESM1309 (YPH499 *dbf2-2*) pSM908 (pRS316-*DBF2*).
ESM2282	ESM1278 (YPH499 *cdc15-1*) pBS9 (pRS316-*CDC15*).
GPY120	TEM1 shuffle strain. Spore from GPY109 (YPH501 *tem1Δ*::KanMx6, pRS316-*TEM1*). MATalpha, *kan+, ura+, leu-, his-, trp-*, 5-FOA sensitive.
AKY2526-1	FAY149 (ESM1192-19 *TRP+ lte1Δ*::kanMX6 pRS316-*LTE1*) *spo12Δ::natNT2*.
SHM295-2	ESM356-1 pAFS125-GFP-*TUB1-URA3*
AKY260	BKY035 (ESM356 *kar9Δ::hisMX6*) pGW399 (pRS316-*KAR9*)
BSY001	BY4741 pRS315.

BSY002	BY4741 pBK030-1 (pRS315-Gal1-*KIN4*-Cyc1).
BSY003	Y06322 (*rtk1-1 kanMX6)* pRS315.
BSY004	Y06322 (*rtk1-1 kanMX6*) pBK030.
BSY005-1	ESM356-1 pRS406/BsgI.
BSY006-1	ESM356-1 pGW410-1 (pRS406-Gal1-*KIN4*)/BsgI.
BSY007-1	BY4741 pGW410-1 (pRS406-Gal1- *KIN4*-Cyc1)/BsgI.
BSY008-1	Y06322 (*rkt1-1* kanMX6) pGW410-1 (pRS406-Gal1- *KIN4*-Cyc1)/BsgI.
UJY011-4	ESM356-1 *SPC42*-EQFP611-KanMX6 Nat-Gal1-GFP-*KIN4 ura3::*pMET25-*KIN4*.
UJY013-2	ESM356-1 *SPC42*-EQFP611-KanMX6 Nat-Gal1-GFP-*KIN4 ura3::*pMET25-*KIN4 Δbfa1*::klTRP1.
UJY014-1	ESM356-1 *SPC42*-EQFP611-KanMX6 Nat-Gal1-GFP-*KIN4 ura3::*pMET25-*KIN4 Δbub2*::hgh..
UJY016-1	ESM356-1 *SPC42*-EQFP611-KanMX6 Nat-Gal1-GFP-*KIN4 ura3::*pMET25-*KIN4 Δrts1*::klTRP1.
BSY015-1	YPH499 *SAN1* :: Pfa6a HisMX6:: *san1Δ*.
BSY020-1	GPY490 (CVY16 (YPH499 *cdc14-1*) pUG120 (*CDC14*-pRS316)) *SAN1* :: PFA6A HisMX6 :: *san1Δ*.
BSY021-1	ESM2283 (ESM1309 (YPH499 *dbf2-2*) pSM908 (pRS316-*DBF2*)) *SAN1*:: PFA6A HisMX6 :: *san1Δ.*
BSY022-1	ESM2285 (ESM1361 (YPH499 *mob1-67*) pSM926 (pRS316-*MOB1*)) *SAN1* :: PFA6A HisMX6 :: *san1Δ*.
BSY023	ESM2282 (ESM1278 (YPH499 *cdc15-1*) pBS9 (pRS316-*CDC15*)) *SAN1* :: PFA6A HisMX6 :: *san1Δ*.
BSY024	GPY491-1 (ESM1276 (YPH499 *cdc14-2*) pUG120 (*CDC14*-pRS316)) *SAN1* :: PFA6A HisMX6 *san1Δ*..
BSY025	JOY79-1 (CLY169 (YPH499 *cdc5-10*) pCL33 (pRS316-*CDC5*)) *SAN1* :: PFA6A HisMX6 *san1Δ*.
BSY038	ESM356 *SAN1* :: PFA6A klTRP *SAN1*-6HA.
BSY039	ESM356 *SAN1*::PFA6A klTRP1-6HA :: *san1Δ*.
BSY040-1	SHM295-2 (ESM356 GFP-*TUB1*) *SAN1*::PFA6A HisMX6 :: *Δsan1*.
SEY039-1	AKY1729 (ESM356 *PDS1*-3HA-his3MX6) *sic1-9myc+ trp1*
BSY049	AKY2526-1 (FAY149 (ESM1192-19 *TRP+ lte1Δ::*kanMX6 pRS316-*LTE1*) *spo12Δ::*natNT2) SAN1 :: PFA6A HisMX6:: *san1Δ.*
BSY051	BKY035 (ESM356 kar9Δ::his) pGW399 (pRS316-KAR9) SAN1 :: PYMN24 pGal1-NatNT2-3HA-SAN1.
BSY054	AKY260 (BKY035(ESM356 *kar9Δ::*hisMX6) pGW399 (pRS316-*KAR9*) SAN1::PFA6A klTRP-6HA *san1Δ.*

Appendix B: Materials and Methods

Strains and Growth Conditions

The *S. cerevisiae* strains used in this study are described in Table A3. Composition of growth media is described in Table A5. Yeast media, (YPD rich solid medium, YPAD rich liquid medium, synthetic medium lacking specific nutrients [SC-X] or 5-Fluoroorotic acid [5'FOA]) have been used as indicated in the figure legends. The auxotroph yeast strains were grown in SC-X medium supplemented with D(+)-Glucose (BioFroxx) as a carbon source unless othherwise stated. For Raffinose and/or Galactose usage as carbon source(s), 2% D-Raffinose (AFG Bioscience #379827), 3% D(+)-Galactose (AFG Bioscience #307688), was used instead of 2% D(+)-Glucose. For solid media preparation, 20 g Bacto Agar (Carl Roth) was added for 1 L media and be autoclaved together. *S. cerevisiae* strains were grown at 30 °C except where noted..
Escherichia coli strain DH5α was used for plasmid amplification purposes. LB (Luria-Bertani) was used as a growth media, unless otherwise stated (Table A5) For, solid medial preparation, 20 g Bacto Agar (Carl Roth) was added for 1 L LB liquid media and be autoclaved together.
For AmpR containing plasmid selection/amplification Ampicillin (100 µg/ml) was added to the liquid medium or agar plate, after being autoclaved and cooled to 50°C-60°C, *E coli* was grown at 37 °C except where noted.

Yeast Transformation

To achieve yeast transformation, first, the competent cells of desired background strains were prepared. This required logarithmically growing (log-phase) yeast cultures. To obtain log-phase cultures, stationary yeast pre-culture (cells grown in media for overnight) was diluted to 0.15 OD_{600} and incubated until the culture reaches an OD_{600} of 0.8-1, which takes approximately 2.5 doubling time. OD measurements were performed using PG Instruments, T60 Visible Spectrophotometer.

Log phase culture was centrifuged in Beckman Coulter Allegra X-22R Centrifuge, and supernatant was discarded. Pellets were washed once with sterile ddH2O and once with LISORB (See Table A5 for composition). After discarding the supernatant, the cell pellet is dissolved in LISORB and denaturated salmon sperm DNA. Salmon sperm DNA (ThermoFisher Scientific #1563250) was denatured by boiling at 95°C for 5 min and followed by incubation on ice for 5 min. LISORB and salmon sperm DNA amounts were scaled proportionally according to the optical density of the culture; $OD_{600\ value}$*300 µL for LISORB and $OD_{600\ value}$*50 µL for salmon sperm DNA, respectively. Obtained competent cells were aliquoted and stored at -80 ºC or used right away for transformation.

Transformation of yeast competent cells was performed as follows: 1-5 µL of exogenous genetic material (plasmid or cassette) was pipetted into 50 µL of competent cells and briefly vortexed. the cell-DNA mix was incubated for 15 minutes at room temperature. After incubation, 300 µL of LiPEG was added into competent cells, vortexed and incubated for another 15 minutes at room temperature. Then, 35 µL of DMSO (Fisher Scientific #BP231-1) was added, vortexed and the mixture was incubated for 15 min at 42˚C water bath. For temperature sensitive strains, the duration of this heat shock step was reduced to 12 minutes. After incubation, the samples were centrifuged at 3200 rpm for 2 minutes, supernatant was discarded, cells were dissolved in sterile PBS and directly plated-out onto their respective agar plates, if an auxotrophy selection marker was used. If antibiotic resistance markers were used, cells were recovered in nonselective medium for 6-12 hours before plating out on the respective agar plates. Colonies were tested with colony PCR to confirm proper integrations for gene deletion, whereas western blot or microscopy was applied for confirmation of gene tagging.

E. coli Competent cell Preparation

E. coli strain (DH5alpha) was streak on a LB agar plate (Table A5) and be incubated at 37°C overnight. In the next day evening, 2-3 mm of cells were inoculated in 50 ml LB medium (Table A5) and be incubated at 37°C rotator to obtain a preculture. In the morning, the pre-culture was diluted to 0.1 OD and started to be inoculated overnight at 18°C shaking incubator. In the next morning, the culture was diluted to 0.2 OD in 100 ml SOB medium (Table A5) inside 500 ml flask. In the evening, a log phase culture was obtained, and this culture was diluted to 0.075 OD in 400 ml SOB medium. In the next day, when OD is 0.6 - 0.8,

the culture flask was placed on ice for 10 min and the culture was transfer into 50 ml centrifuge tubes. Centrifuge was performed at 2500xg for 10 min at 4 °C. The supernatant was discarded totally, using a vacuum aspirator. The pellets were resuspended with ice cold Freeze-Thaw buffer (FTB) (Table A5) as 15 ml FTB would be used for 50 ml culture pellet. The tubes were incubated on ice for 10 min and be centrifuged for 10 min with 2500 x g at 4°C. FTB was discarded and the cell suspensions from 50 ml falcon tubes were combined into a smaller number, using fresh FTB (on ice). Again, Centrifuge was performed at 2500xg for 10 min at 4 °C and the supernatant was discarded. All the cell pellets were combined in one falcon and the pellets were dissolved in 0.3 ml of DMSO and 2.4 ml FTB, per 0.6 OD 50 ml culture. While the cells were kept on ice, they were dispensed into 100µl aliquots using ice-cold sterile microfuge tubes. The cells were, then, snap-frozen by immersing in liquid nitrogen.

E. coli Transformation

For bacterial transformations, 1-5 µL of exogenous genetic material (plasmid) was pipetted into 50 µL of ice - thawed competent DH5α cells. Transformation solutions were mixed gently and incubated for 30 minutes on ice followed by a heat shock (incubation at 42˚C for 90 sec and rest on ice for 2-5 min). Then transformants were plated out onto ampicillin containing agar plates and incubated at 37°C. The transformants were taken for further work 12-16 hours later.

Dosage suppressor Screen protocol

a. High Efficiency Yeast Transformation protocol

Log-phase cultures of BSY008 (*rtk1-1* pGal1-*KIN4*) were prepared as explained above (see Yeast Transformation). Then, culture was centrifuged at 3200 rpm for 5 minutes at room temperature. The supernatant was discarded, and cells were resuspended with 25 ml ddH20 and be spinned again. Then, cells were resuspended with 1 ml LiAc (1 M) with pipetting. Cell suspension was transferred into a 1.5 ml centrifuge tube and centrifuged for 15 sec at maximum rpm. Supernatant was aspirated. 400 µl of fresh LiAc (1 M) was added, the solution was gently vortexed, and 50 µl of competent cells were aliquoted a 1.5 ml centrifuge tube. LiAc was completely removed by aspiration after centrifugation. On the cell pellet, immediately following were added in the given order and amount:

PEG %50	240 µl
LiAc (1 M)	36 µl
Denatured Salmon sperm DNA (10mg/ml)	10 µl
2-micron yeast genomic library (100 ng/µl*)	20 µl
ddH20	54 µl

* The optimum concentration of DNA was determined in a plot experiment where DNA amounts ranging from 500 ng, 1000 ng, 1500 ng, 2000 ng and 3000 ng were transformed into yeast using the same protocol. 2000 ng DNA led the optimum efficiency.

The cell pellet was resuspended with the transformation solution by vortexing and the mixture was incubated at 30°C for 30 min. After incubation, heat shock was applied at 42°C for 30 min. At the end of heat shock, the mixture was centrifuged at 6000 rpm for 15 sec and the supernatant was aspirated. 2 ml SC-Leu medium was pipetted onto the pellet and cells were resuspended by pipetting. Then, the cell suspension was incubated at 23°C shaking incubator for 90 minutes (less than one doubling time). The transformation solution was kept at 4 °C for 2 days until the transformation efficiency was calculated.

b. Calculation of transformation efficiency and amount of desired transformants

To calculate the transformation efficiency, 10-fold dilutions (from 1 to 10^{-4}) were prepared from the 2 mL transformation solution (see above) using sterile PBS. Each dilution was plated-out as three replicates onto SC-Leu plates. After two days, the number of transformants were counted.

The number of the desired transformants per plate was calculated as follows:
Yeast genome contains 12.000.000 base pairs. YEplac 181-library (2um, LEU2, AmpR) contained DNA fragments with insert size: 3000-5000 kb (4000 bp as average)

To achieve to cover the entire genome, we needed to get at least 3000 colonies (assuming every fragment distinctly contains different regions in the genome). To ensure that every single fragment was

placed into at least one competent cell and every competent cell carries at least one DNA fragment, we required at least 3*3 times coverage of the genome. In this case, 27 000 transformants were necessary. However, we could obtain approximately 23 000 transformants. Due to possessing high coverage possibility of the genomic library in this condition, we continued our experiments with these transformants.

c. Selection of desired colonies

Transformation solution was diluted to get approximately 150 colonies per 200 µl. From this 200 µl was plated on each SC-LEU agar plate. A total number of 196 plates were used to obtain a total number of 27 000 transformants. Plates were incubated at 23°C for 2-3 days. Each plate was then replica plated on two SC-LEU Glucose plates and one SC-LEU Raffinose/Galactose plate. One of the SC-LEU Glucose plates were incubated at 23°C to be used as the stock. The other SC-LEU Glucose and SC-LEU Raffinose/Galactose plate were incubated at 30°C, which is the semi-permissive temperature for *rkt1-1*. Then, the transformants that cannot grow on SC-LEU Raffinose/Galactose plate but can grow on SC-LEU Glucose plate at 30°C were selected as desired colonies. These colonies were picked from the SC-LEU plate incubated at 23°C and their growth on SC-LEU Raffinose/Galactose plates were analyzed again by colony streaking. 370 colonies with the desired phenotype were kept for plasmid isolation.

d. Selection and amplification of desired plasmids

We isolated plasmids form 370 yeast colonies showing the desired phenotype colonies. These plasmids were transformed into *E. coli* for further amplification. 3 colonies from *E. coli* were selected considering the possibility of multiple plasmid presence in yeast. Plasmids from 3 colonies were run on agarose gel to see if they are different. Those plasmids were kept for back transformation experiments.

e. Back transformation and selection

Obtained plasmids were transformed into the starting strain (back transformation). Then, the growth of colonies were checked with usage of drop tests onto SC-LEU GLU and SC-LEU RAF/GAL plates to distinguish even the small differences in the growth when exposing to the galactose-bearing environment. In the end, we identified 6 plasmids that caused lethality at 30°C on SC-LEU RAF/GAL plates.

g. Plasmid sequencing

The 6 plasmids were sequenced by Sanger sequencing (Macrogen) using M13F and M13R primers.

Gene Cloning

PBS004 (pRS425-*NSE4*), PBS005 (pRS425-*PHO2*), PBS006 (pRS425-*SAN1*), were constructed as follows: each respective gene was amplified from yeast chromosomal DNA using Phusion Polymerase PCR procedure with NSE4-BamHI-Fw and NSE4-SalI-Rev primers for *NSE4* cloning, PHO2-BamHI-Fw and PHO2-SalI-Rev primers for *PHO2* cloning, SAN1-Fw-BamHI and SAN1-Rev-SalI primers for *SAN1* cloning). PCR products were extracted from the gel using NucleoSpin Gel and PCR Clean-up Kit (Macherey-Nagel) following the protocol. Cleaned up DNA was digested with BamHI F.D and SalI F.D (Thermofischer Scientific-FD0054 and FD0644) restriction enzymes. For restriction digestion of PCR products, 10 µl of 10X Fast Digest Buffer (B64 – Thermofischer Scientific), 1 µl of BamHI F.D restriction enzyme, 2 µl of SalI F.D restriction enzyme, 60 µl of PCR clean-up solution and ddH2O up to 100 µl restriction solution was mixed in 1.5 ml microcentrifuge tube and the mixture was incubated 25-30 min at 37°C. pRS425 backbone was digested in the same way, with usage of 5 µg plasmid DNA directly. ddH2O amount was altered accordingly.

Then, digested backbone was ligated with each insert (BamHI/SalI fragments from PCR products) using T4 ligase (LSG-EL0011). To determine the ratio in between the plasmid and the insert, 3 µl from both were loaded into AGE side by side and the amounts of DNA were compared. For our case, 1 µl plasmid and 7,5 µl insert were used for each ligation reaction, with the addition of 1 µl of 10X T4 ligase buffer (LSG-EL0011) and 0.5 µl of T4 ligase enzyme (LSG-EL0011). This 10 µl ligation mixes were incubated at room temperature for 1 hour. After ligation reaction was completed, 100 µl *E. coli* DH5α competent cells were directly transformed with the ligation mixtures and the transformant solutions were plated out onto LB agar plates with ampicillin (see Table A5). Isopropyl β-D-1-thiogalactopyranoside (IPTG) (100mM in

ddH2O) (Table A5) is used along with X-gal (20 mg/ml X-Gal in DMF) (Table A5) for blue-white screening for the selection of positive transformants, in which the insert was placed inside lacZα gene (Ullmann et al., 1967). The agar plates were incubated at 37°C overnight. 6-12 transformants were selected for each transformation and the transformants were inoculated in LB liquid medium with ampicillin (Table A5) for 9-18 hours. Plasmid isolation from *E. coli* was performed (see "plasmid isolation from *E. coli*") and newly constructed plasmids were confirmed with restriction digestion using BamHI F.D. and SalI F.D and also KspAI F.D (Thermofischer Scientific-ER103) enzyme, as an additional control. After incubation at 37°C for 25-30 minutes to complete the digestion, AGE was applied using the digestion mixtures. The plasmids which showed the expected results in AGE were kept at -20°C for further use.

Colony formation test (Drop test)

Yeast strains were inoculated into appropriate liquid media and grown until stationary phase (overnight at 30°C unless otherwise stated) The OD_{600} of cultures were diluted to 1 OD_{600} (10^0) and 10 times serially dilutions were made until 10^{-4} OD_{600}. 7.5 microliter of the culture suspensions were dropped side by side from 10^0 to 10^{-4} onto appropriate plates. The plates were incubated at different temperatures and scanned at 2-3 days later.

Chromosomal DNA purification from yeast

To prepare chromosomal DNA, the stationary cultures were centrifuged at 14000 rpm for 1 minute. The supernatant was aspirated, and the cells were resuspended with 300 µl %6 SET (Table A5). The mix was incubated in 65^0C for 15 min and transferred to ice. 150 µl of cold P3 buffer (Table A5) was added and incubated on ice for 15 minutes. Then, the mix was centrifuged at 14000 rpm for 10 min. The supernatant was decanted into a new tube and 500 µl of isopropanol was pipetted onto it. The mixture was invert-rotated and centrifuged at 14000 rpm for 1min. The pellet was washed with 200 µl %70 cold ethanol (Merck #1.00983.2500). The DNA was resuspended in 25-30 µl ddH2O with 1 µl of 1mg/ml RNAase (Neofroxx #1263) and be incubated at 37 ºC for 15 minutes.

Plasmid isolation from yeast

A stationary yeast culture was centrifuged, and the medium was aspirated. The cell pellet was resuspended in 0.5 mL of S buffer (Table A5). The solution was incubated at 37˚C for 1 hour with gentle shaking in every 15-20 minutes. 0.1 ml lysis buffer (Table A5) was added, and the mixture was vortexed. Incubation was done at 65 ˚C for 30 min and 166 µl P3 buffer was added (Table A5). The mixtures were incubated on ice for 10 min. After incubation, the solution was spinned at highest speed for 10 min. The supernatant was decanted to a fresh eppendorf and the DNA was precipitated by adding 0.8 ml cold 100% EtOH. The solution was incubated on ice for 10 min and spin for 10 min at highest speed. Supernatant was discarded and the pellet was washed by centrifugation with 0.5 mL 70% EtOH and the pellet was air dried. After disolving the pellet in 20 µl sterile water, the plasmid DNAs could be kept at -20˚C for further use. Because the yield is not much, the plasmids that were isolated from the yeast were amplified in E. coli.

Plasmid isolation from E. coli

A streak of *E. coli* colonies was inoculated in 2-3 ml TY with appropriate antibiotics and grown at 37 °C overnight at shaker. The culture was pelleted at 6000 rpm 5 min at RT. The supernatant was discarded, and the pellet was dissolved in 300 µl P1 buffer (Table A5). 300 µl P2 buffer (Table A5) was added into the suspension of cells and the tubes invert-rotated to mix. 300 µl cold P3 buffer (Table A5) was mixed inverting the tubes several times again. The solution was centrifuged at 14000 rpm for 10-15 min at RT. The supernatant was decanted onto 600 µL isopropanol (ACS #0312.2500) by inversion. The mix was then centrifuged at 14000 rpm for 1 min at RT. The obtained DNA pellet washed with 70 % EtOH. The pellet was air dried and resuspended in 20-30 µl of ddH2O.

Agarose Gel Electrophoresis

Agarose Gel Electrrophoresis was performed with use of in 0.8% (w/v) agarose gel in TAE buffer (Table A5). 4 µl DNA ladder (NEB N3232S) - loading dye (NEB B7025S) mix and 12 µl of DNA samples each mixed with 3 µl loading dye (composition in the Table A5) were loaded into wells. Running was performed at 120V, 300 mA and for 45-75 minutes. Post-running EtBr treatment was done for at least 15 minutes at room temperature to achieve visualization under UV light.

Preparation of Yeast total Protein extracts

Sample collection: 1 mL cell culture of known OD600 were pelleted at 14000 rpm for 2 min, supernatant was aspirated, and pellet was immediately frozen at -20 C.

Protein extraction: Pellets were put on ice, resuspended in 800 µL ice cold ddH2O. 150 µL1.85 M NaOH was added and vortexed. Then, 150 µL (w/w) 55% cold TCA (Merck #100807) was added and vortexed. After 10-15 min incubation on ice, protein precipitates were pelleted at 14000rpm at +4°C for 20-30 min and the supernatant was aspirated. Tubes were centrifuged again for 1 min at room temperature to remove the remnants of TCA. Finally, the pellets were resuspended in appropriate amount of HU-DTT (Table A5). The appropriate amount was calculated 75µl HU-DTT per protein pellet obtained from 1 ml of 1 OD_{600} culture.) The protein solutions were boiled at 65°C for 15 min and centrifuged at maximum rpm for 1 minute, before loading on SDS-PAGE gels.

Western blot analysis

SDS-PAGE gels were prepared using BioRAD Mini-Protean II gel apparatus.

The separating gel was prepared by the stock concentrations of the 1.5M Tris-HCl pH 8.8, 10 (w/v) % SDS, 8 or 10% polyacrylamide mixture (30%: 0.8% w/v acrylamide:bisacrylamide) and polymerized by addition of 10% (w/v) ammonium persulfate (APS) (Sigma #A3678) and TEMED (Sigma). Stacking gels contained 0.5 M Tris-HCl pH 6.8, 10% SDS, 4% polyacrylamide mixture, and were polymerized with 10% APS and TEMED. The amount of the materials per gel are stated below:

Separating Gel	8%	10%
Acrylamide / Bis	1,3 ml	1,68 ml
H_2O	2,38 ml	2,0 ml
1.5 M Tris-HCl pH 8.8	1,25 ml	1,25 ml
10% SDS	50 µl	50 µl
TEMED	2,5 µl	2,5 µl
10% APS	25 µl	25 µl

Stacking Gel	4%
Acrylamide / Bis	325 µl
H_2O	1,55 ml
0.5 M Tris-HCl pH 6.8	625 µl
10% SDS	25 µl
TEMED	2,5 µl
10% APS	12,5 µl

All lysates were loaded on 8% or 10% SDS–polyacrylamide gels for electrophoresis and after running at 200V for 20mA for 1.5 hour in 1X Laemmli buffer (Table A5), the gels were transferred onto nitrocellulose membranes (Merck, GE10600002). Blotting was performed at 0.1 mA/gel, 25 V, 90 min using Semi-Dry Transblot system (BioRAD TransBlot® Turbo™ Transfer System) When blotting was completed, the membranes were stained with Ponceau S for 5-10 minutes to observe the proteins. The membrane was then labelled at the edges of its wells and cut from specific sizes if necessary. For antibody treatment, the membrane is then destained in 0.02 % Tween containing 1xPBS (PBS-T) (Table A5) and was blocked in 1xPBS-T buffer supplemented with 5% nonfat dried milk (PanReac AppliChem) for either 1 hr at RT or overnight at 4°C with gentle shaking. After blocking, the membrane was incubated with the primary antibodies (Table A4) for 1 hr at RT or overnight at 4°C. Then, the membrane was washed with PBS-T three times, five minutes each. Then the membrane was incubated with secondary antibodies (Table A4) for 1 hr at RT or overnight at 4°C. The membrane was washed with PBS-T three times, five minutes each.

Signal was detected using chemiluminescence ECL and exposing on X-ray films (Carestream Medical X-ray Green/MXG Film).

Table A4: Antibody list used for Western Blot studies

Name of the Antibody	Specification	Origin of the Antibody	Dilution Ratio	reference / description
Anti-HA	Primary	Mouse	1:50 in 3% milk with PBS-T (0.02 % Tween-20)	monoclonal
Anti-Clb2	Primary	Rabbit	1:3000 in 3% milk with PST-T (0.02 % Tween-20)	Polyclonal, Gislene Pereira's gift
Anti-Kin4	Primary	Rabbit	1:3000 in 3% milk with PST-T (0.02 % Tween-20)	Polyclonal, Gislene Pereira's gift
Anti-Tubulin	Primary	Rabbit	1:50000 in 3% milk with PBS-T (0.02 % Tween-20)	Abcam EPR13799 rabbit monoclonal
Anti-mouse with HRP	Secondary	Goat	1:1000 in 3% milk with PBS-T (0.02 % Tween-20)	Advansta R-5071-500
Anti-rabbit with HRP	Secondary	Goat	1:1000 in 3% milk with PBS-T (0.02 % Tween-20)	Advansta R-5062-500

Microscopy analysis

Imaging was performed using Carl ZEISS Axio Observer 7 motorized inverted epifluorescence microscope equipped with Colibri 7 LED light source, Axiocam 702 Monochrome camera, 100X and 63X Plan Apochromat immersion oil objective lenses, Filter sets 95 (GFP/Cherry), 20 (Rhodamin), FITC and DAPI, and an XL incubation and climate chamber. Image acquisition and analysis was performed with ZEN Software and ImageJ/Fiji software.

For budding and mitotic index calculations, cell fixed with 70% Ethanol were visualized. Before microscopy analysis, ethanol precipitated cells were spun down, and ethanol was aspirated totally. The cells were resuspended in DAPI solution (DAPI suspended in PBS as 1 mg/ml). The analyses were done under 63X objective, with DAPI filter.

For time-lapse experiments, cells were grown into filter sterilized SC medium and kept at log phase for 2 days. Then, 150 µl of 6% Concanavalin A (*Canavalia ensiformis* Jack Bean, type IV Sigma C2010-G) was pipetted on the glass center of the glass bottomed petri dish (WVR 10810-054and incubated for 5-10 minutes at room temperature. The Concanavalin A was taken back and taken to -20°C for further use. The glass bottom petri dish was washed with ddH2O three times. After washing, 150 µl of 0.3-0.5 OD_{600} sample was pipetted onto glass bottom petri dish and incubated at 30˚C for 30 minutes. Sample was, then, washed with filter sterilized SC medium 3-4 times. 2-3 mL of SC medium was added onto the dish. The experiments were done at 30°C, under 100X Plan APO 1.25NA objective, a GFP/RFP/MCHERRY/EQFP filter, which all were controlled by ZEN elements software. Z stacks of 10 sections were acquired in 1 min intervals for 1 hour. Light intensity was 7.5% and exposure time was 35 ms for GFP tagged strains.

Time course experiments

Stationary yeast cultures diluted to 0.1 OD and inoculated at 23°C or 30°C until log phase into proper medium. When OD is around 0.5, the cultures were diluted to 0.4 OD and α mating pheromone was added (1 mg/ml in DMSO- from Sigma #T6901). 1,5 doubling time later, the cells were quickly checked under bright field microscope to ensure 95% of the cells had the shmoo tip. Cells were released from alpha factor arrest by 2 times washing with the fresh medium and suspended in final medium (pre-warmed) as 0.4 OD cultures. From these cultures, first samples (t0) were taken: 1 ml of culture was taken for protein pellets (1-2 min centrifuged for 14000 rpm, medium discarded and pellets were taken to -20°C), 300 µl onto 700 µl of 100% ethanol (for ethanol fixation into 70% ethanol-kept in 4°C) and lastly 300 µl onto 600 µl ddH2O

(1:3) for spectrophotometry analysis to determine the necessary HU-DTT amount (see below) for protein samples. At the end of each interval (e.g., every 10 minutes), the same process was repeated, and samples were collected for western blot and microscopy analyses.

PCR-based methods

Colony PCR

Colony PCR was the protocol used for gene cloning purposes and confirming positive candidates in the strain constructions (e.g., gene deletion) together with Western Blot and microscopy. To prepare cell lysates, small amount of yeast cells from a colony were picked up and suspended in 50 µl of 0.01% Sarkosyl and 0.02N NaOH. The solution was boiled for 15 minutes with vigorous shaking and 0.6 µl of cell extract was used for standard 25 µl of PCR reaction with Taq polymerase (NEB M0273S). Reactions were performed as follows - The same protocol can also be used for amplification from plasmid or chromosomal DNA:

cell lysate	0.6 µl
10 µM Primer 1	1.25 µl
10 µM Primer 2	1.25 µl
2 mM dNTPs (Table A5)	2.5 µl
10X PCR Buffer 1 (Table A5)	2.5 µl
ddH2O	16.8 µl
Taq polymerase	0.2 µl

PCR Cycle conditions for colony PCR:

Pre-denaturation:	5 min at 95 ºC
Denaturation:	30 sec. at 95ºC
Annealing:	30 sec at 52-62ºC*
Elongation:	X** min at 72ºC -> turn to denaturation step for 35 times
Final elongation:	10 min at 72ºC
	4ºC (end)

*Annealing temperature of primers is calculated according to base content of primers: 2 x (A+T) + 4 x (G+C)

** X min = is calculated based on length of expected product (1 min per 1000bp).

Cassette PCR

Cassette PCR is used to produce “cassettes”, which are the parts that would be integrated into yeast genome for deletion of the gene, promoter-based over expression or epitope tagging (Janke et al., 2004). Template plasmid DNAs that possess the desired integration product was used to produce cassettes via reaction below for 50 µl solution:

Template (20 ng/µl)	5 µl
10 µM Primer 1	3.2 µl
10 µM Primer 2	3.2 µl
2 mM dNTPs	10.62 µl
PCR Buffer	5 µl
ddH2O	22.38 µl
Enzyme mix*	0.6 µl

*To have proofreading activity 1 part of Vent polymerase (NEB MO254S) was used with 2 parts of Taq polymerase (NEB M0273S).

PCR Cycle conditions for cassette PCR:

1) 2 min at 95 ºC
2) 20 sec. at 95ºC
3) 20 sec at 53ºC
4) X* min at 68ºC -> turn to step 2 for 10 times
5) 30 sec at 94ºC
6) 30 sec at 52ºC
7) X* min at 68ºC, increment of 20 sec per step, -> turn to step 5 to step 7 for 20 times
   4ºC (end)

* X min = is calculated based on length of expected product (1 min per 1000bp).

PCR with Phusion polymerase

For gene cloning, we needed a polymerase that has the proofreading activity to ensure that the insert could be cloned without any mutation in its sequence that might alter its function. We used Phusion® High-Fidelity DNA Polymerase (NEB M0530)

	50 µl Reaction	**Final Concentration**
Nuclease-free water	to 50 µl	
5X Phusion HF or GC Buffer	10 µl	1X
2 mM dNTPs	5 µl	200 µM
10 µM Forward Primer	2.5 µl	0.5 µM
10 µM Reverse Primer	2.5 µl	0.5 µM
Template DNA	2 µl	< 250 ng
Phusion DNA Polymerase	0.5 µl	1.0 units/50 µl PCR

The PCR reaction was performed as follows:

STEP		**TEMP**	**TIME**
Initial Denaturation		98°C	30 seconds
Denaturation	(35 cycles)	98°C	10 seconds
Annealing		54-62°C	30 seconds
Elongation		72°C	30 seconds per kb*
Final Elongation		72°C	10 minutes
Hold		4 °C	

*The size of the expected *NSE4*- and *PHO2* and *SAN1*-bearing PCR products were 1.9, 2.1 kb and 2,5 kb respectively. Accordingly, elongation times for them were 1 min, 1 min and 1,5 min, respectively.

Table A5: Media, Buffer and Reagent Compositions

Name	**Description**
SC or SC-X (X= URA or LEU or HIS or TRP)	3.4 g Bacto yeast nitrogen base without amino acids without ammonium sulfate (Conda pronadisa), 1 g SC-X (or SC) drop out mix, 10 g D (+)-Glucose (BioFroxx), 0.05 g Adenine (Sigma # A8626) and ddH2O up to 500 ml are mixed and autoclaved

YPAD medium	5 g Bacto Yeast Extract (Conda pronadisa), 10 g Bacto Peptone (Merck), 10 g D (+)-Glucose (BioFroxx), 0.05 g Adenine (Sigma), ddH2O up to 500 ml are mixed. Autoclaved or filter sterilized.
SOB medium	20 g Tryptone, 5 g Yeast extract, 10 mL of 1 M NaCl, 5 mL of 0.5 M KCl and ddH2O up to 980 ml were combined and autoclaved together. After that, 10 mL of 1M MgS04 (filter sterilized) + 10 mL 1M MgCl2 Solution (filter sterilized) were added onto the medium.
LB-Medium	5 g NaCl, 5 g Yeast Extract, 10 g Bacto Tryptone, ddH2O up to 1 L. Autoclaved and Ampicillin 100 µg/ml or Kanamycin 50 µg/ml were added after cooling to 50-60^{0}C, if is necesary
LB-agar	5 g NaCl, 5 g Yeast Extract, 10 g Bacto Tryptone are mixed with ddH2O up to 1 L. 20 g Bacto-agar is added and the mixture is autoclaved. Ampicillin 100 µg/ml or Kanamycin 50 µg/ml is added after cooling to 50-60^{0}C, if is necesary.
5-FOA agar	6.7 g Bacto yeast nitrogen base without amino acids without ammonium sulfate (Conda pronadisa), 2 g SC-URA drop-out mix, 20 g Glucose, 0.1 g Uracil, 1 g 5-FOA (US Biological), ddH2O up to 500 ml were mixed and filter-sterilized, then added onto autoclaved 20 g Bacto-agar in 500 ml ddH2O
LiSorb solution	100 mM Lithium acetate (LiOAc), 10 mM Tris pH 8, 1 mM EDTA pH 8, 1 M Sorbitol (Merck), filter sterilized
LiPEG solution	100 mM LiOAc, 10 mM Tris pH 8, 1 mM EDTA pH 8, 40% PEG3350; filter sterilized
%6 SET	3ml %20 SDS + 0.2ml 0,5 M EDTA PH 8.0 + 0.3 ml 1M Tris PH 8.0 + 6,5 ml ddH2O
1X PBS	137 mM NaCl, 2.7 mM KCl, 10 mM Na2HPO4, 1.76 mM KH2PO4. pH 7.2-7.4
1X PBS-T	137 mM NaCl, 2.7 mM KCl, 10 mM Na2HPO4, 1.76 mM KH2PO4. pH 7.2-7.4, 0.05% Tween-20 (AppliChem)
P1 buffer	50mM Tris HCl pH:8, 10mM EDTA + 0,1 mg/ml RNAse A
P2 buffer	200mM NaOH, 1%SDS
P3 buffer	3M KAc pH: 5.5
2 mM dNTP mix	20 µl dATP (100 mM), 20 µl dCTP (100 mM), 20 µl dTTP (100 mM) and 20 µl dGTP (100 mM) + 920 µl ddH2O
HU-DTT	8 M urea, 5% SDS, 200 mM Tris-Cl pH 6.8, 0.1 mM EDTA, bromophenol blue, 100 mM 15 mg/ml DTT
1X Laemmli buffer	25 mM Tris base, 192 mM Glycine, 0.1% SDS, pH 8.3
Ponceau S	0,2 % (w/w) Ponceau S (Sigma #P3504) 3% (w/w) TCA in ddH2O

1X Blotting buffer	25 mM Tris-base, 190 mM glycine, 0.025% SDS, 20% methanol
Home-made ECL	ECL Solution 1: 20 ml 1 M Tris pH 8.5, 2 ml 250 mM luminol (in DMSO, Sigma # A-8511), 889 µl 90 mM p-coumaric acid (in DMSO, Sigma # C-9008), 178 ml H2O ECL Solution 2: 20 ml 1 M Tris, pH 8.5, 180 ml H2O, 123 µl 30% H2O2 (Sigma # H-1009)
10X PCR Buffer 1	500 mM Tris-HCl (pH 9.2), 160 mM (NH4)2SO4, 17.5 mM MgCl2
Freeze-Thaw Buffer	PIPES (10mM, pH:6.7), CaCl2 (15mM), KCl (50mM), MnCl2 (55mM) Filter sterilized

Appendix C: Genetic Screen Assessments

Assessment using Agarose Gel Electrophoresis

After the candidate plasmid transformation into *E. coli*, three single colonies were picked per plasmid and their plasmid DNAs are isolated again. Isolated triplicates were directly loaded into 0.8% agarose gels as 3 microliters per well with 1 microliter loading dye to check if they are identical or not. If all the triplicates represented the same pattern for the respective plasmid, the most concentrated one was used for further studies. If a different pattern occurs among triplicates, every different plasmid was evaluated individually in drop tests.

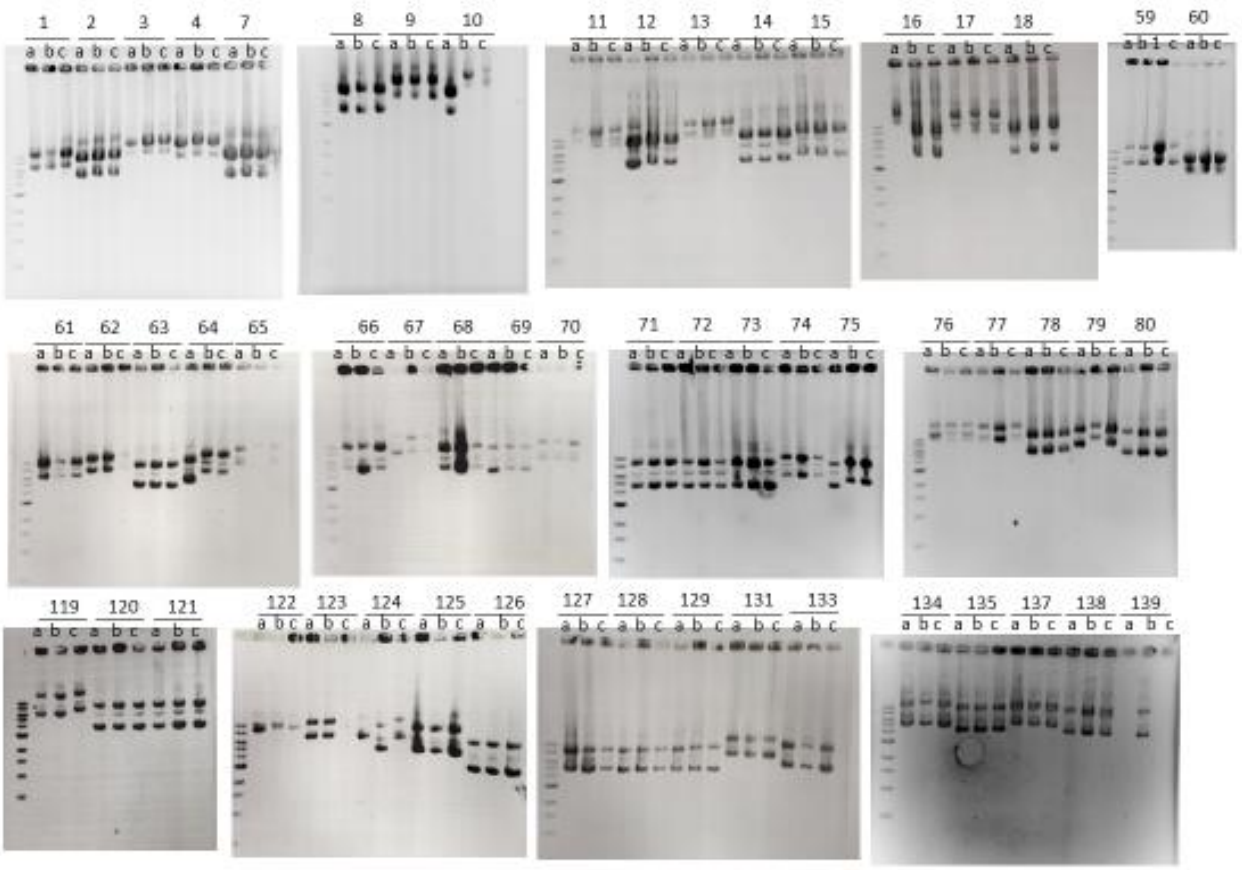

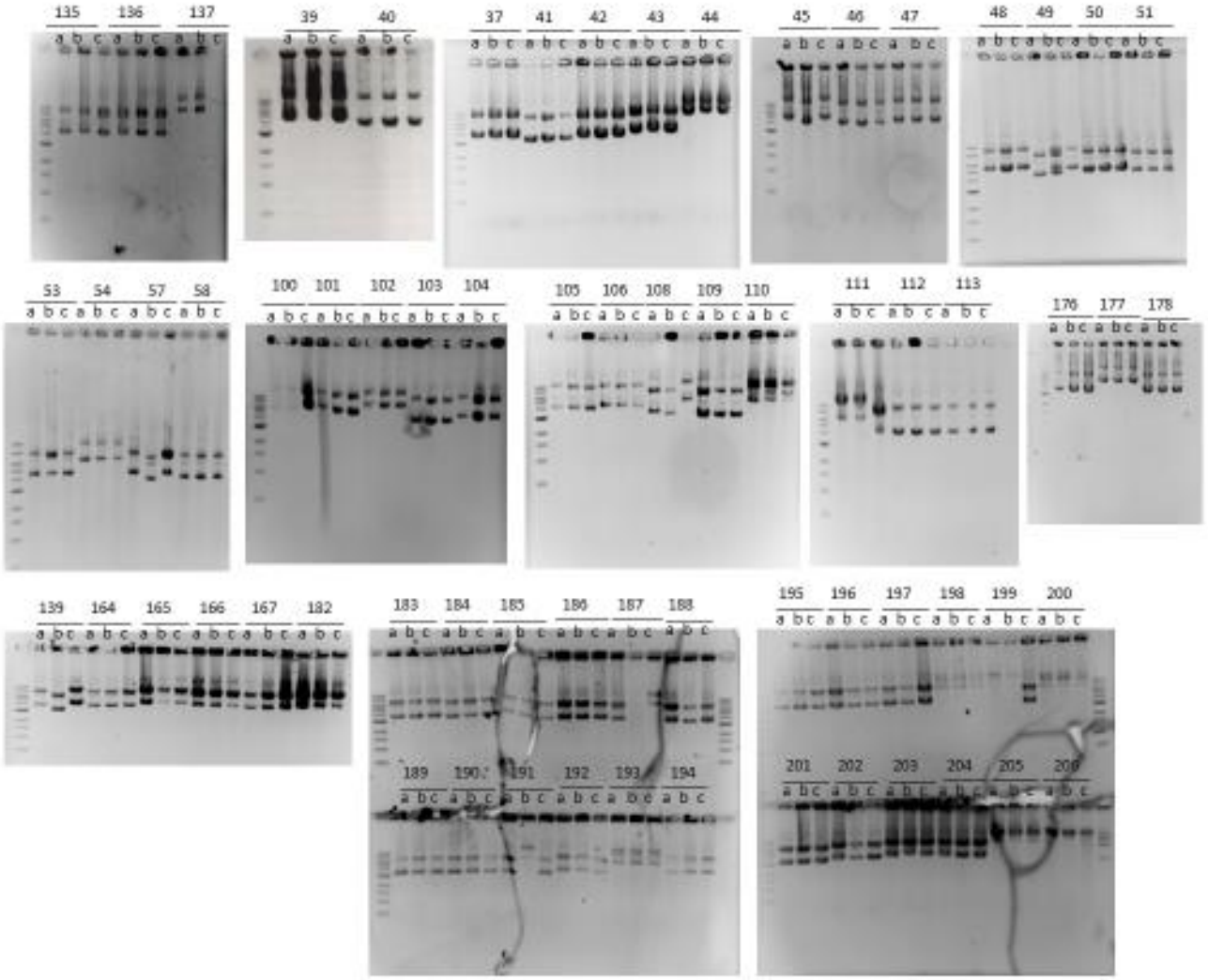
135 136 137
39 40
37 41 42 43 44
45 46 47
48 49 50 51
53 54 57 58
100 101 102 103 104
105 106 108 109 110
111 112 113
176 177 178
139 164 165 166 167 182
183 184 185 186 187 188
189 190 191 192 193 194
195 196 197 198 199 200
201 202 203 204 205 206

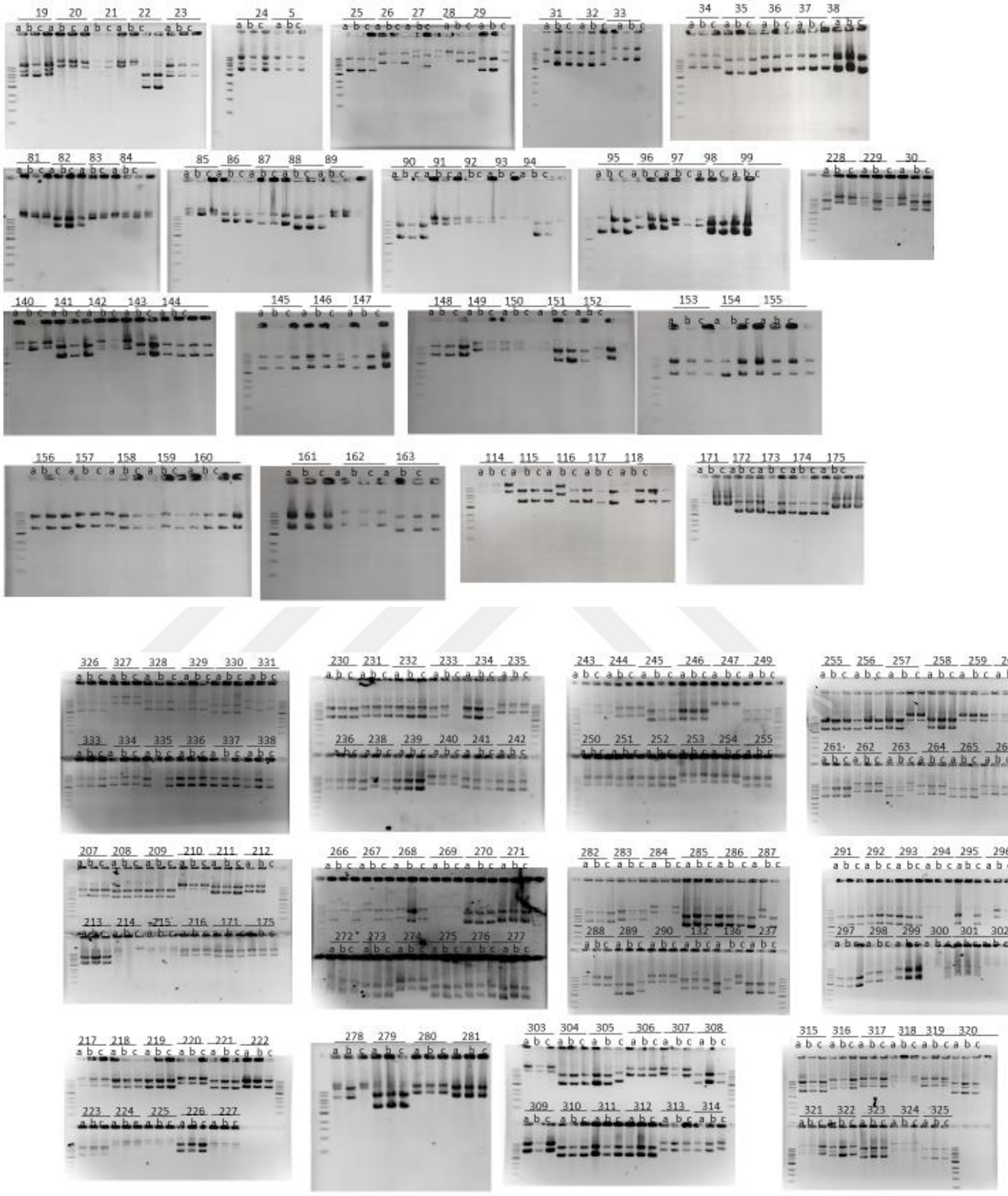

Figure AC1: Agarose Gel Electrophoresis analyses of 370 candidates obtained from the high transformation efficiency based genetic screen.

Assessment using colony formation tests

The candidate plasmids were transformed into starting strain BSY008 and empty plasmid pRS425 were transformed to both BSY007 (*WT* Gal1-*KIN4*) and BSY008 (*mt* Gal1-*KIN4*). BSY007 and BSY008 with Prs425 served as positive and negative controls, respectively and dropped as the first two lanes in this order. A pool of colonies from all transformants were inoculated into SC-LEU medium until stationary phase and 7.5 microliter of the serially diluted cultures were dropped onto SC-LEU and SC-LEU RAF/GAL plates to check the growth of plasmid-bearing strains, in comparison to controls (see Materials and Methods for *Colony Formation Test*).

First assessment: In the first assessment, 10^{-1} to 10^{-3} drops were used in the drop test.

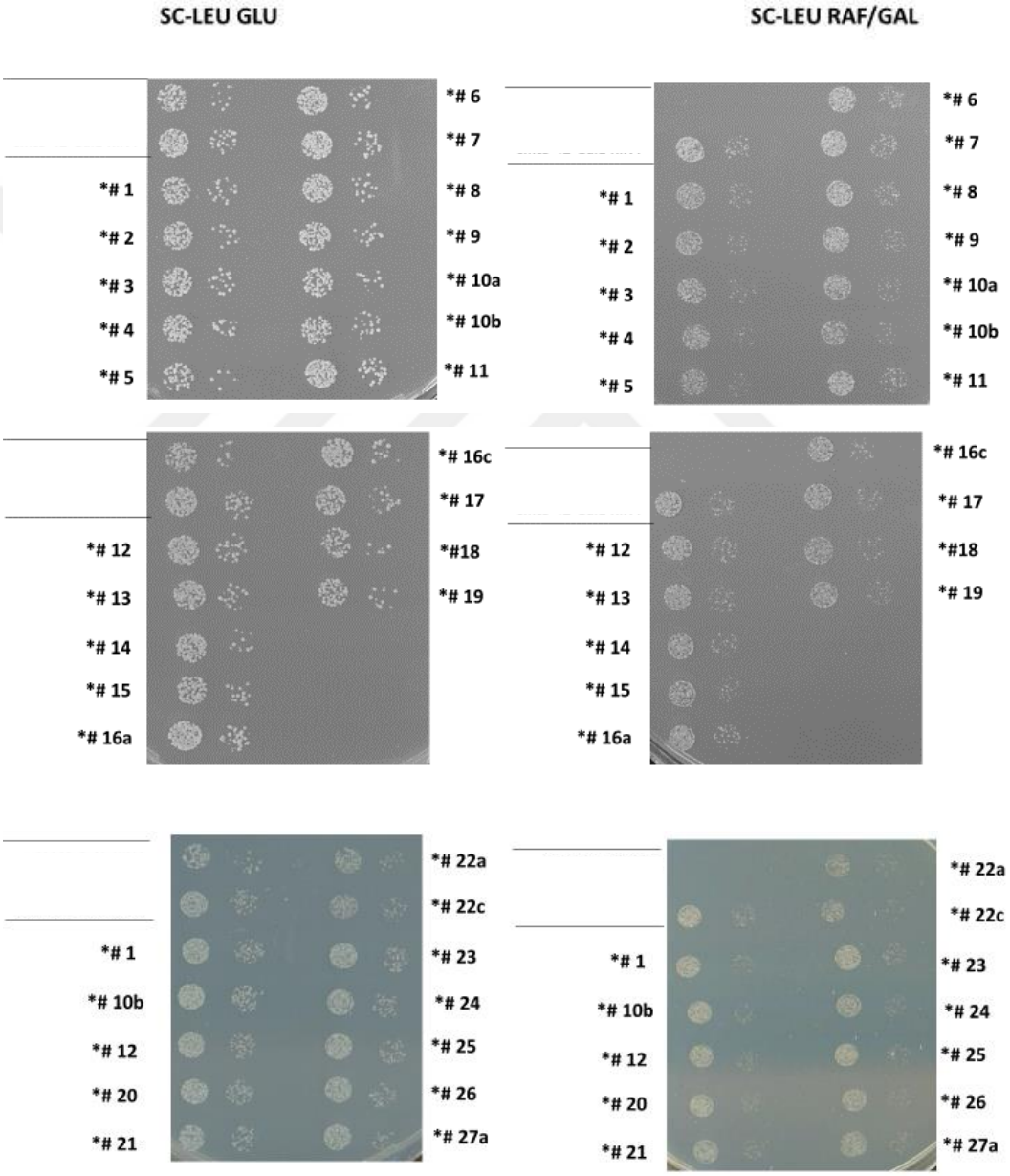

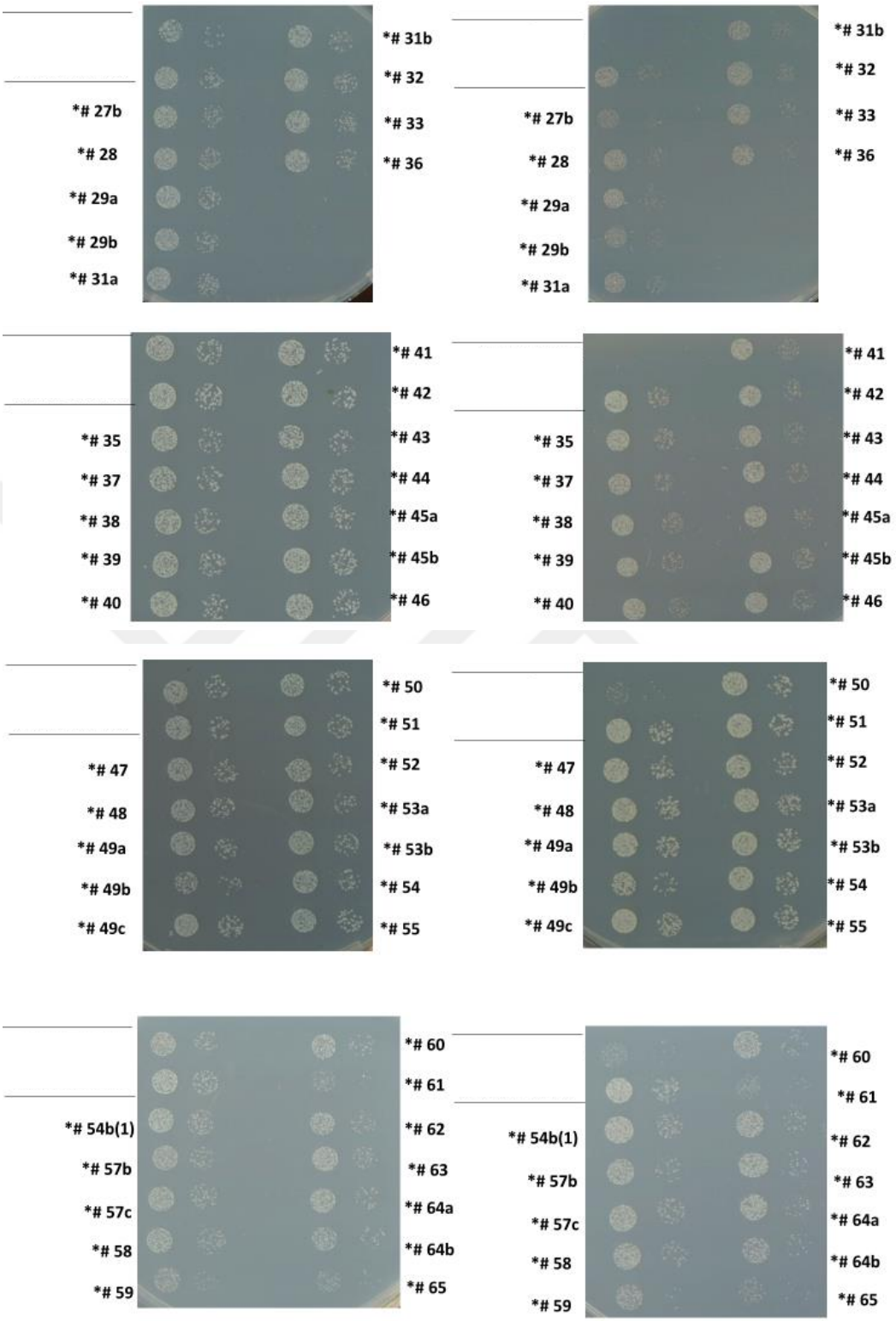
*# 31b
*# 32
*# 27b
*# 33
*# 28
*# 36
*# 29a
*# 29b
*# 31a
*# 41
*# 42
*# 35
*# 43
*# 37
*# 44
*# 38
*# 45a
*# 39
*# 45b
*# 40
*# 46
*# 50
*# 51
*# 47
*# 52
*# 48
*# 53a
*# 49a
*# 53b
*# 49b
*# 54
*# 49c
*# 55
*# 60
*# 61
*# 54b(1)
*# 62
*# 57b
*# 63
*# 57c
*# 64a
*# 58
*# 64b
*# 59
*# 65

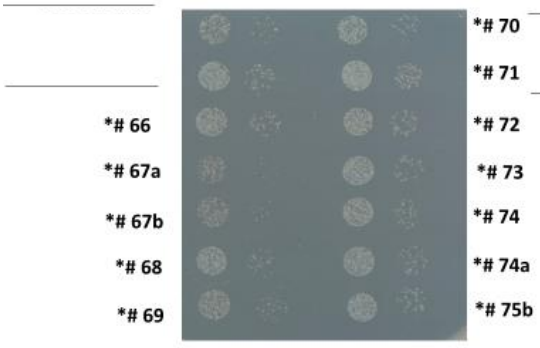
*# 66
*# 67a
*# 67b
*# 68
*# 69
*# 70
*# 71
*# 72
*# 73
*# 74
*# 74a
*# 75b

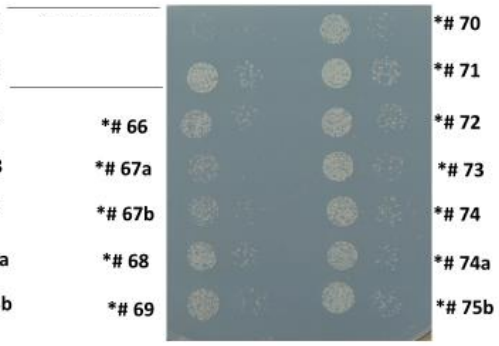
*# 66
*# 67a
*# 67b
*# 68
*# 69
*# 70
*# 71
*# 72
*# 73
*# 74
*# 74a
*# 75b

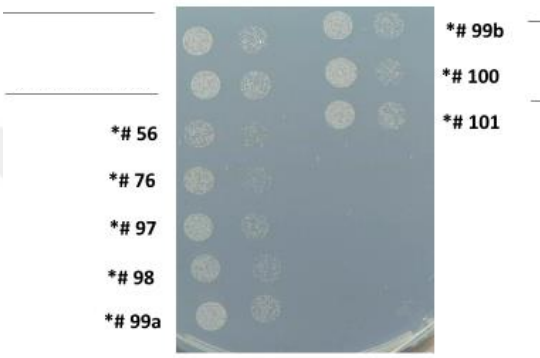
*# 56
*# 76
*# 97
*# 98
*# 99a
*# 99b
*# 100
*# 101

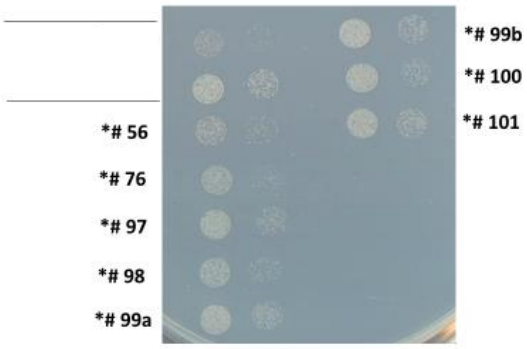
*# 56
*# 76
*# 97
*# 98
*# 99a
*# 99b
*# 100
*# 101

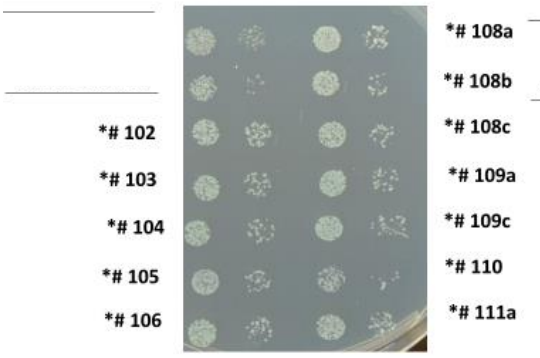
*# 102
*# 103
*# 104
*# 105
*# 106
*# 108a
*# 108b
*# 108c
*# 109a
*# 109c
*# 110
*# 111a

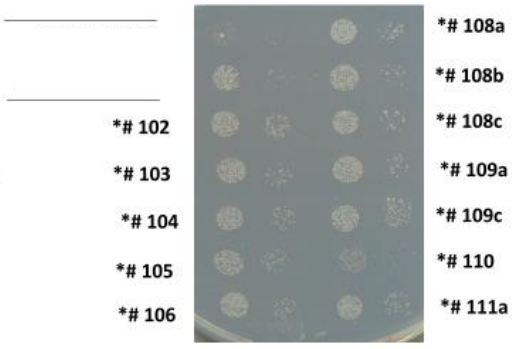
*# 102
*# 103
*# 104
*# 105
*# 106
*# 108a
*# 108b
*# 108c
*# 109a
*# 109c
*# 110
*# 111a

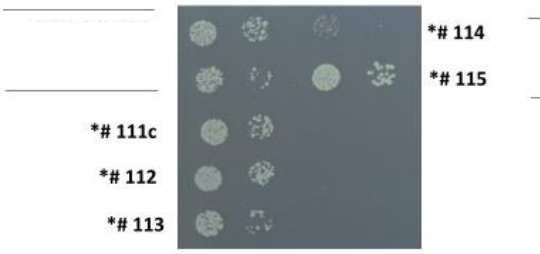
*# 111c
*# 112
*# 113
*# 114
*# 115

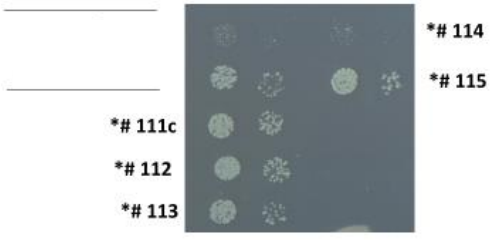
*# 111c
*# 112
*# 113
*# 114
*# 115

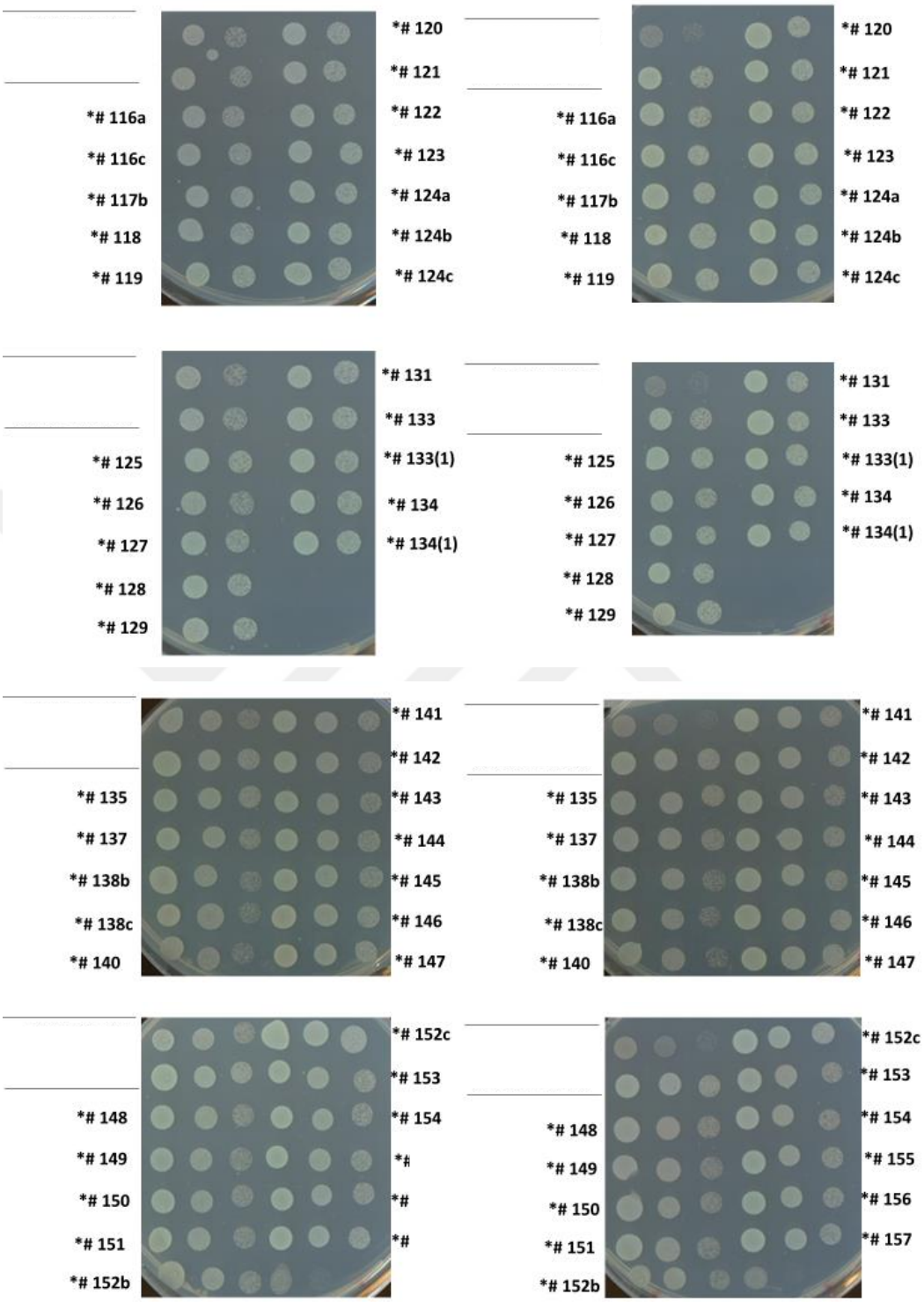
*# 116a
*# 116c
*# 117b
*# 118
*# 119
*# 120
*# 121
*# 122
*# 123
*# 124a
*# 124b
*# 124c
*# 116a
*# 116c
*# 117b
*# 118
*# 119
*# 120
*# 121
*# 122
*# 123
*# 124a
*# 124b
*# 124c
*# 125
*# 126
*# 127
*# 128
*# 129
*# 131
*# 133
*# 133(1)
*# 134
*# 134(1)
*# 125
*# 126
*# 127
*# 128
*# 129
*# 131
*# 133
*# 133(1)
*# 134
*# 134(1)
*# 135
*# 137
*# 138b
*# 138c
*# 140
*# 141
*# 142
*# 143
*# 144
*# 145
*# 146
*# 147
*# 135
*# 137
*# 138b
*# 138c
*# 140
*# 141
*# 142
*# 143
*# 144
*# 145
*# 146
*# 147
*# 148
*# 149
*# 150
*# 151
*# 152b
*# 152c
*# 153
*# 154
*#
*#
*#
*# 148
*# 149
*# 150
*# 151
*# 152b
*# 152c
*# 153
*# 154
*# 155
*# 156
*# 157

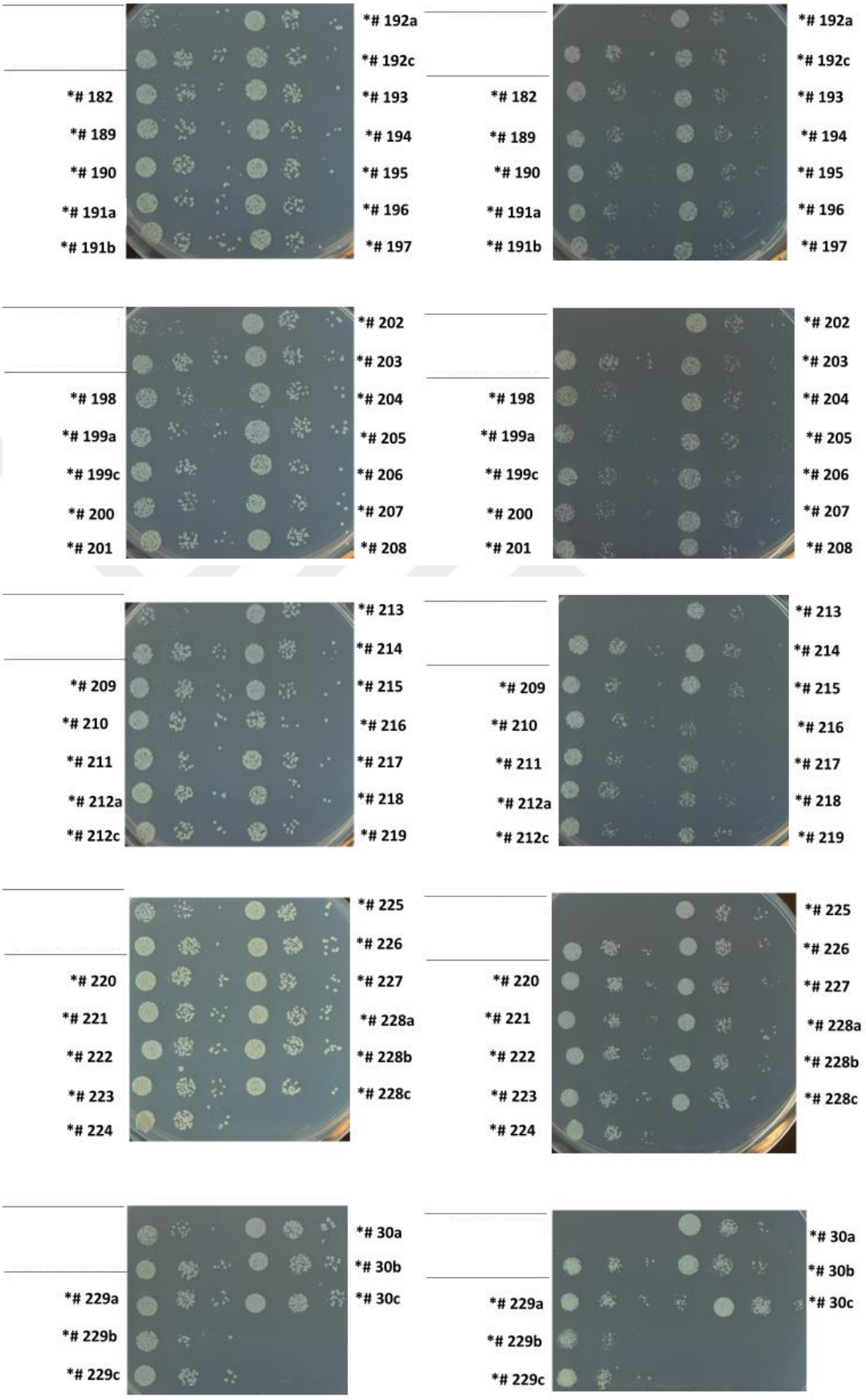
*# 182
*# 189
*# 190
*# 191a
*# 191b
*# 192a
*# 192c
*# 193
*# 194
*# 195
*# 196
*# 197
*# 198
*# 199a
*# 199c
*# 200
*# 201
*# 202
*# 203
*# 204
*# 205
*# 206
*# 207
*# 208
*# 209
*# 210
*# 211
*# 212a
*# 212c
*# 213
*# 214
*# 215
*# 216
*# 217
*# 218
*# 219
*# 220
*# 221
*# 222
*# 223
*# 224
*# 225
*# 226
*# 227
*# 228a
*# 228b
*# 228c
*# 229a
*# 229b
*# 229c
*# 30a
*# 30b
*# 30c

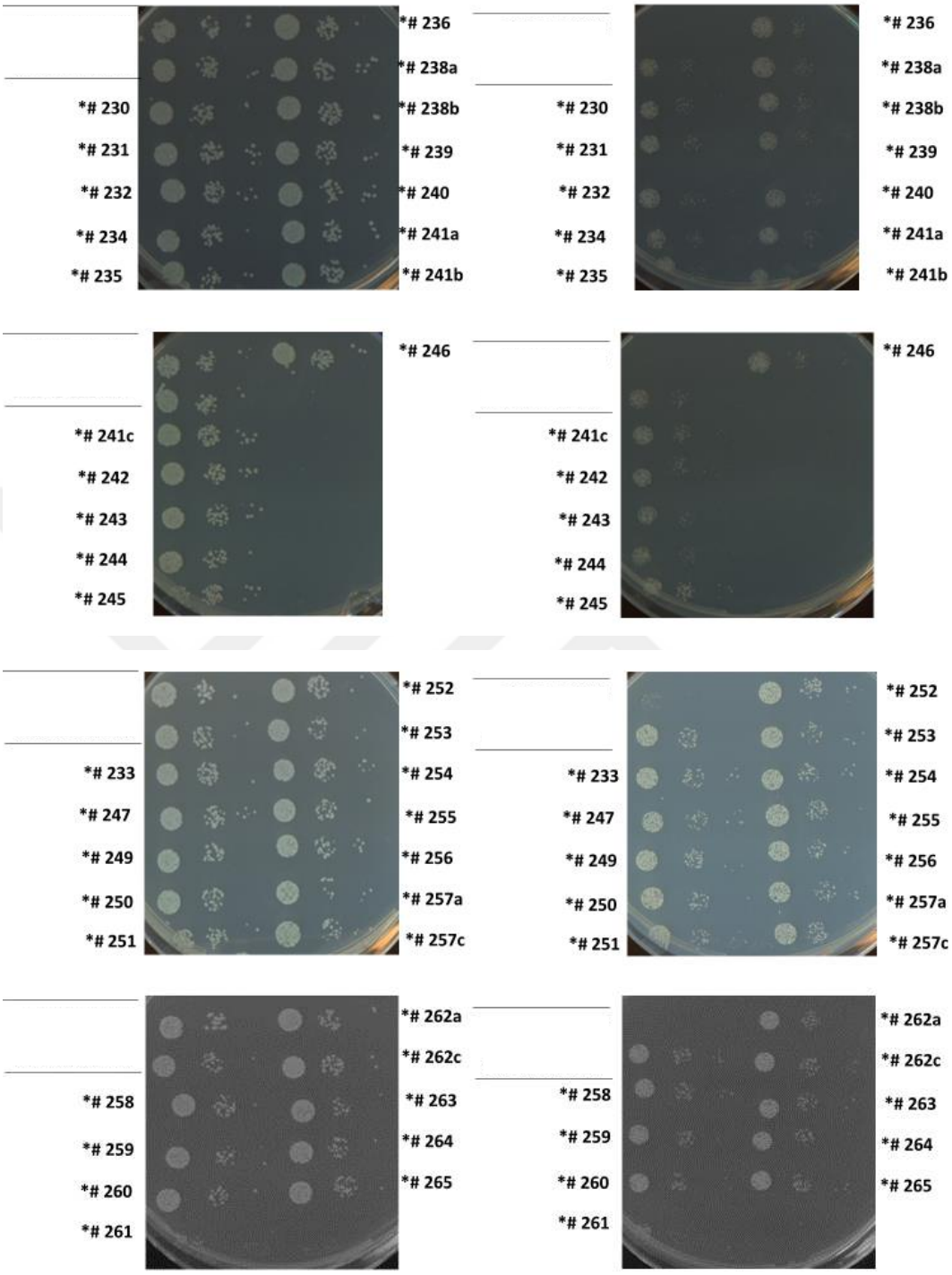
*# 230
*# 231
*# 232
*# 234
*# 235
*# 236
*# 238a
*# 238b
*# 239
*# 240
*# 241a
*# 241b
*# 230
*# 231
*# 232
*# 234
*# 235
*# 236
*# 238a
*# 238b
*# 239
*# 240
*# 241a
*# 241b
*# 241c
*# 242
*# 243
*# 244
*# 245
*# 246
*# 241c
*# 242
*# 243
*# 244
*# 245
*# 246
*# 233
*# 247
*# 249
*# 250
*# 251
*# 252
*# 253
*# 254
*# 255
*# 256
*# 257a
*# 257c
*# 233
*# 247
*# 249
*# 250
*# 251
*# 252
*# 253
*# 254
*# 255
*# 256
*# 257a
*# 257c
*# 258
*# 259
*# 260
*# 261
*# 262a
*# 262c
*# 263
*# 264
*# 265
*# 258
*# 259
*# 260
*# 261
*# 262a
*# 262c
*# 263
*# 264
*# 265

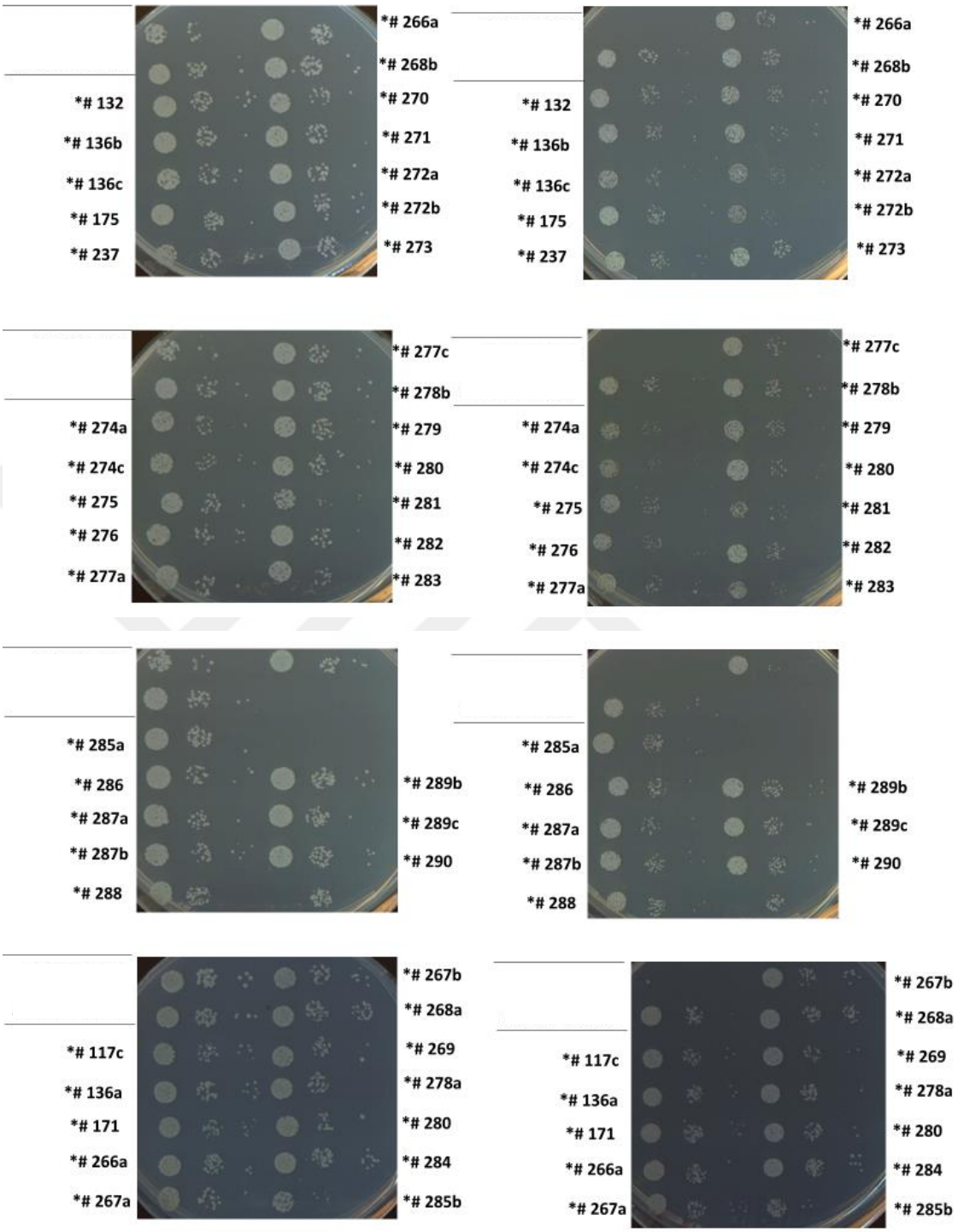
*# 266a
*# 268b
*# 270
*# 271
*# 272a
*# 272b
*# 273
*# 132
*# 136b
*# 136c
*# 175
*# 237
*# 277c
*# 278b
*# 279
*# 280
*# 281
*# 282
*# 283
*# 274a
*# 274c
*# 275
*# 276
*# 277a
*# 289b
*# 289c
*# 290
*# 285a
*# 286
*# 287a
*# 287b
*# 288
*# 267b
*# 268a
*# 269
*# 278a
*# 280
*# 284
*# 285b
*# 117c
*# 136a
*# 171
*# 266a
*# 267a

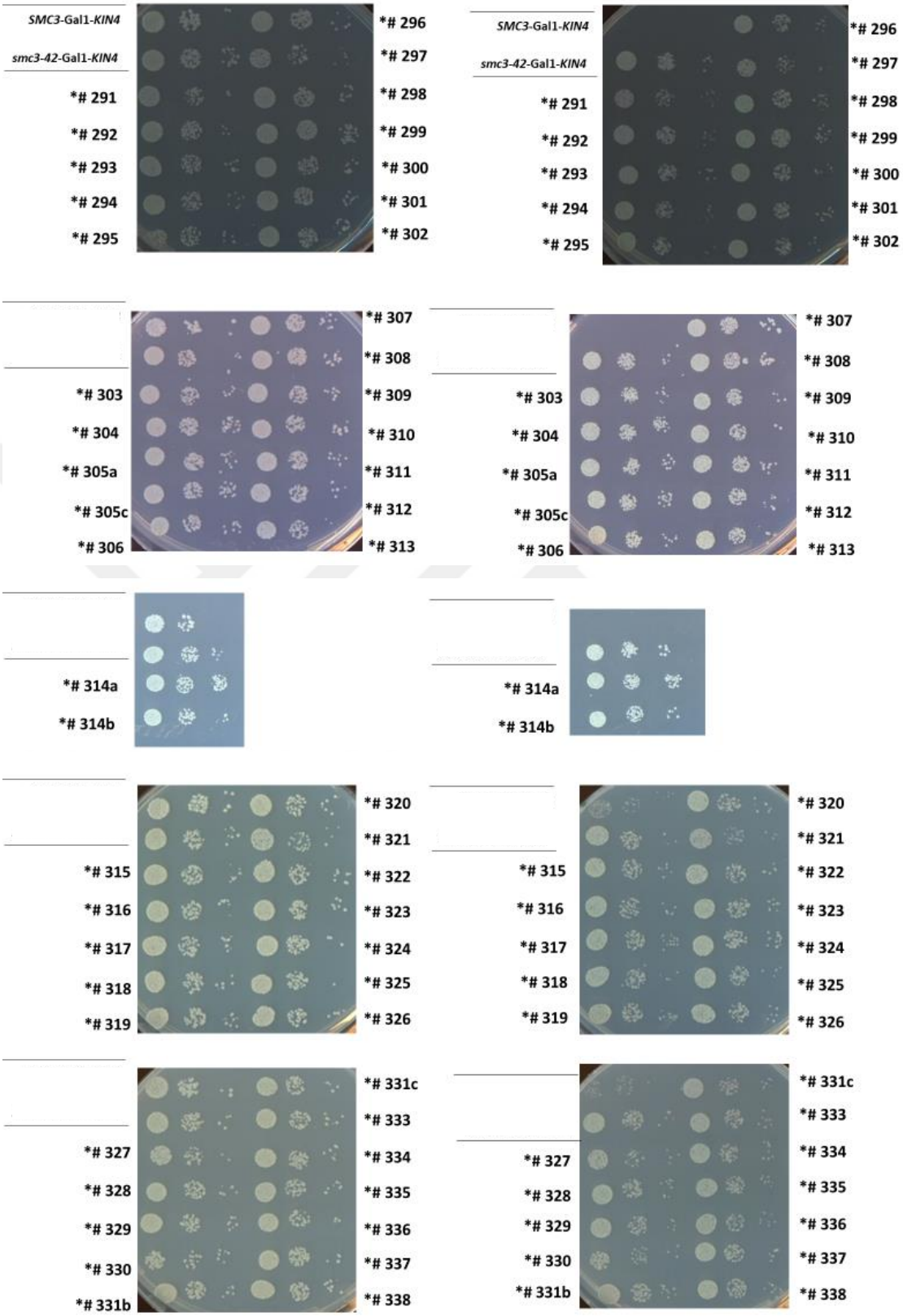
SMC3-Gal1-KIN4
smc3-42-Gal1-KIN4
*# 291
*# 292
*# 293
*# 294
*# 295
*# 296
*# 297
*# 298
*# 299
*# 300
*# 301
*# 302
*# 303
*# 304
*# 305a
*# 305c
*# 306
*# 307
*# 308
*# 309
*# 310
*# 311
*# 312
*# 313
*# 314a
*# 314b
*# 315
*# 316
*# 317
*# 318
*# 319
*# 320
*# 321
*# 322
*# 323
*# 324
*# 325
*# 326
*# 327
*# 328
*# 329
*# 330
*# 331b
*# 331c
*# 333
*# 334
*# 335
*# 336
*# 337
*# 338

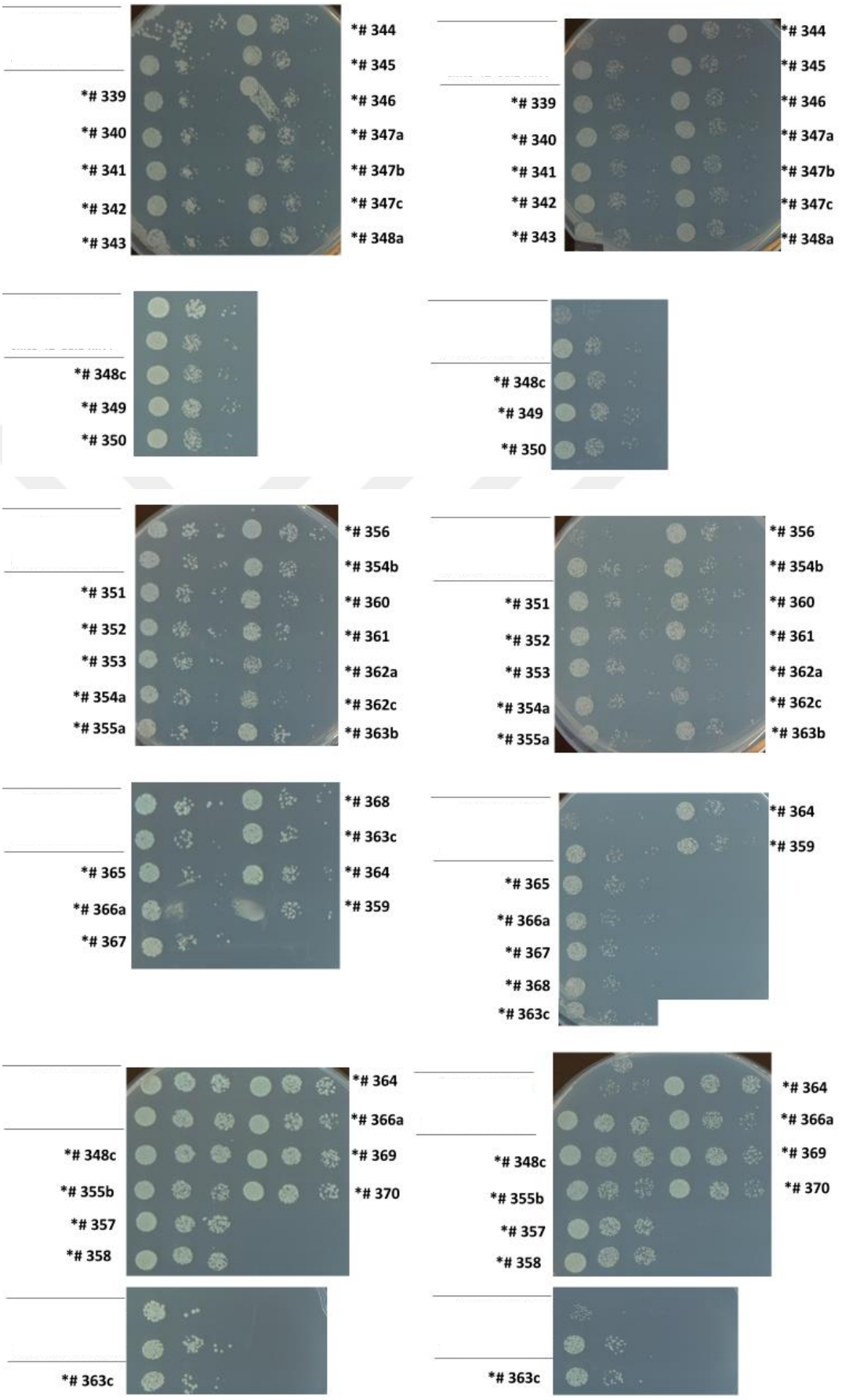
*# 344
*# 345
*# 346
*# 347a
*# 347b
*# 347c
*# 348a
*# 339
*# 340
*# 341
*# 342
*# 343
*# 348c
*# 349
*# 350
*# 356
*# 354b
*# 360
*# 361
*# 362a
*# 362c
*# 363b
*# 351
*# 352
*# 353
*# 354a
*# 355a
*# 368
*# 363c
*# 364
*# 359
*# 365
*# 366a
*# 367
*# 369
*# 370
*# 355b
*# 357
*# 358

Figure AC2: Drop test analyses of 370 candidates obtained from the high transformation efficiency based genetic screen (first assessment).

Second assessment: In final assessment, 24 pre-hits were assessed and 6 of them were selected as hits (see the main text--Chapter 2)

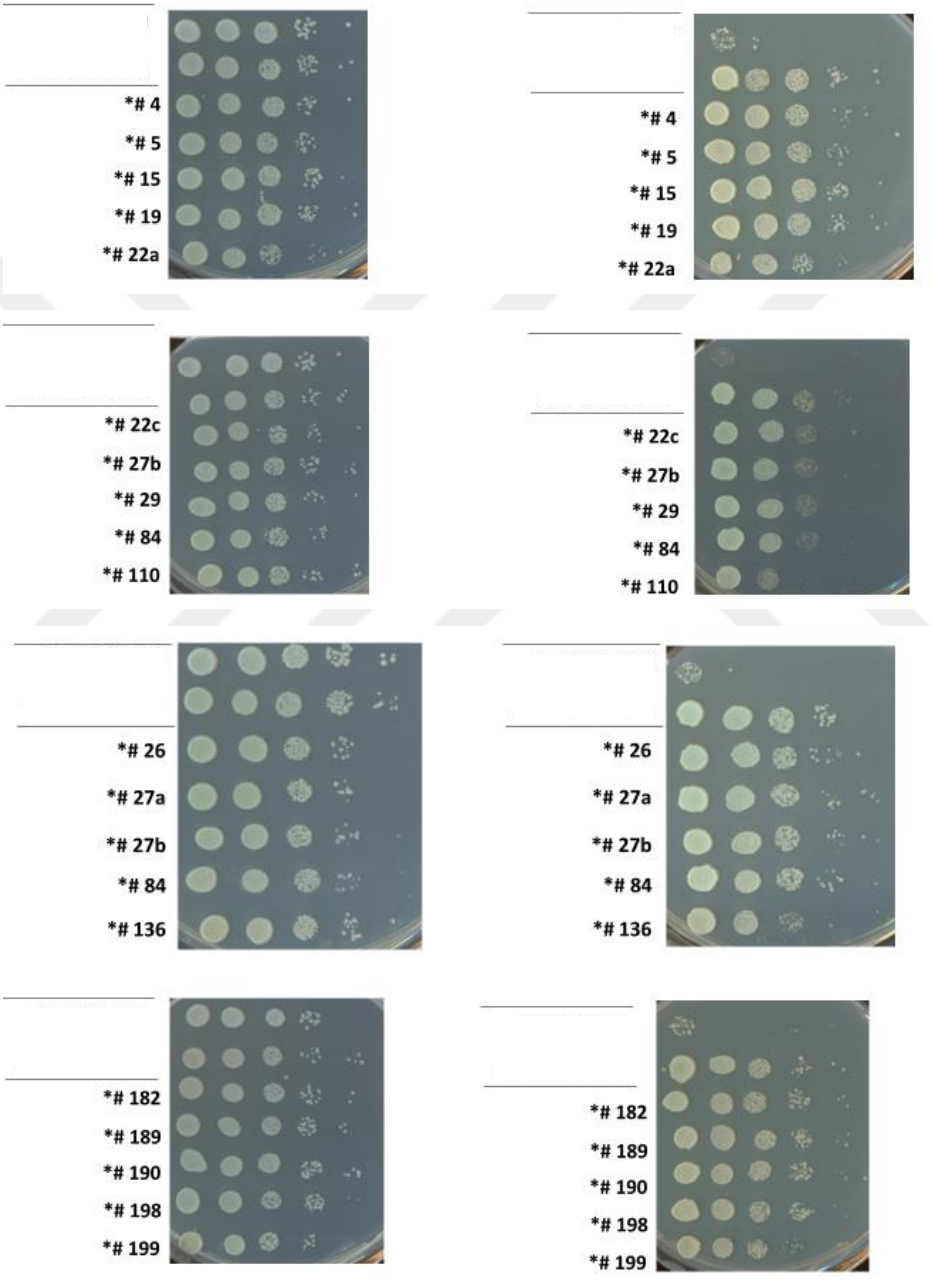

Figure AC3: Drop test analyses of 24 candidates obtained from the high transformation efficiency based genetic screen (second assessment).

Appendix D: Chromosomal Fragments Carried by Hit Plasmids

#84

Interested gene:

SAN1

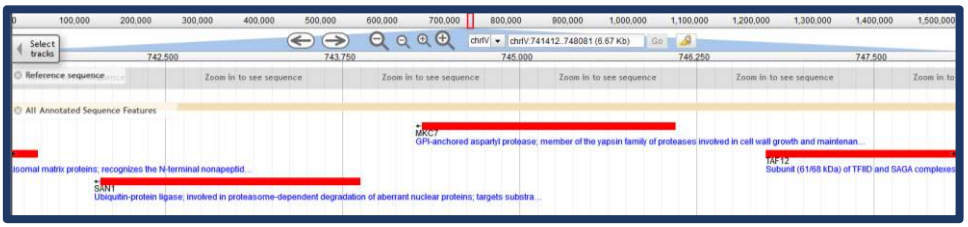

#216 #229 #274

Interested gene:

SAN1

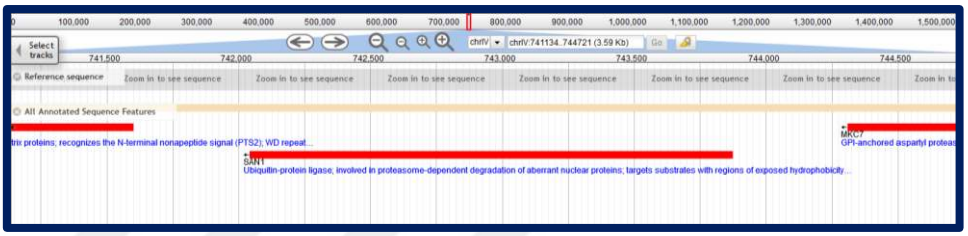

#27 #272

Interested gene:

NSE4 & PHO2

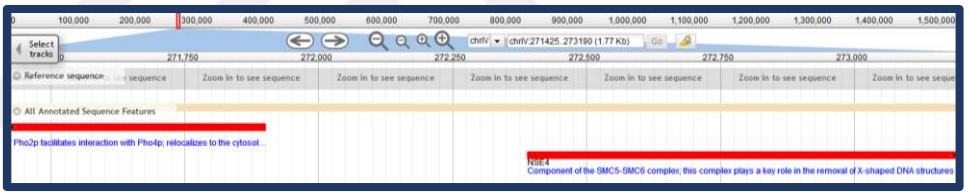

BIBLIOGRAPHY

Akiyoshi, B., and Biggins, S. (2010). Cdc14-dependent dephosphorylation of a kinetochore protein prior to anaphase in Saccharomyces cerevisiae. Genetics *186*, 1487-1491.

Arlt, H., Perz, A., and Ungermann, C. (2011). An overexpression screen in Saccharomyces cerevisiae identifies novel genes that affect endocytic protein trafficking. Traffic *12*, 1592-1603.

Azzam, R., Chen, S.L., Shou, W., Mah, A.S., Alexandru, G., Nasmyth, K., Annan, R.S., Carr, S.A., and Deshaies, R.J. (2004). Phosphorylation by cyclin B-Cdk underlies release of mitotic exit activator Cdc14 from the nucleolus. Science *305*, 516-519.

Bardin, A.J., Visintin, R., and Amon, A. (2000). A mechanism for coupling exit from mitosis to partitioning of the nucleus. Cell *102*, 21-31.

Bertazzi, D.T., Kurtulmus, B., and Pereira, G. (2011). The cortical protein Lte1 promotes mitotic exit by inhibiting the spindle position checkpoint kinase Kin4. J Cell Biol *193*, 1033-1048.

Bos, J.L., Rehmann, H., and Wittinghofer, A. (2007). GEFs and GAPs: critical elements in the control of small G proteins. Cell *129*, 865-877.

Branzei, D., and Foiani, M. (2008). Regulation of DNA repair throughout the cell cycle. Nat Rev Mol Cell Biol *9*, 297-308.

Buvelot, S., Tatsutani, S.Y., Vermaak, D., and Biggins, S. (2003). The budding yeast Ipl1/Aurora protein kinase regulates mitotic spindle disassembly. J Cell Biol *160*, 329-339.

Byers, B., and Goetsch, L. (1975). Behavior of spindles and spindle plaques in the cell cycle and conjugation of Saccharomyces cerevisiae. J Bacteriol *124*, 511-523.

Cai, Q., Wang, W., Gao, Y., Yang, Y., Zhu, Z., and Fan, Q. (2009). Ce-wts-1 plays important roles in Caenorhabditis elegans development. FEBS Lett *583*, 3158-3164.

Caydasi, A.K., Ibrahim, B., and Pereira, G. (2010a). Monitoring spindle orientation: Spindle position checkpoint in charge. Cell Div *5*, 28.

Caydasi, A.K., Kurtulmus, B., Orrico, M.I., Hofmann, A., Ibrahim, B., and Pereira, G. (2010b). Elm1 kinase activates the spindle position checkpoint kinase Kin4. J Cell Biol *190*, 975-989.

Caydasi, A.K., Lohel, M., Grunert, G., Dittrich, P., Pereira, G., and Ibrahim, B. (2012). A dynamical model of the spindle position checkpoint. Mol Syst Biol *8*, 582.

Caydasi, A.K., Micoogullari, Y., Kurtulmus, B., Palani, S., and Pereira, G. (2014). The 14-3-3 protein Bmh1 functions in the spindle position checkpoint by breaking Bfa1 asymmetry at yeast centrosomes. Mol Biol Cell *25*, 2143-2151.

Caydasi, A.K., and Pereira, G. (2009). Spindle alignment regulates the dynamic association of checkpoint proteins with yeast spindle pole bodies. Dev Cell *16*, 146-156.

Cenamor, R., Jimenez, J., Cid, V.J., Nombela, C., and Sanchez, M. (1999). The budding yeast Cdc15 localizes to the spindle pole body in a cell-cycle-dependent manner. Mol Cell Biol Res Commun *2*, 178-184.

Chan, C.S., and Tye, B.K. (1980). Autonomously replicating sequences in Saccharomyces cerevisiae. Proc Natl Acad Sci U S A *77*, 6329-6333.

Chan, L.Y., and Amon, A. (2009). The protein phosphatase 2A functions in the spindle position checkpoint by regulating the checkpoint kinase Kin4. Genes Dev *23*, 1639-1649.

Chan, L.Y., and Amon, A. (2010). Spindle position is coordinated with cell-cycle progression through establishment of mitotic exit-activating and -inhibitory zones. Mol Cell *39*, 444-454.

Charvin, G., Oikonomou, C., Siggia, E.D., and Cross, F.R. (2010). Origin of irreversibility of cell cycle start in budding yeast. PLoS Biol *8*, e1000284.
Cheng, L., Hunke, L., and Hardy, C.F. (1998). Cell cycle regulation of the Saccharomyces cerevisiae polo-like kinase cdc5p. Mol Cell Biol *18*, 7360-7370.
Chibazakura, T. (2004). Cyclin proteolysis and CDK inhibitors: two redundant pathways to maintain genome stability in mammalian cells. Cell Cycle *3*, 1243-1245.
Chibazakura, T., McGrew, S.G., Cooper, J.A., Yoshikawa, H., and Roberts, J.M. (2004). Regulation of cyclin-dependent kinase activity during mitotic exit and maintenance of genome stability by p21, p27, and p107. Proc Natl Acad Sci U S A *101*, 4465-4470.
Chin, C.F., Bennett, A.M., Ma, W.K., Hall, M.C., and Yeong, F.M. (2012). Dependence of Chs2 ER export on dephosphorylation by cytoplasmic Cdc14 ensures that septum formation follows mitosis. Mol Biol Cell *23*, 45-58.
Clemente-Blanco, A., Sen, N., Mayan-Santos, M., Sacristan, M.P., Graham, B., Jarmuz, A., Giess, A., Webb, E., Game, L., Eick, D.*, et al.* (2011). Cdc14 phosphatase promotes segregation of telomeres through repression of RNA polymerase II transcription. Nat Cell Biol *13*, 1450-1456.
Costanzo, M., Nishikawa, J.L., Tang, X., Millman, J.S., Schub, O., Breitkreuz, K., Dewar, D., Rupes, I., Andrews, B., and Tyers, M. (2004). CDK activity antagonizes Whi5, an inhibitor of G1/S transcription in yeast. Cell *117*, 899-913.
D'Amours, D., Stegmeier, F., and Amon, A. (2004). Cdc14 and condensin control the dissolution of cohesin-independent chromosome linkages at repeated DNA. Cell *117*, 455-469.
D'Aquino, K.E., Monje-Casas, F., Paulson, J., Reiser, V., Charles, G.M., Lai, L., Shokat, K.M., and Amon, A. (2005). The protein kinase Kin4 inhibits exit from mitosis in response to spindle position defects. Mol Cell *19*, 223-234.
Dasgupta, A., Ramsey, K.L., Smith, J.S., and Auble, D.T. (2004). Sir Antagonist 1 (San1) is a ubiquitin ligase. J Biol Chem *279*, 26830-26838.
de Barros Lopes, M., Ho, J.Y., and Reed, S.I. (1990). Mutations in cell division cycle genes CDC36 and CDC39 activate the Saccharomyces cerevisiae mating pheromone response pathway. Mol Cell Biol *10*, 2966-2972.
Deshaies, R.J., Chau, V., and Kirschner, M. (1995). Ubiquitination of the G1 cyclin Cln2p by a Cdc34p-dependent pathway. EMBO J *14*, 303-312.
Donovan, J.D., Toyn, J.H., Johnson, A.L., and Johnston, L.H. (1994). P40SDB25, a putative CDK inhibitor, has a role in the M/G1 transition in Saccharomyces cerevisiae. Genes Dev *8*, 1640-1653.
Downey, M., Houlsworth, R., Maringele, L., Rollie, A., Brehme, M., Galicia, S., Guillard, S., Partington, M., Zubko, M.K., Krogan, N.J.*, et al.* (2006). A genome-wide screen identifies the evolutionarily conserved KEOPS complex as a telomere regulator. Cell *124*, 1155-1168.
Ducommun, B., Brambilla, P., Felix, M.A., Franza, B.R., Jr., Karsenti, E., and Draetta, G. (1991). cdc2 phosphorylation is required for its interaction with cyclin. EMBO J *10*, 3311-3319.
Evans, T., Rosenthal, E.T., Youngblom, J., Distel, D., and Hunt, T. (1983). Cyclin: a protein specified by maternal mRNA in sea urchin eggs that is destroyed at each cleavage division. Cell *33*, 389-396.
Falk, J.E., Chan, L.Y., and Amon, A. (2011). Lte1 promotes mitotic exit by controlling the localization of the spindle position checkpoint kinase Kin4. Proc Natl Acad Sci U S A *108*, 12584-12590.

Faust, A.M., Wong, C.C., Yates, J.R., 3rd, Drubin, D.G., and Barnes, G. (2013). The FEAR protein Slk19 restricts Cdc14 phosphatase to the nucleus until the end of anaphase, regulating its participation in mitotic exit in Saccharomyces cerevisiae. PLoS One *8*, e73194.
Fraschini, R., D'Ambrosio, C., Venturetti, M., Lucchini, G., and Piatti, S. (2006). Disappearance of the budding yeast Bub2-Bfa1 complex from the mother-bound spindle pole contributes to mitotic exit. J Cell Biol *172*, 335-346.
Fredrickson, E.K., Gallagher, P.S., Clowes Candadai, S.V., and Gardner, R.G. (2013). Substrate recognition in nuclear protein quality control degradation is governed by exposed hydrophobicity that correlates with aggregation and insolubility. J Biol Chem *288*, 6130-6139.
Furge, K.A., Cheng, Q.C., Jwa, M., Shin, S., Song, K., and Albright, C.F. (1999). Regions of Byr4, a regulator of septation in fission yeast, that bind Spg1 or Cdc16 and form a two-component GTPase-activating protein with Cdc16. J Biol Chem *274*, 11339-11343.
Gardner, R.G., Nelson, Z.W., and Gottschling, D.E. (2005). Degradation-mediated protein quality control in the nucleus. Cell *120*, 803-815.
Geymonat, M., Spanos, A., de Bettignies, G., and Sedgwick, S.G. (2009). Lte1 contributes to Bfa1 localization rather than stimulating nucleotide exchange by Tem1. J Cell Biol *187*, 497-511.
Geymonat, M., Spanos, A., Smith, S.J., Wheatley, E., Rittinger, K., Johnston, L.H., and Sedgwick, S.G. (2002). Control of mitotic exit in budding yeast. In vitro regulation of Tem1 GTPase by Bub2 and Bfa1. J Biol Chem *277*, 28439-28445.
Geymonat, M., Spanos, A., Walker, P.A., Johnston, L.H., and Sedgwick, S.G. (2003). In vitro regulation of budding yeast Bfa1/Bub2 GAP activity by Cdc5. J Biol Chem *278*, 14591-14594.
Godfrey, M., Kuilman, T., and Uhlmann, F. (2015). Nur1 dephosphorylation confers positive feedback to mitotic exit phosphatase activation in budding yeast. PLoS Genet *11*, e1004907.
Gruneberg, U., Campbell, K., Simpson, C., Grindlay, J., and Schiebel, E. (2000). Nud1p links astral microtubule organization and the control of exit from mitosis. EMBO J *19*, 6475-6488.
Gryaznova, Y., Koca Caydasi, A., Malengo, G., Sourjik, V., and Pereira, G. (2016). A FRET-based study reveals site-specific regulation of spindle position checkpoint proteins at yeast centrosomes. Elife *5*.
Hao, Y., Chun, A., Cheung, K., Rashidi, B., and Yang, X. (2008). Tumor suppressor LATS1 is a negative regulator of oncogene YAP. J Biol Chem *283*, 5496-5509.
Hartwell, L.H., Culotti, J., Pringle, J.R., and Reid, B.J. (1974). Genetic control of the cell division cycle in yeast. Science *183*, 46-51.
Harvey, K.F., Pfleger, C.M., and Hariharan, I.K. (2003). The Drosophila Mst ortholog, hippo, restricts growth and cell proliferation and promotes apoptosis. Cell *114*, 457-467.
Higuchi, T., and Uhlmann, F. (2005). Stabilization of microtubule dynamics at anaphase onset promotes chromosome segregation. Nature *433*, 171-176.
Hu, F., Wang, Y., Liu, D., Li, Y., Qin, J., and Elledge, S.J. (2001). Regulation of the Bub2/Bfa1 GAP complex by Cdc5 and cell cycle checkpoints. Cell *107*, 655-665.
Jaspersen, S.L., Charles, J.F., Tinker-Kulberg, R.L., and Morgan, D.O. (1998). A late mitotic regulatory network controlling cyclin destruction in Saccharomyces cerevisiae. Mol Biol Cell *9*, 2803-2817.
Jaspersen, S.L., and Morgan, D.O. (2000). Cdc14 activates cdc15 to promote mitotic exit in budding yeast. Curr Biol *10*, 615-618.

Jaspersen, S.L., and Winey, M. (2004). The budding yeast spindle pole body: structure, duplication, and function. Annu Rev Cell Dev Biol *20*, 1-28.
Johnston, G.C., Pringle, J.R., and Hartwell, L.H. (1977). Coordination of growth with cell division in the yeast Saccharomyces cerevisiae. Exp Cell Res *105*, 79-98.
Justice, R.W., Zilian, O., Woods, D.F., Noll, M., and Bryant, P.J. (1995). The Drosophila tumor suppressor gene warts encodes a homolog of human myotonic dystrophy kinase and is required for the control of cell shape and proliferation. Genes Dev *9*, 534-546.
Kang, J., Shin, D., Yu, J.R., and Lee, J. (2009). Lats kinase is involved in the intestinal apical membrane integrity in the nematode Caenorhabditis elegans. Development *136*, 2705-2715.
Keng, T., Clark, M.W., Storms, R.K., Fortin, N., Zhong, W., Ouellette, B.F., Barton, A.B., Kaback, D.B., and Bussey, H. (1994). LTE1 of Saccharomyces cerevisiae is a 1435 codon open reading frame that has sequence similarities to guanine nucleotide releasing factors. Yeast *10*, 953-958.
Khmelinskii, A., Lawrence, C., Roostalu, J., and Schiebel, E. (2007). Cdc14-regulated midzone assembly controls anaphase B. J Cell Biol *177*, 981-993.
Kim, J., Luo, G., Bahk, Y.Y., and Song, K. (2012). Cdc5-dependent asymmetric localization of bfa1 fine-tunes timely mitotic exit. PLoS Genet *8*, e1002450.
Knapp, D., Bhoite, L., Stillman, D.J., and Nasmyth, K. (1996). The transcription factor Swi5 regulates expression of the cyclin kinase inhibitor p40SIC1. Mol Cell Biol *16*, 5701-5707.
Knop, M., and Schiebel, E. (1997). Spc98p and Spc97p of the yeast gamma-tubulin complex mediate binding to the spindle pole body via their interaction with Spc110p. EMBO J *16*, 6985-6995.
Koch, C., Moll, T., Neuberg, M., Ahorn, H., and Nasmyth, K. (1993). A role for the transcription factors Mbp1 and Swi4 in progression from G1 to S phase. Science *261*, 1551-1557.
Koch, C., Schleiffer, A., Ammerer, G., and Nasmyth, K. (1996). Switching transcription on and off during the yeast cell cycle: Cln/Cdc28 kinases activate bound transcription factor SBF (Swi4/Swi6) at start, whereas Clb/Cdc28 kinases displace it from the promoter in G2. Genes Dev *10*, 129-141.
Lavoie, B.D., Hogan, E., and Koshland, D. (2004). In vivo requirements for rDNA chromosome condensation reveal two cell-cycle-regulated pathways for mitotic chromosome folding. Genes Dev *18*, 76-87.
Lee, M.G., and Nurse, P. (1987). Complementation used to clone a human homologue of the fission yeast cell cycle control gene cdc2. Nature *327*, 31-35.
Lee, S.E., Frenz, L.M., Wells, N.J., Johnson, A.L., and Johnston, L.H. (2001). Order of function of the budding-yeast mitotic exit-network proteins Tem1, Cdc15, Mob1, Dbf2, and Cdc5. Curr Biol *11*, 784-788.
Liu, C., Yang, Z., Yang, J., Xia, Z., and Ao, S. (2000). Regulation of the yeast transcriptional factor PHO2 activity by phosphorylation. J Biol Chem *275*, 31972-31978.
Maekawa, H., Priest, C., Lechner, J., Pereira, G., and Schiebel, E. (2007). The yeast centrosome translates the positional information of the anaphase spindle into a cell cycle signal. J Cell Biol *179*, 423-436.
Meitinger, F., Petrova, B., Lombardi, I.M., Bertazzi, D.T., Hub, B., Zentgraf, H., and Pereira, G. (2010). Targeted localization of Inn1, Cyk3 and Chs2 by the mitotic-exit network regulates cytokinesis in budding yeast. J Cell Sci *123*, 1851-1861.
Mendenhall, M.D. (1993). An inhibitor of p34CDC28 protein kinase activity from Saccharomyces cerevisiae. Science *259*, 216-219.

Metzger, M.B., Scales, J.L., Dunklebarger, M.F., Loncarek, J., and Weissman, A.M. (2020). A protein quality control pathway at the mitochondrial outer membrane. Elife *9*.
Miller, D.P., Hall, H., Chaparian, R., Mara, M., Mueller, A., Hall, M.C., and Shannon, K.B. (2015). Dephosphorylation of Iqg1 by Cdc14 regulates cytokinesis in budding yeast. Mol Biol Cell *26*, 2913-2926.
Miller RK, R.M. (1998). Kar9p is a novel cortical protein required for cytoplasmic microtubule orientation in yeast. The Journal of Cell Biology *140(2):377-390*.
Mirchenko, L., and Uhlmann, F. (2010). Sli15(INCENP) dephosphorylation prevents mitotic checkpoint reengagement due to loss of tension at anaphase onset. Curr Biol *20*, 1396-1401.
Mohl, D.A., Huddleston, M.J., Collingwood, T.S., Annan, R.S., and Deshaies, R.J. (2009). Dbf2-Mob1 drives relocalization of protein phosphatase Cdc14 to the cytoplasm during exit from mitosis. J Cell Biol *184*, 527-539.
Molk, J.N., Schuyler, S.C., Liu, J.Y., Evans, J.G., Salmon, E.D., Pellman, D., and Bloom, K. (2004). The differential roles of budding yeast Tem1p, Cdc15p, and Bub2p protein dynamics in mitotic exit. Mol Biol Cell *15*, 1519-1532.
Morgan, D.O. (1995). Principles of CDK regulation. Nature *374*, 131-134.
Morgan, D.O. (1997). Cyclin-dependent kinases: engines, clocks, and microprocessors. Annu Rev Cell Dev Biol *13*, 261-291.
Nakajima, Y., Cormier, A., Tyers, R.G., Pigula, A., Peng, Y., Drubin, D.G., and Barnes, G. (2011). Ipl1/Aurora-dependent phosphorylation of Sli15/INCENP regulates CPC-spindle interaction to ensure proper microtubule dynamics. J Cell Biol *194*, 137-153.
Nash, P., Tang, X., Orlicky, S., Chen, Q., Gertler, F.B., Mendenhall, M.D., Sicheri, F., Pawson, T., and Tyers, M. (2001). Multisite phosphorylation of a CDK inhibitor sets a threshold for the onset of DNA replication. Nature *414*, 514-521.
Nasmyth, K., and Dirick, L. (1991). The role of SWI4 and SWI6 in the activity of G1 cyclins in yeast. Cell *66*, 995-1013.
Nasmyth, K., and Nurse, P. (1981). Cell division cycle mutants altered in DNA replication and mitosis in the fission yeast Schizosaccharomyces pombe. Mol Gen Genet *182*, 119-124.
Niu, W., Li, Z., Zhan, W., Iyer, V.R., and Marcotte, E.M. (2008). Mechanisms of cell cycle control revealed by a systematic and quantitative overexpression screen in S. cerevisiae. PLoS Genet *4*, e1000120.
Nurse, P., and Bissett, Y. (1981). Gene required in G1 for commitment to cell cycle and in G2 for control of mitosis in fission yeast. Nature *292*, 558-560.
Nurse, P., Thuriaux, P., and Nasmyth, K. (1976). Genetic control of the cell division cycle in the fission yeast Schizosaccharomyces pombe. Mol Gen Genet *146*, 167-178.
Oka, T., Mazack, V., and Sudol, M. (2008). Mst2 and Lats kinases regulate apoptotic function of Yes kinase-associated protein (YAP). J Biol Chem *283*, 27534-27546.
Olafsson, G., and Thorpe, P.H. (2015). Synthetic physical interactions map kinetochore regulators and regions sensitive to constitutive Cdc14 localization. Proc Natl Acad Sci U S A *112*, 10413-10418.
Orr-Weaver, T.L., Szostak, J.W., and Rothstein, R.J. (1981). Yeast transformation: a model system for the study of recombination. Proc Natl Acad Sci U S A *78*, 6354-6358.
Palani, S., Meitinger, F., Boehm, M.E., Lehmann, W.D., and Pereira, G. (2012). Cdc14-dependent dephosphorylation of Inn1 contributes to Inn1-Cyk3 complex formation. J Cell Sci *125*, 3091-3096.

Panasenko, O., Landrieux, E., Feuermann, M., Finka, A., Paquet, N., and Collart, M.A. (2006). The yeast Ccr4-Not complex controls ubiquitination of the nascent-associated polypeptide (NAC-EGD) complex. J Biol Chem *281*, 31389-31398.
Pereira, F.B., Teixeira, M.C., Mira, N.P., Sa-Correia, I., and Domingues, L. (2014). Genome-wide screening of Saccharomyces cerevisiae genes required to foster tolerance towards industrial wheat straw hydrolysates. J Ind Microbiol Biotechnol *41*, 1753-1761.
Pereira, G., Hofken, T., Grindlay, J., Manson, C., and Schiebel, E. (2000). The Bub2p spindle checkpoint links nuclear migration with mitotic exit. Mol Cell *6*, 1-10.
Pereira, G., Manson, C., Grindlay, J., and Schiebel, E. (2002). Regulation of the Bfa1p-Bub2p complex at spindle pole bodies by the cell cycle phosphatase Cdc14p. J Cell Biol *157*, 367-379.
Pereira, G., and Schiebel, E. (2003). Separase regulates INCENP-Aurora B anaphase spindle function through Cdc14. Science *302*, 2120-2124.
Pereira, G., Tanaka, T.U., Nasmyth, K., and Schiebel, E. (2001). Modes of spindle pole body inheritance and segregation of the Bfa1p-Bub2p checkpoint protein complex. EMBO J *20*, 6359-6370.
Petersen, J., and Hagan, I.M. (2003). S. pombe aurora kinase/survivin is required for chromosome condensation and the spindle checkpoint attachment response. Curr Biol *13*, 590-597.
Prasad, R., Kawaguchi, S., and Ng, D.T. (2010). A nucleus-based quality control mechanism for cytosolic proteins. Mol Biol Cell *21*, 2117-2127.
Queralt, E., Lehane, C., Novak, B., and Uhlmann, F. (2006). Downregulation of PP2A(Cdc55) phosphatase by separase initiates mitotic exit in budding yeast. Cell *125*, 719-732.
Queralt, E., and Uhlmann, F. (2008). Separase cooperates with Zds1 and Zds2 to activate Cdc14 phosphatase in early anaphase. J Cell Biol *182*, 873-883.
Ratsima, H., Ladouceur, A.M., Pascariu, M., Sauve, V., Salloum, Z., Maddox, P.S., and D'Amours, D. (2011). Independent modulation of the kinase and polo-box activities of Cdc5 protein unravels unique roles in the maintenance of genome stability. Proc Natl Acad Sci U S A *108*, E914-923.
Richardson, P.M., and Zon, L.I. (1995). Molecular cloning of a cDNA with a novel domain present in the tre-2 oncogene and the yeast cell cycle regulators BUB2 and cdc16. Oncogene *11*, 1139-1148.
Rock, J.M., and Amon, A. (2011). Cdc15 integrates Tem1 GTPase-mediated spatial signals with Polo kinase-mediated temporal cues to activate mitotic exit. Genes Dev *25*, 1943-1954.
Rock, J.M., Lim, D., Stach, L., Ogrodowicz, R.W., Keck, J.M., Jones, M.H., Wong, C.C., Yates, J.R., 3rd, Winey, M., Smerdon, S.J.*, et al.* (2013). Activation of the yeast Hippo pathway by phosphorylation-dependent assembly of signaling complexes. Science *340*, 871-875.
Rosenbaum, J.C., Fredrickson, E.K., Oeser, M.L., Garrett-Engele, C.M., Locke, M.N., Richardson, L.A., Nelson, Z.W., Hetrick, E.D., Milac, T.I., Gottschling, D.E.*, et al.* (2011). Disorder targets misorder in nuclear quality control degradation: a disordered ubiquitin ligase directly recognizes its misfolded substrates. Mol Cell *41*, 93-106.
Rozelle, D.K., Hansen, S.D., and Kaplan, K.B. (2011). Chromosome passenger complexes control anaphase duration and spindle elongation via a kinesin-5 brake. J Cell Biol *193*, 285-294.

Schmidt, S., Sohrmann, M., Hofmann, K., Woollard, A., and Simanis, V. (1997). The Spg1p GTPase is an essential, dosage-dependent inducer of septum formation in Schizosaccharomyces pombe. Genes Dev *11*, 1519-1534.
Schneider, B.L., Yang, Q.H., and Futcher, A.B. (1996). Linkage of replication to start by the Cdk inhibitor Sic1. Science *272*, 560-562.
Schnell, R., D'Ari, L., Foss, M., Goodman, D., and Rine, J. (1989). Genetic and molecular characterization of suppressors of SIR4 mutations in Saccharomyces cerevisiae. Genetics *122*, 29-46.
Schwob, E., Bohm, T., Mendenhall, M.D., and Nasmyth, K. (1994). The B-type cyclin kinase inhibitor p40SIC1 controls the G1 to S transition in S. cerevisiae. Cell *79*, 233-244.
Sen, R., Ferdoush, J., Kaja, A., and Bhaumik, S.R. (2016). Fine-Tuning of FACT by the Ubiquitin Proteasome System in Regulation of Transcriptional Elongation. Mol Cell Biol *36*, 1691-1703.
Shirayama, M., Matsui, Y., Tanaka, K., and Toh-e, A. (1994a). Isolation of a CDC25 family gene, MSI2/LTE1, as a multicopy suppressor of ira1. Yeast *10*, 451-461.
Shirayama, M., Matsui, Y., and Toh, E.A. (1994b). The yeast TEM1 gene, which encodes a GTP-binding protein, is involved in termination of M phase. Mol Cell Biol *14*, 7476-7482.
Shirayama, M., Toth, A., Galova, M., and Nasmyth, K. (1999). APC(Cdc20) promotes exit from mitosis by destroying the anaphase inhibitor Pds1 and cyclin Clb5. Nature *402*, 203-207.
Shirayama, M., Zachariae, W., Ciosk, R., and Nasmyth, K. (1998). The Polo-like kinase Cdc5p and the WD-repeat protein Cdc20p/fizzy are regulators and substrates of the anaphase promoting complex in Saccharomyces cerevisiae. EMBO J *17*, 1336-1349.
Shou, W., Azzam, R., Chen, S.L., Huddleston, M.J., Baskerville, C., Charbonneau, H., Annan, R.S., Carr, S.A., and Deshaies, R.J. (2002). Cdc5 influences phosphorylation of Net1 and disassembly of the RENT complex. BMC Mol Biol *3*, 3.
Shou, W., Seol, J.H., Shevchenko, A., Baskerville, C., Moazed, D., Chen, Z.W., Jang, J., Shevchenko, A., Charbonneau, H., and Deshaies, R.J. (1999). Exit from mitosis is triggered by Tem1-dependent release of the protein phosphatase Cdc14 from nucleolar RENT complex. Cell *97*, 233-244.
Sillje, H.H., ter Schure, E.G., Rommens, A.J., Huls, P.G., Woldringh, C.L., Verkleij, A.J., Boonstra, J., and Verrips, C.T. (1997). Effects of different carbon fluxes on G1 phase duration, cyclin expression, and reserve carbohydrate metabolism in Saccharomyces cerevisiae. J Bacteriol *179*, 6560-6565.
Stegmeier, F., and Amon, A. (2004). Closing mitosis: the functions of the Cdc14 phosphatase and its regulation. Annu Rev Genet *38*, 203-232.
Stegmeier, F., Huang, J., Rahal, R., Zmolik, J., Moazed, D., and Amon, A. (2004). The replication fork block protein Fob1 functions as a negative regulator of the FEAR network. Curr Biol *14*, 467-480.
Stegmeier, F., Visintin, R., and Amon, A. (2002). Separase, polo kinase, the kinetochore protein Slk19, and Spo12 function in a network that controls Cdc14 localization during early anaphase. Cell *108*, 207-220.
Stoepel, J., Ottey, M.A., Kurischko, C., Hieter, P., and Luca, F.C. (2005). The mitotic exit network Mob1p-Dbf2p kinase complex localizes to the nucleus and regulates passenger protein localization. Mol Biol Cell *16*, 5465-5479.

Straight, A.F., Shou, W., Dowd, G.J., Turck, C.W., Deshaies, R.J., Johnson, A.D., and Moazed, D. (1999). Net1, a Sir2-associated nucleolar protein required for rDNA silencing and nucleolar integrity. Cell *97*, 245-256.
Sullivan, M., Higuchi, T., Katis, V.L., and Uhlmann, F. (2004). Cdc14 phosphatase induces rDNA condensation and resolves cohesin-independent cohesion during budding yeast anaphase. Cell *117*, 471-482.
Sullivan, M., Lehane, C., and Uhlmann, F. (2001). Orchestrating anaphase and mitotic exit: separase cleavage and localization of Slk19. Nat Cell Biol *3*, 771-777.
Sullivan, M., and Uhlmann, F. (2003). A non-proteolytic function of separase links the onset of anaphase to mitotic exit. Nat Cell Biol *5*, 249-254.
Svensson, J.P., Pesudo, L.Q., Fry, R.C., Adeleye, Y.A., Carmichael, P., and Samson, L.D. (2011). Genomic phenotyping of the essential and non-essential yeast genome detects novel pathways for alkylation resistance. BMC Syst Biol *5*, 157.
Tamborrini, D., Juanes, M.A., Ibanes, S., Rancati, G., and Piatti, S. (2018). Recruitment of the mitotic exit network to yeast centrosomes couples septin displacement to actomyosin constriction. Nat Commun *9*, 4308.
Tanaka, T.U., Rachidi, N., Janke, C., Pereira, G., Galova, M., Schiebel, E., Stark, M.J., and Nasmyth, K. (2002). Evidence that the Ipl1-Sli15 (Aurora kinase-INCENP) complex promotes chromosome bi-orientation by altering kinetochore-spindle pole connections. Cell *108*, 317-329.
Tapon, N., Harvey, K.F., Bell, D.W., Wahrer, D.C., Schiripo, T.A., Haber, D., and Hariharan, I.K. (2002). salvador Promotes both cell cycle exit and apoptosis in Drosophila and is mutated in human cancer cell lines. Cell *110*, 467-478.
Tinker-Kulberg, R.L., and Morgan, D.O. (1999). Pds1 and Esp1 control both anaphase and mitotic exit in normal cells and after DNA damage. Genes Dev *13*, 1936-1949.
Tomson, B.N., Rahal, R., Reiser, V., Monje-Casas, F., Mekhail, K., Moazed, D., and Amon, A. (2009). Regulation of Spo12 phosphorylation and its essential role in the FEAR network. Curr Biol *19*, 449-460.
Tucker, M., Staples, R.R., Valencia-Sanchez, M.A., Muhlrad, D., and Parker, R. (2002). Ccr4p is the catalytic subunit of a Ccr4p/Pop2p/Notp mRNA deadenylase complex in Saccharomyces cerevisiae. EMBO J *21*, 1427-1436.
Tucker, M., Valencia-Sanchez, M.A., Staples, R.R., Chen, J., Denis, C.L., and Parker, R. (2001). The transcription factor associated Ccr4 and Caf1 proteins are components of the major cytoplasmic mRNA deadenylase in Saccharomyces cerevisiae. Cell *104*, 377-386.
Tyers, M., Tokiwa, G., and Futcher, B. (1993). Comparison of the Saccharomyces cerevisiae G1 cyclins: Cln3 may be an upstream activator of Cln1, Cln2 and other cyclins. EMBO J *12*, 1955-1968.
Tyers, M., Tokiwa, G., Nash, R., and Futcher, B. (1992). The Cln3-Cdc28 kinase complex of S. cerevisiae is regulated by proteolysis and phosphorylation. EMBO J *11*, 1773-1784.
Uhlmann, F., Wernic, D., Poupart, M.A., Koonin, E.V., and Nasmyth, K. (2000). Cleavage of cohesin by the CD clan protease separin triggers anaphase in yeast. Cell *103*, 375-386.
Ullmann, A., Jacob, F., and Monod, J. (1967). Characterization by in vitro complementation of a peptide corresponding to an operator-proximal segment of the beta-galactosidase structural gene of Escherichia coli. J Mol Biol *24*, 339-343.
Valerio-Santiago, M., and Monje-Casas, F. (2011). Tem1 localization to the spindle pole bodies is essential for mitotic exit and impairs spindle checkpoint function. J Cell Biol *192*, 599-614.

van Leeuwen, J., Pons, C., Mellor, J.C., Yamaguchi, T.N., Friesen, H., Koschwanez, J., Usaj, M.M., Pechlaner, M., Takar, M., Usaj, M.*, et al.* (2016). Exploring genetic suppression interactions on a global scale. Science *354*.

Verma, R., Annan, R.S., Huddleston, M.J., Carr, S.A., Reynard, G., and Deshaies, R.J. (1997). Phosphorylation of Sic1p by G1 Cdk required for its degradation and entry into S phase. Science *278*, 455-460.

Visintin, R., and Amon, A. (2001). Regulation of the mitotic exit protein kinases Cdc15 and Dbf2. Mol Biol Cell *12*, 2961-2974.

Visintin, R., Craig, K., Hwang, E.S., Prinz, S., Tyers, M., and Amon, A. (1998). The phosphatase Cdc14 triggers mitotic exit by reversal of Cdk-dependent phosphorylation. Mol Cell *2*, 709-718.

Visintin, R., Hwang, E.S., and Amon, A. (1999). Cfi1 prevents premature exit from mitosis by anchoring Cdc14 phosphatase in the nucleolus. Nature *398*, 818-823.

Visintin, R., Prinz, S., and Amon, A. (1997). CDC20 and CDH1: a family of substrate-specific activators of APC-dependent proteolysis. Science *278*, 460-463.

Visintin, R., Stegmeier, F., and Amon, A. (2003). The role of the polo kinase Cdc5 in controlling Cdc14 localization. Mol Biol Cell *14*, 4486-4498.

Wang, Y., Hu, F., and Elledge, S.J. (2000). The Bfa1/Bub2 GAP complex comprises a universal checkpoint required to prevent mitotic exit. Curr Biol *10*, 1379-1382.

Willems, A.R., Lanker, S., Patton, E.E., Craig, K.L., Nason, T.F., Mathias, N., Kobayashi, R., Wittenberg, C., and Tyers, M. (1996). Cdc53 targets phosphorylated G1 cyclins for degradation by the ubiquitin proteolytic pathway. Cell *86*, 453-463.

Wittenberg, C., Sugimoto, K., and Reed, S.I. (1990). G1-specific cyclins of S. cerevisiae: cell cycle periodicity, regulation by mating pheromone, and association with the p34CDC28 protein kinase. Cell *62*, 225-237.

Woodbury, E.L., and Morgan, D.O. (2007). Cdk and APC activities limit the spindle-stabilizing function of Fin1 to anaphase. Nat Cell Biol *9*, 106-112.

Xu, T., Wang, W., Zhang, S., Stewart, R.A., and Yu, W. (1995). Identifying tumor suppressors in genetic mosaics: the Drosophila lats gene encodes a putative protein kinase. Development *121*, 1053-1063.

Yeh, E., Skibbens, R.V., Cheng, J.W., Salmon, E.D., and Bloom, K. (1995). Spindle dynamics and cell cycle regulation of dynein in the budding yeast, Saccharomyces cerevisiae. J Cell Biol *130*, 687-700.

Yellman, C.M., and Roeder, G.S. (2015). Cdc14 Early Anaphase Release, FEAR, Is Limited to the Nucleus and Dispensable for Efficient Mitotic Exit. PLoS One *10*, e0128604.

Yoshida, S., Asakawa, K., and Toh-e, A. (2002). Mitotic exit network controls the localization of Cdc14 to the spindle pole body in Saccharomyces cerevisiae. Curr Biol *12*, 944-950.

Zachariae, W., Schwab, M., Nasmyth, K., and Seufert, W. (1998). Control of cyclin ubiquitination by CDK-regulated binding of Hct1 to the anaphase promoting complex. Science *282*, 1721-1724.

Zeng, X., Kahana, J.A., Silver, P.A., Morphew, M.K., McIntosh, J.R., Fitch, I.T., Carbon, J., and Saunders, W.S. (1999). Slk19p is a centromere protein that functions to stabilize mitotic spindles. J Cell Biol *146*, 415-425.

Zhou, X., Li, W., Liu, Y., and Amon, A. (2020). Cross-compartment signal propagation in the Mitotic Exit Network. bioRxiv, 2020.2010.2001.322719.